MONITORING URBAN HEAT ISLAND INTENSITY OF DHAKA MEGA CITY USING MULTI-TEMPORAL AND MULTI SPECTRAL SATELLITE IMAGERY

BY

NIGAR SULTANA PARVIN

A thesis submitted to the University of Birmingham for the degree of

MASTER OF PHILOSOPHY

Department of Environmental Health and Risk management

School of Geography Earth and Environmental Science (GEES)

University of Birmingham

United Kingdom

May 2024.

Declaration

This work, named "Monitoring urban heat island vulnerability in Dhaka using multi spectral and multi temporal satellite imagery," is only being submitted in conjunction with the Master of Philosophy (MPhil) in Environmental health and risk management at the University of Birmingham, UK. To the best of my knowledge, no part of this thesis has been submitted to support a request for a different degree or accreditation from this or other university.

Furthermore, I confirm that the research and analysis in this paper were conducted by myself. My work is not plagiarised since, in the instances when I have utilised someone else's work, it has been properly cited with references in places like tables, images, and the text body.

Dedication

I would like to dedicate my MPhil thesis to my mother Begum Ashura Salim who always inspired me for my studies.

Acknowledgement

I am highly grateful to my supervisors Professor Christian Pfrang, Professor Lee Chapman, Dr. Emma Ferranti for their advice and contribution to complete this research project. I wish to express my gratitude to the government of Bangladesh for the scholarship by which I have been selected to pursue my post graduate research in the United Kingdom.

I acknowledge my friends and colleagues for their cooperation for supplying ground datasets from Bangladesh meteorological department (BMD), Centre for geographical information system (CEGIS) and Bangladesh Bureau of Statistics (BBS). I also thankful to my friend Dr Dan Abudu for his support in writing python and GEE code for analysis.

I would like to appreciate my family (husband, son, and daughter) who sacrifice their time and love to complete my study.

Abstract

Land surface temperature (LST) with high spatial and temporal resolution is a significant parameter for Urban Heat Island (UHI) determination. Moreover, such data are not currently available due to sensor design or compromises between temporal and spatial resolution. Therefore, development and corroboration of certain data are highly valuable. Landsat and Moderate Resolution Imaging Spectroradiometer (MODIS) data are frequently fused to produce Landsat like imagery using the spatiotemporal fusion technique, which may be used to increase spatiotemporal resolution. However, integrated MODIS and Landsat satellite datasets for LST estimation is still a unique approach for Dhaka, Bangladesh. This study evaluated the effectiveness of using multi-temporal and multi-spatial satellite imagery for assessing the intensity of Dhaka city's UHI from 2011 to 2022. To obtain the seasonal changes and ensure frequent monitoring, the UHI was estimated for the Winter to Summer transitional period (January to May) of year 2011 and 2022, respectively. The study demonstrates the usefulness of combining MODIS and Landsat (5TM and 9 TIRS /OLI) to obtain high spatial and temporal resolution imagery required for accurate UHI estimation. The Spatial and Temporal Adaptive Reflectance Fusion Model (STARFM) was used to fuse the satellite imagery, which generated synthetic Landsat imagery by applying the STARFM algorithm to MODIS daily datasets. These synthetic images, along with the original Landsat images, used to calculate the LST of Dhaka for the respective seasons and years. Human activities continuously influence the land use. It is important to observe and detect the changes of land use to protect and sustain the environment. Dhaka megacity is considered one of the most populous cities in the world, which is the capital of Bangladesh. The study also focused on the dynamic changes in land use which substantially transformed to urban area between the years 2011 and 2022. Population and housing Census for the respective years has been used to explore the transformation trends of land use within the city. This study also attempts to investigate the interaction between population growth and land use changing patterns, especially examining the density of population and their distribution within the study period. Within this investigation, land use has been categorised into four distinct feature classes: built areas, greenspaces, water bodies and bare soil. Within the limit of this study, an accuracy assessment has been carried out to ensure accuracy and clarity of the classified maps illustrating land use and land cover. Between year 2011 to 2022, the built-up area within Dhaka has experienced a notable increase of 24.9%, contrarily, there has been a significant decline of -7.36% in greenspaces, -2.48% in water bodies and -15.06 % in bare land. Dense vegetation cover has declined and very few has replaced with moderate vegetation rather than built area. The study's findings provide a concise and accurate depiction of the urban growth of Dhaka over the past twelve years. The results shed light on the modifications, expansions, and developments of Dhaka's thana scale landscape that observed within this study period.

List of Figures

List of Tables

Abbreviations

BMD- Bangladesh Meteorological department

CEGIS- Centre for Environmental and Geographic Information System

DNCC- Dhaka North City Corporation

DSCC- Dhaka South City Corporation

ESA- European Space Agency

ETM+ - Enhanced Thematic mapper plus

GEE - Google Earth Engine

GIS- Geographical information system

LST- Land surface temperature

LULC- Land use and Land cover

MNDWI- Modified Normalized different water index

MODIS- Moderate resolution imaging Spectroradiometer

NASA - National Aeronautics and Space Administration

NDBI- Normalized different built up index

NDVI- Normalized difference vegetation index

NDWI- Normalized different water index

NIR- Near Infra-Red of the electromagnetic spectrum

OLI2- Operational Land Imager 2

RS- Remote sensing

STARFM- Spatial temporal adaptive reflectance fusion model

SWIR- Short wave Infra-Red

TIRS - Thermal infrared Sensor

TIRS2- Thermal Infrared Sensor 2

TM- Thematic Mapper

UAV- Unmanned aerial vehicles

UCL- Urban Canopy layer

UHI – Urban Heat Island

USGS- United states geological survey

Thana – Administrative unit in Dhaka

Table of contents

1.CHAPTER ONE - INTRODUCTION

Urban Heat Islands (UHIs) have arisen as a major problem in urban environments across the world, aggravating the effects of climate change and providing a variety of difficulties to the well-being and sustainability of city people. As one of the world's fastest-growing megacities, Dhaka, Bangladesh's capital, is facing mounting challenges related to UHI impacts caused by rapid urbanisation, population increase, and inadequate infrastructure. It is important to comprehend the dynamics of urban heat island (UHI) and its susceptibility in Dhaka in order to develop mitigation and adaptation methods that effectively promote a robust and environmentally friendly urban environment.

This chapter examines numerous characteristics present and prior academic research that are significant to current topic. The chapter contextualises the study, examines the methodologies used, and logically connects the advantages and disadvantages of each evaluated approach. Additionally, the literature review demonstrates the project's scientific and general demands, producing a knowledge basis for research assessment and documentation. subsequently, several of the study questions included in the research goals are introduced.

Dhaka, the capital of Bangladesh is one of the fastest growing megacities experiencing higher temperature over the last decade depicted by hot summer days and daytime scorching heat (Islam, 2008; Uddin, et al, 2022). Annual daytime temperature of Dhaka has increased by 2.74 degree Celsius in last 20 years (Dewan, A, et al, 2021), whilst the world fights to keep rising temperatures to less than 1.5 degrees Celsius (UNEP,2015). Several variables have been considered for the increasing temperature in Dhaka (Uddin, et al, 2022; Parvin et al, 2017; Abrar R, 2022) but one factor that is recurrently focused by the researchers, is the phenomenon known as Urban Heat Island (UHI) effect (Oke, et al., 2017; Tomlinson, C.J, et al, 2012; Tashnim, et al, 2016;). UHI is one of the most important environmental issues which is related

to urban climate and sustainability of the cities (Liu et al., 2020). However, the heat in urban area is normally apparent at night, paradoxical diurnal behaviour also noticed in urban heat island (Dewan, A., et al, 2021).

Urban microclimate variation is generally related with the urban heat island (UHI) which is considered as the phenomenon of intense heat occurring in urban areas than to its surrounding rural areas (Oke, et al., 2017). Changing in natural surfaces and increased uses of heat reflective building materials reducing heat evaporation and transformation rates, exacerbates UHI phenomenon. It's also modifying microclimate, airflow as well as atmosphere and causing UHI (Karakuş, 2019), is studied in many cities regardless of their locations, size, and different degrees. Population density is one of the other causes of UHI in a conurbation (Oke et al.,2017) which is associated with releasing of anthropogenic heat (Smith et al. 2009). Many studies have found that UHI can vary in air temperature from 2^0C to 15^0C (Aflaki et al,2017). A UHI impact specifically influences human thermal comfort and increases the energy consumption in the cities for cooling in summer (Raja et al., 2021), causes less dense fogs in winter and increase chemical oriented smog (Oke, 2017). UN Habitat (2022) reported that 78% of global energies consumed by the cities and producing 60% of the greenhouse gas emission. Germination and proper growth of plants take longer time in urban area than the rural due to effect of UHI (Ishola et al., 2016).

Air temperature experienced in UHIs are usually higher at night and lower at daytime (Bohnenstengel et al., 2014). From a health perspective, this is increasing diseases such as respiratory problem, physical distress, heatstroke, heat cramps and exhaustion and heat related mortality (US-EPA, 2017). Elderly people who are at high risk of illness, workers whose exposure to heat, homeless populations are the sufferers of UHI effects (Hsu, et al., 2021; Han, D et al., 2023), however most of the thermal impact research has been carried out in industrialised countries located in the mid-latitudes, whereas little is known about the heat related mortality in less developed, particularly in tropical countries (Burkart et al., 2021) like Bangladesh. Heat exposure increases total days of hospitalisation, which caused an increase in the amount of hospital admissions and severity of disease in Adelaide, Australia (Liu, J et al., 2022). Total urban area of the world has extended by 168% since 2001 to 2018, which is mostly high in in Asia and Africa (Dewan A, et al., 2021). A recent study shows that 60% of Dhaka city is urbanized with built-up area and rest of the areas are consisting of low vegetation and water (Abrar R, 2022).

According to the most recent World Population Review report, Dhaka is the sixth most populous city in the world with a population density of 23,234 people per square kilometre as of 2022. In reference to the latest Census of Bangladesh, total urban population in Dhaka city is 11.22 million (BBS, 2022). Dhaka's population has drastically increased from 2.2 to 10 million from 1975 to 2015 (Karim, 2024; Islam, et al.,2022). The increased population and urban area caused the changing of land use from permeable to impermeable which significantly increase the temperature of the city. (Corner, J., et al, 2014). Many studies indicated a positive correlation between impermeable area and land surface temperature (LST) of the city (Karakuş, 2019; Zou, Z. et al., 2021). More than half of the inhabitants living in informal housing in Bangladesh where 35% of population lives in slum in Dhaka (Ahmed, 2014). They have limited opportunity to sustain with thermal comfort, weather related sickness and mortality (Uddin, et al., 2022). Typhoid fever (Chua, et al., 2021), dengue fever (Imai, C., et al, 2015) and other infectious diseases are the evidence of the heat effects in Dhaka (Ali, S., et al, 2022). The city experienced a temperature of 41.2 degree Celsius on 25th April 2021, which was recorded as the highest in a decade. Dhaka has continuously the focus of researcher for various significant challenges are progressively affecting Bangladesh.

There are multiple approaches to observe and estimate the UHI effect (Ishola, et al., 2016). Structural design and configuration of land use and land cover has high impact on UHI (Guo G. etal.,2015; Hsu, et al., 2021). The UHI of a region or area can be assessed using various methods which includes portable thermal camera, authorised database, ground temperature from weather stations, and remotely sensed datasets (Weng, Q. et al., 2014). Several studies (Dewan A, et al, 2021 ; Padmanaban, 2019)used multiple data sources to enhance this information from both at the ground level and atmosphere to measure UHI and surface urban heat island (SUHI).Although the influence is stronger in the summer and winter, this range of sources provides access to data collected throughout the day or night (Santamouris, 2014). Earth observation systems and satellite images has been comprehensively used to research the characteristics of urban climate change. The key point of using remotely sensed satellite image is that it can monitor surface UHI in efficient way and across multi spectral and various spatial scales (Varentsov et al., 2019; Padmanaban, 2019). Land surface temperature (LST) is considered as an important parameter of physics and the climate system from local area to global scales (Zhao C. et al., 2018). The land surface where the incoming solar energy interacts with and heats the ground or the surface of the canopy in vegetated regions is where LST detects the emission of thermal radiation (Khan A. et al, 2019).

The use of satellite imagery to model land use dynamics, land surface temperatures and isolate heat hotspots over time has proved very significant in UHI studies because it can generate accurate results over very large geographical extents thereby providing timely and cost-efficient results (Deilami et al., 2018). However, most studies conducted focus on the use of single satellite imagery for a single period (Abrar et al., 2022), or the use of two satellite imagery over two short periods of time (Parvin, 2017). An attempt at exploring the use of extensive datasets for UHI estimation such as the case of Birmingham city UK (Tomlinson, et al., 2012) have shown great accuracy comparable to ground based measurements. It is noteworthy that because of climate dynamics, accurate modelling of UHI requires near-timely datasets as compared to isolated days in a month. However, for the case of Dhaka megacity with minimal daily to weekly climate variations, a similar temporal dataset can accurate UHI modelling. The use of extensive datasets further increases the reliability of UHI models in supporting decision making.

The feasibility of using more than two satellite imagery in a month to assess UHI vulnerabilities in Dhaka city is still an open research area. This study aims to fuse MODIS datasets, which is high in temporal resolution with the Landsat data which although better in spatial resolution, they have poor spectral resolution. MODIS daily-time (MOD11A1) datasets are used to estimate the LST for Dhaka. Fusion of MODIS and LANDSAT different series (5,9) of datasets has done to increase the granularity of the LST produced.

However, to the best of our knowledge, the use of integrated multi-temporal and multi-spatial remote sensing data for UHI estimation for Dhaka is novel.

In this study, we aim to assess the use of multi-temporal and multi-spectral satellite imagery for UHI vulnerability of Dhaka city from 2011 to 2022. The selected years correspond the respective censuses. To properly understand the seasonal changes in the study area and ensure frequent monitoring, we estimated UHI for Dhaka's winter (Jan/Feb) and summer seasons (March-May) in 2011 and 2022 respectively. The study demonstrated the utility of fusing MODIS and Landsat 5 and 9 to obtain imagery with both high spatial and temporal resolutions necessary for accurate UHI estimation. Ground climate datasets about Dhaka city provided the surface air temperatures for comparison and accuracy assessment. The study results will assist policy makers, urban planners, and the community to effectively monitor UHI and related public health hazards and contribute to the UN's Sustainable Development Goals 11 and 13.

1.1 Background of the study

According to the United Nations Department of Economic and Social Affairs projections, nearly seven out of ten people will be living in an urban area by the year 2050 (UN, 2018). This translates to about 2.5 billion people added to the current urban population and nearly 2.25 billion people (90%) filling urban areas in Asia and Africa largely because of their current low levels of urbanization. Urban footprints will therefore significantly increase, altering the environmental and ecological habitats of previously undisturbed areas. The magnitude of ensuring risks to climate, health and safety of the communes are disastrous if not properly understood and contained. In Asian continent for instance, much as her rural population are high, several of her major cities have populations in excess of thirteen million people such as over seven cities in China (Wang et al., 2019), Mumbai city in India (Vinayak et al., 2021), Istanbul city in Turkey (Halicioglu et al., 2021) and Dhaka city is Bangladesh (Yin et al., 2021). These cities must contend with both rural-urban migration problems and the devastating consequences of urbanization.

Urban Heat Islands (UHIs) have arisen as a major problem in urban environments across the world, aggravating the effects of climate change and providing a variety of difficulties to the well-being and sustainability of city people. UHIs phenomenon is characterised by inner cities becoming far warmer than the rural urban peripheries at night. This is because, during day, the concrete and steel materials of the cities absorb and retain much daytime heat and dissipates the heat at night. Consequently, urban dwellers feel much warmer at night compared to other dwellers surrounding the urban areas. The changing climatic conditions resulting into higher temperatures or prolonged heat seasons can compound UHI effect on urban areas and has the potential of causing several heat related illnesses such as burns, heat exhaustion and heat stroke, when the body cannot adequately cool itself through sweating and heat dissipation. Additionally, UHI may worsen other illnesses such as diabetes, respiratory problems, kidney disorders and mental health, because the affected individuals may find it more difficult to manage their condition in higher temperatures.

In Dhaka city, the effect of climate change has the potential of undercutting urbanisation progress by endangering the social and environmental safety of the communities through increased risks of urban heat islands (UHI), floods, droughts, traffic congestion and poor air quality. Several studies have reported the existence of UHI in Dhaka (Abrar et al., 2022;

Maharjan et al., 2021; Raja et al., 2021) and adverse effects of extreme heat waves in 2002 (Karim et al., 2024; Wu et al., 2018) and from 2003 to 2014 (Sultana et al., 2020). Dhaka's high population density, poorly planned buildings and infrastructural developments makes it most susceptible to heat-related illness, compounded by climate change. It also makes it a great potential source of man-made climate-change contributors through increased emission of greenhouse gases.

In mitigating the devastating impacts on the health of UHI Dhaka city dwellers, several approaches have been employed. Prominent among the studies is the use of satellite imagery to model land use dynamics, land surface temperatures and isolate heat hotspots overtime. The use of satellite imagery has proved very significant because once augmented with ground-based datasets, it can generate accurate results over very large geographical extents thereby providing timely and cost-efficient results. The feasibility of using two or more satellite imagery spanning twenty years or more to assess land cover and LST dynamics remains an open research area. More so, given that climate change is a recent phenomenon, assessing the vulnerability of Dhaka city dwellers to heat-related illness over such time periods can provide valuable insights into the contributions of climate change and non-climate change contributors.

Landsat, EOS MODIS, AVHRR are continuously used to derived land surface temperature (LST) to determine UHIs (NASA,2022). Landsat data have proven its necessity in monitoring LST; however, its 16-day revisit cycle is a limitation of the application of Landsat for rapid changes of surface and land surface temperature (Zhao G., et al., 2020; Guan X., et al., 2021). Landsat overpasses Bangladesh in the morning hours which is 10.30 am at morning (USGS-Landsat) according to Bangladesh local time (GMT+6), so Landsat data is not adequate to provide a real picture of UHI which sometimes intensifies at the end of the day (Guo G. et al., 2015). In some region which are prone to rain during summer, the cloud cover is high in satellite images with moderate high resolution, such as Landsat (Guan X., et al, 2021). One solution is to integrate the temporal resolution sensor such as Moderate Resolution Imaging spectroradiometer (MODIS) with the spatial resolution of Landsat (Walker, J., et al, 2012; Hazaymeh et al., 2015; Long, D et al.,2020).

Ground-based measurements, however, are limited to providing high temporal resolution of the atmospheric state of the region being studied (Weng, Q et al., 2014) and are not able to give large geographical coverage for a limited amount of time. Researching, tracking, and getting the spatial features of the changes in land cover and the LST of different cities is

made easier by the remotely sensed measurement approach, which can be used to characterise and quantify the UHI on multi-temporal scales (Long, D et al.,2020 ; Guan X., et al, 2021). Estimating the energy balance and surface heating is aided by having a solid grasp of how the LST varies over various surfaces.

In this study, we aim to assess the heat vulnerability of Dhaka city from 2002 to 2022 using multi-temporal and multi-spectral satellite imagery. The study will utilise satellite optical imagery from Landsat 5 TM, Landsat 9 and Sentinel-2 to quantify land cover changes over a twenty-year period and determine the land surface temperature of subsequent years. Ground climate datasets about Dhaka city will provide the needed surface air temperatures for the study. The study results will assist local public health experts and policy makers, urban planners, and the community to effectively monitor public UHI and related public health hazards and contribute to the UN's Sustainable Development Goals 11 and 13.

1.2 Problem statement

The urban heat island (UHI) phenomenon in Dhaka poses a variety of issues, including higher energy consumption for cooling purposes, an increased risk of heat-related diseases, and decreased agricultural production in outskirts of cities regions. As a result, thorough study is desperately needed to determine how vulnerable Dhaka is to the effects of UHI and to create focused solutions that would lessen its negative consequences. By using cutting-edge remote sensing methods and geographical analysis to track and assess Dhaka Mega City's UHI sensitivity, this study seeks to close this gap.

1.3 Aim of the study

The study aims to assess the urban heat island intensity of Dhaka city using multi-temporal and multi-spectral satellite imagery.

1.3.1 Objectives

The objectives of the study are to:

i. Quantify the land use land cover changes over Dhaka city from 2011 to 2022.
ii. Estimate the urban heat island of Dhaka city and its change over time using multi-temporal satellite imagery, census, and ground weather data.

iii. Determine the significant land use land cover variables for heat vulnerability in Dhaka City.

iv. Recommend adaptability measures for heat vulnerability interventions in Dhaka City.

1.3.2 Research questions

1. How have spatial patterns of UHI and heatwaves evolved over the study period in Dhaka?
2. How much land use and land cover changes over the study period?
3. How do land use/land cover factors relate to the geographical distributions of UHI susceptibility within Dhaka Mega City as indicated by multi-spectral satellite imagery?

1.4 Study area

Dhaka is in South Asia (figure 1), positioned along the bank of the Buriganga River, and its geographical coordinates are approximately 23^0 42' N latitude and 90^0 22' longitude. The city is also near other water bodies such as the Sita Lakshya River, Turag River, Balu River, and Tongi canal. The regional topography of the city is characterised by flat and low- lying land surface with an elevation of 1 to 14m above the sea level where most of the built-up areas situated at 6-8m (FAP 8A,1991; Kafy et al., 2021). There are three distinct seasons are experiencing within the city, hot and dry summer Mar- May, monsoon rainy season from Jun-Oct, cool and dry winter from Nov-Feb (Corner, J. et al., 2014). Dhaka is comprising with two municipalities: Dhaka South City Corporation (DSCC), which has 90 wards, and Dhaka North City Corporation (DNCC), which has 54 wards. The city comprises with 53 thanas (administrative unit such as parish) covering all these wards.

According to Dhaka South and North City Corporation, the total area of Dhaka metropolitan area is 1528 square kilometres, and the built-up megacity (study area) covering an area of 306.4 sq.km. The city is the capital of Bangladesh's and most densely populated city with 33591 residents /sq.km. Dhaka is considered one of the largest metropolises in South Asia. Based on the preliminary report of the population housing census, it has been indicated that the population of the country's capital city, Dhaka, stands at 10.2 million (1,02,78,882 individuals), this figure represents a notable growth, approximately 1.5 times higher than the population of

about 7 million (69,70,105) recorded in 2011 census (BBS, 2023). According to the Mayor of Dhaka North city corporation DNCC, 2000 people move to Dhaka from other rural areas of the country every day. Some previous study reported that Dhaka's population reached to 22 million (NASA 2022; Macrotrends, 2023; Masrur et al., 2022). Expansion of Dhaka has been largely influenced by its elevation, higher population, and economic development.

The city also presents a prospective research topic for Urban Heat Island (UHI) studies due to its distinctive combination of meteorological, socioeconomic, and physical factors. The city Dhaka, among the world's most populated cities, is fast developing and witnessing significant urbanisation, which has influenced land-use patterns and increased impervious surfaces. Because of these changes, urban heat islands are expanding, which also contributes to the formation of local microclimates. The city's topography, which consists of open regions, narrow streets, and high-rise buildings, also influences the spatial distribution of temperature variations.

Investigating Dhaka's urban heat island (UHI) may provide insights into the intricate relationships between urban form, changes in land use, and climatic conditions. Dhaka's climate is tropical monsoon. There are three different seasons in this geographical location. Summer, rainy and winter. Summer season is hot and dry which lasts from March to May, June to October is rainy season and November to February considered as dry and cold winter (Corner, J. et al.,2014).

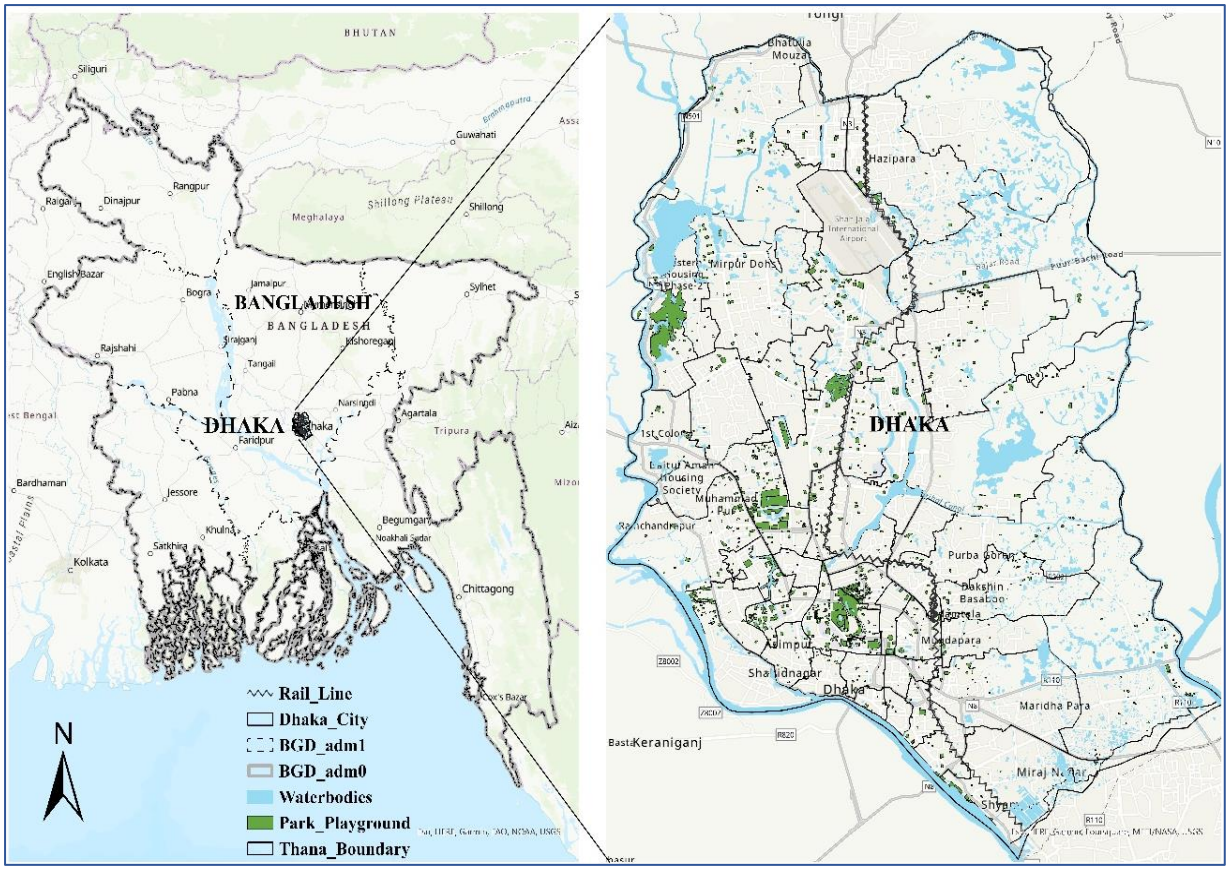

Figure 1: Study area Dhaka Megacity, Source: CEGIS, 2023.

1.7.1 Weather in Dhaka

It is notable that there is always temperature rise from January to April, and then the temperature starts to drop in May as the season transitions to fall. However, in some years such as 2011, 2012, 2015, 2017, 2019 and 2020, temperatures in May were higher than April. From experience of the city's temperature, the lower half of May is usually hotter than April while temperatures begin dropping towards the end of the month. This attributes to general lower average temperatures in May as compared to April. However, as reported in Parvin et., al (2017), there are cases where daily temperatures of Dhaka have exceeded the 40-degree Celsius mark, for instance in 2014 where the city experienced temperatures at 42.2 ^{0}C. (Figure 2,3,4, and 5) provide the chart representation of the daily average temperature and rainfall variation of Dhaka in 2011 and 2022, respectively.

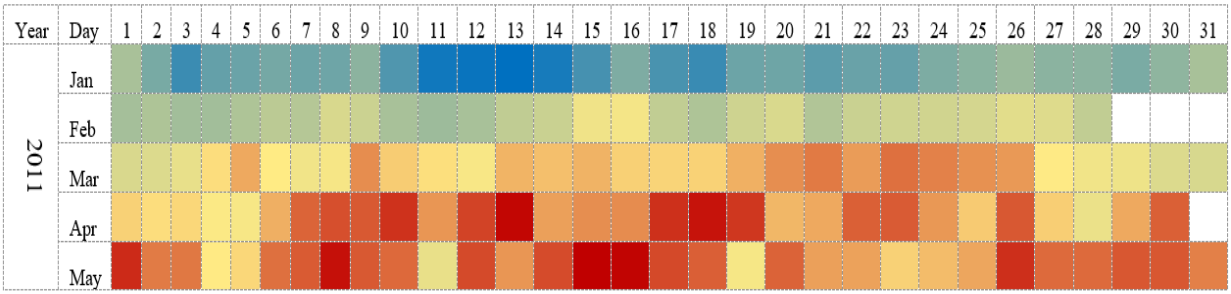

Figure 2 : Heat map of Dhaka from January to May daily temperature, 2011(Source: BMD)

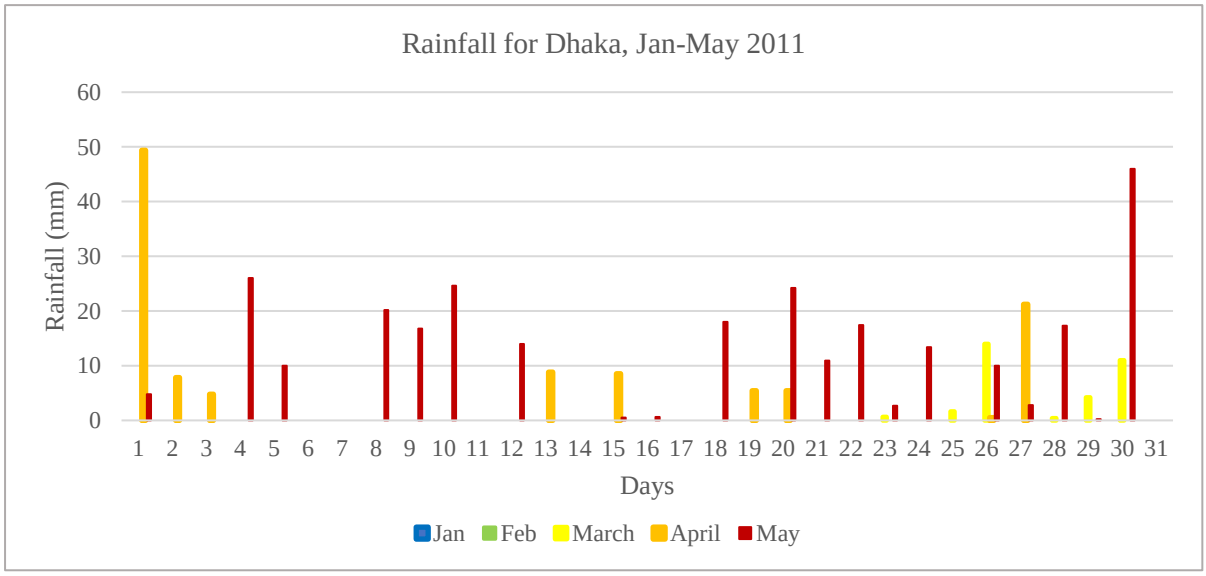

Figure 3: Rainfall of Dhaka_ January to May 2011(Source: BMD)

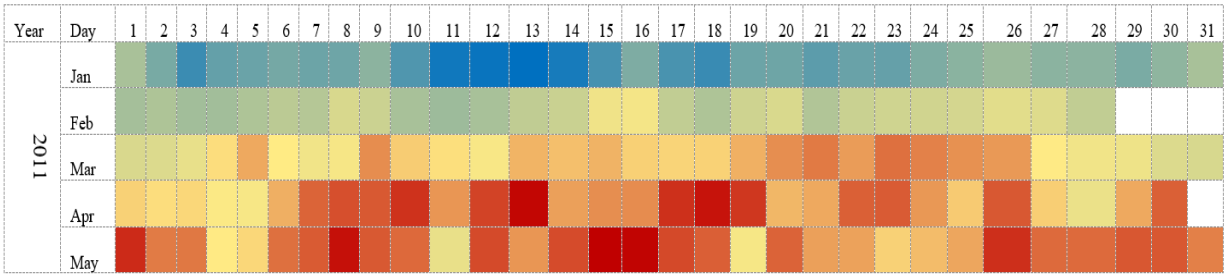

Figure 4: Heat map of Dhaka_ January to May 2022 (Source: BMD)

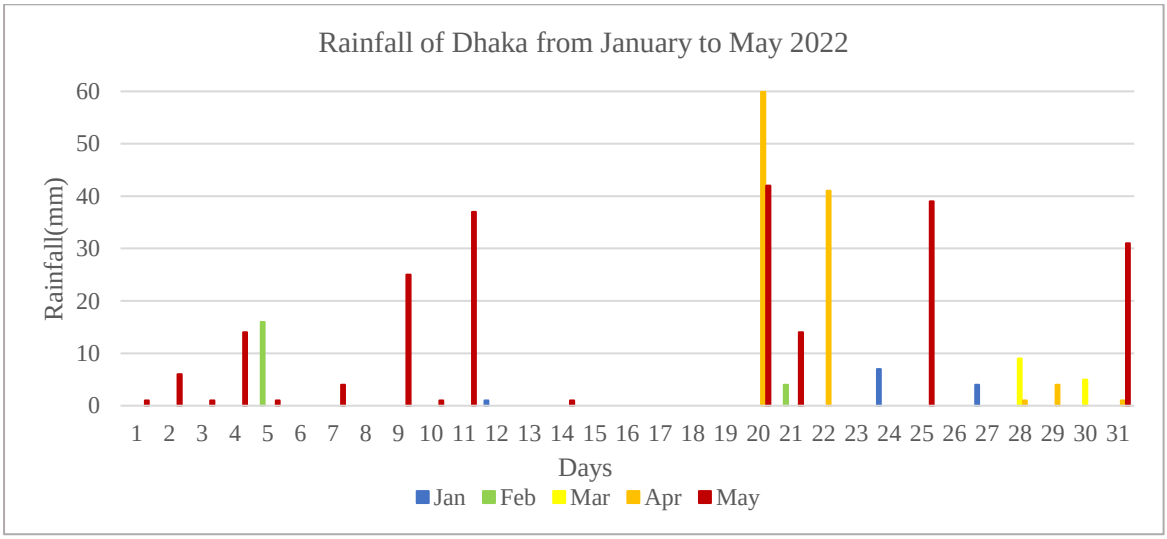

Figure 5: Rainfall of Dhaka_ January to May 2022 (Source: BMD)

From figures 3 and 5, it is evident that there is usually none or limited rainfall during the transition months of January and February, despite the low temperatures (figures 2 and 4) experienced in these months. This is attributed to the cool breeze from the previous winter season that is still felt in the two months. However, the months of April and May experiences rainfall on almost a daily basis yet showing higher temperatures greater than other months. This scenario is common in Dhaka in the months of April and May, where cyclones built from the Bay of Bengal makes landfall with devasting effects in Dhaka and the neighbouring cities. In the two years considered in this study, the cyclone impacted Dhaka on the 30th of May 2011 and 20th April 2022 respectively. In 2022, a 60-mm rainfall was recorded as compared to 46mm recorded in 2011. Climate change effects could also likely be intensifying the cyclones and making them more frequent.

2. CHAPTER TWO -LITERATURE REVIEW

2.1. Introduction

This chapter examines numerous characteristics present and prior academic research that are significant to current topic of land use land cover (LULC) and urban heat island (UHI) modelling, with a specific focus on Dhaka. The chapter contextualises the study, examines the methodologies used, and logically connects the advantages and disadvantages of each evaluated approach. Additionally, the literature review demonstrates the project's scientific and general demands, producing a knowledge basis for research assessment and documentation. subsequently, several of the study questions included in the research goals are addressed. The review investigates the existing knowledge and identifies research to establish a seminal basis for current and future research. This is done by examining the methodologies used, and logically connecting the advantages and disadvantages of each evaluated approach.

Dhaka became uncomfortable to live in due to its unplanned urbanisation and high population density. Urban expansion is increasingly changing the scenery. Land conversion to residential area, open and green landscapes have been replaced by carriageways and other infrastructure. Surface that was once permeable and moist becomes impenetrable and dry. Geographical expansion and current population growth have been made in a disproportionate manner. Dhaka's water resources are already under stress (Moshfika et al., 2022) due to its uncontrolled expansion, which is already reducing the city's sustainability (Hossain, et al., 2018). The city and its sizable population are impacted by climate change and numerous meteorological phenomena. Heat stress is becoming increasingly common in the city for rapid and extensive urbanisation, which is a serious health hazard. In regard to sustainable development, scientists have pointed out the need of establish a balance between the needs of humans and those related to the environment. (Fonseca, et al., 2020).

2.2 An overview of Urban Heat Island Phenomenon

UHI is a condition that escalates with the size and demographics of an urban area. As a result, if people continue to live in the cities, the urban heat island issue will continue to get worsen.

The effects of UHI are strongly related to the patterns of climate change (Ivajnšič D. et al., 2019), with the expectation that rising mean temperatures. It has more rapid and substantial impact on the physical and mental health of people live in urban area, particularly the elderly and obese.

UHI arises with the anthropogenic activities which related to increase temperature in metropolitan areas in compared to neighbouring rural areas. It also depends on urbanization and land use changes (Xiang, Y et al., 2023; Oke et al., 1982). This effect is primarily driven by the replacement of natural surfaces with buildings, roads, and other heat-absorbing materials, leading to alterations in energy balance, heat retention, and atmospheric dynamics within urban environments (Figure 6).
Since the 1980s, this phenomenon has been recognized and investigated. It is brought on by:

- Physical properties of surfaces, including asphalt and concrete, absorb solar radiation instead of reflecting it.
- Absence of naturally occurring absorbent surfaces, like vegetation, which helps preserve a steady energy balance in rural regions.
- The strengthening of the vertical surface, which increases its surface area for receiving and reflecting solar radiation and blocks breezes that may otherwise cause the temperature to drop.

- The primary sources of heat created by human activity include automobiles, industrial processes, heating and cooling facilities and constructions, etc.
- High number of contaminants that change the radiative characteristics of the atmosphere.

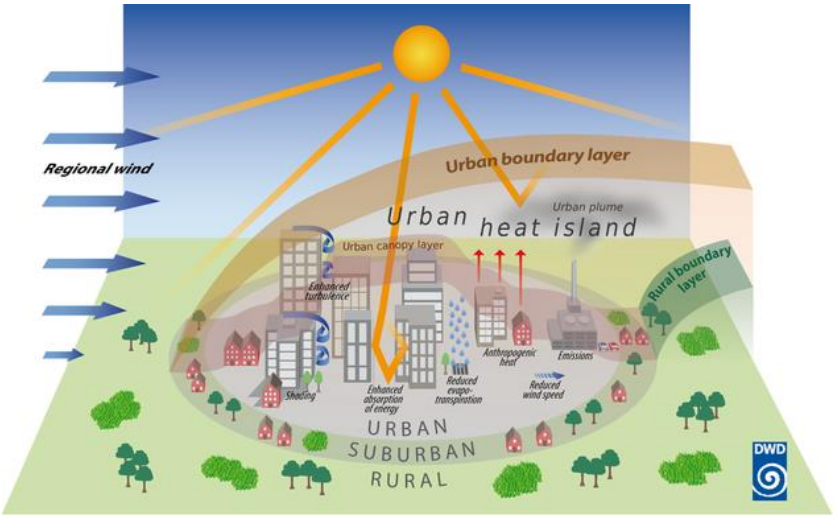

Figure 6: Illustration of UHI development (WMO, 2020)

There are many regional variables that make UHI severe in areas like South Asia. Cities in South Asia have seen significant changes in land use due to the region's fast urbanisation and population increase, including the transformation of once-forested landscapes into concrete jungles. Cities like Mumbai in India (Vinayak et al., 2021) and Dhaka, Bangladesh (Yin et al., 2021) have a numerous high-rise buildings, pavements, and infrastructure that increased daytime heat absorption and release at nighttime. This has impacts on UHI. South Asian cities has high population density, and their anthropogenic activities produced more energy which contribute to UHI. These activities include industrial works, transportation, household energy consumption etc.

UHI has wide ranging consequences in South Asia. Frequent heatwaves and their severity in cities are notable. Urban residents may be at risk for their health and well-being due to heat and UHI effects, especially vulnerable groups such as elderly, children, and people with other medical conditions (Fonseca et al., 2020). UHI could made the regional environment worse which would be more harmful for precipitation patterns, ecosystem, biodiversity and moreover increase air pollution (Wu et al., 2018).

Urban planning, green infrastructure development and policy makers should work together to address UHI in local area as well as South Asia. More plantation for natural cooling, changes in rooftop design can boost low heat absorption. Energy effective building materials and pavement technologies can help to control UHI effects (Eastin et al., 2018). Citizen awareness and community engagement are essential for sustainable urban growth.

With the challenges of UHI, South Asia provides plenty of opportunities for innovation and collaboration to mitigate this serious issue. Governments, urban planners, scientist, and private sectors may work for regional collaboration to exchange knowledge, build capacity, and implement initiatives to address urban heat island impacts. To make their cities sustainable, adaptive, and liveable for the future, south Asian cities should integrate their plans, policy, and legislation.

2.3 Urban Heat Island Dynamics

Some of the variables that impact the dynamics of UHI are briefly discussed as follows.

Impermeable feature: Urban areas are prone to have more impermeable features, such as roads, buildings, and pavement. These surfaces absorb sunlight during the day and hold the heat daylong and release them at night. Due to the release of heat at night, temperature within the city increase and contribute to the UHI.

Decreased Vegetation: The process of urbanization frequently results in the elimination of grass and trees, which helps evapotranspiration to naturally cool the area. The cooling effect is lessened by this loss in foliage cover, which raises the temperature.

Anthropogenic Heat: Heat is released into the environment by human activities including energy use, transportation, and industrial operations. This causes temperatures in metropolitan areas to rise even more.

Density and Height of Buildings: Tall buildings and closely spaced urban buildings may hinder air circulation, trap heat, and form urban canyons where heat concentrates, all of which worsen the UHI impact.

Thermal waste: During moments of peak energy usage, the heat load in metropolitan areas is increased by the heat produced by automobiles, air conditioning systems, and industrial activities.

Urban Design: The extent of the UHI impact is influenced by elements such as building materials, roadway layout, especially the presence or lack of green areas. For instance,

roadways oriented in specific orientations could improve ventilation or heat retention. Solar radiation is absorbed by glass surfaces, particularly in areas like Dhaka that receive a lot of sunshine. This absorbed heat is subsequently reflected in the surrounding environment, contributing to increased temperatures in cities, especially in densely populated regions with nearby buildings.

Urban Geometry: The features of an urban canyon (urban regions with roadways cutting through areas of dense structures may be found in urban geometry (Deng J. et al., 2020), which is made up of many components such as city blocks, walls, floors, and pavements Short-wave radiation can be trapped by urban canyons, preventing considerable amounts of it from escaping as long-wave radiation (Nasrollahi N. et al., 2023). After sunset, canyons of the highway absorbed radiation and insufficient air flow lead the UHI to swiftly worsen (Vujovic S. et al.,2021).

2.4 Urban Heat Island Characteristics in Dhaka City

Urban heat island (UHI) existence in Dhaka has been studied in various academic research (Abrar et al., 2022; Maharajan et al., 2021; Raja et al., 2021); especially, extreme heat events in different periods which took place in 2002 (Karim et al., 2024; Wu et al., 2018) and from 2003 to 2014 (Sultana et al., 2020). There is correlation in between climate change, environmental degradation, and unplanned urbanisation has shown with the UHI phenomenon in Dhaka city. Dhaka is considered one of the most populous cities in the world, experiencing exponential growth in its population and land use changes over the last few decades. It is continuously impacting on changing the microclimate and topography of the capital city (Sharmin et al., 2020). Green space has been disappeared by the replacement of concrete pavements, roads, housing, and industrial areas which increase heat absorption and holding it within the urban areas.

Dhaka is sensitive to heat trapping characteristics as the city is situated in low-lying delta location. The city is also adjacent to agricultural areas which exacerbate this condition. Anthropogenic, geographical location and climatic influences are noticeable for the UHI of Dhaka (Raja et al., 2021). Lack of green spaces, elevated humidity and slow wind speeds amid summer season restrict natural cooling systems and increase accumulation of heat in cities, which intensify the impacts of UHI.

There are several repercussions of UHI within Dhaka that affect every part of city life. Particularly in the summer, the metropolis endures intense heat waves with temperatures that are significantly higher than those in rural regions (Abrar et al., 2022). Especially for poor people residing in slums and homeless with inadequate access to basic amenities and infrastructure, the extreme temperatures pose serious health hazards to them. It also Increase the risk of heat-related diseases and fatalities (Karim et al, 2024; Moshfika et al., 2022).

Moreover, Dhaka's energy use and air pollution become worse due to UHI. The increased consumption of power for cooling, which generally met by fans and air conditioners, results in higher energy use and raises greenhouse gas emissions. It contributes to climate change. In addition, heat-induced chemical reactions promote the development of urban air pollutants, intensifying Dhaka's dwellers respiratory health concerns and other difficulties with air quality. It has put continuous pressure on the water resources of Dhaka (Moshfika et al., 2022).

Resolving the UHI phenomenon in Dhaka requires collaborative and sustainable strategies with an emphasis on preservation of the environment and resilience in urban areas. Increased green spaces can lower the effects of UHI by fostering biodiversity, absorbing carbon dioxide and offering tree shade and fresh air (Irfeey et al., 2023). However, the use of effective urban planning, cool roof technology and sustainable construction materials could control heat absorption. It also enhances thermal comfort within the urban areas (Raja et al., 2021).

Two types of components have significant influence on UHI formation. Firstly, manmade factors that are related to the length of the day light and secondly, natural effects (Zhou et al., 2018; Mushtaha et al., 2021). Environment friendly transportation, climate-resilient infrastructure, and energy efficiency all these need to receive highest attention in policy interventions to reduce the effects of UHI in Dhaka. Promoting sustainable public transportation, pedestrian path, options will help reduce traffic congestion and automobile emissions, which will enhance air quality and reduce heat emissions (Manisalidis, I. et al., 2020).

2.5 Land Use Land Cover Changes and Urban Heat Island

Urban land use classes such as industrial, residential and transportation continuously release heat which raises the intensity of UHI in a particular location (Liang, X et al., 2021; Oke et al., 2004). Industrial areas increase anthropogenic heat which contributes to the intensity of UHI

in the canopy layer (Mohan M et al., 2020). Chimneys and roof tops also have the impact on enhancing the UHI in urban boundary layer (Oke, 2017).

Urban areas are always in demand of additional structures to accommodate the growing population. However, permeable surfaces like vegetation or plantation should be replaced with impermeable surfaces such as asphalt, brick, and concrete (Martilli et al., 2020). One of the key influences on UHI production in urban environments is the ratio of vegetated surfaces to impervious surfaces (Dutta D., et al, 2021; Liang, X et al., 2021).

Study shown that development of 10% impervious surface in the city, increased the average temperature by 0.40C, before sunrise (Bachir, N., et al., 2021). However, no mention has been made of the relative humidity of the study area. When the relative humidity declines, it signals an increase in air temperature since it shows the lack of moisture in the surrounding atmosphere (Vujovic S. et al., 2021). As a result, the link between relative humidity and temperature should be investigated and included in urban research. Apart from relative humidity, surface albedo is one of the most crucial factors to consider in land cover research. Albedo is the reflecting capacity of a surface. Shortwave radiation from the sun is different from individual surfaces. It aids in determining the daily net radiation budget. White surfaces contain high albedo, and it reflects more radiation than black surfaces (low albedo) (Irfeey et al., 2023).

Various land cover types exhibit different temperature patterns, causing temperature fluctuations in metropolitan areas. Roof regions had the greatest temperature during the day followed by pavement, bare soil, and air temperature (Proutsos et al., 2022). Monitoring and examining the spatial distribution of different kinds of land cover types in an urban area involves measure the trends of urban expansion and understand the increase in land surface temperature (Vani, M et al,2020; Dutta D., et al, 2021; Oke, 1982).Urban expansion that results in changes in land cover types may be assessed using multiple image classification algorithms (MohanRajan S. et al.,2020; Chugtai et al., 2021).

2.6 Methodologies for LULC Classification and UHI Estimation

In mitigating the devastating impacts of UHI Dhaka city dwellers, several approaches have been employed. Modelling of land use patterns, land surface temperatures, and the identification of heat hotspots throughout time using satellite data, probably the most important research. The use of satellite imagery has proved very significant because once augmented with ground-based datasets, it may provide precise findings over extremely wide geographic ranges,

delivering data in a fast and economical manner. But most of the research is done on using one satellite image for a single period (Abrar et al., 2022). or using two satellite images for two short time periods (Parvin & Abudu, 2017; Rashid, et al., 2022). The feasibility of using two or more satellite imagery spanning twenty years or more to assess land cover and LST dynamics remains an open research area. Further, considering the current state of climate change, measuring the sensitivity of Dhaka residents to heat-related disease throughout such time periods might offer helpful information into the implications of both global warming and non-climate change components.

2.6.1Urban Heat Island Estimation Methods

UHI impact can be calculated by various methods which examine and analyse temperature variations between urban and rural areas. These methods apply for ground- based observations, satellite imagery and computer modelling to process the magnitude of UHI effects. Some commonly used methods are:

Ground based temperature monitoring is widely used techniques which collect air and surface temperature by employing temperature sensors. High resolution data from these sensors used to compare temperature variations in a straight way for rural and urban areas. Drones and other mobile devices can record temperature across the city or study areas.

Remote sensing is a common and standard method for the researcher to estimate UHI. Landsat and MODIS satellite sensors are fitted with thermal infrared sensor which can detect the thermal radiation released by earth surface (Hulley et al., 2020). Land surface temperature (LST) at different temporal and spatial resolutions are calculated using this satellite datasets. It allows for mapping and monitoring the UHI effect across the areas by comparing spatially between rural and urban regions. MODIS and Sentinel has their own LST products which provide the variation of UHI throughout the urban and rural areas in the world. They have different temporal and spatial resolutions.

Mobile sensing and citizen science includes collecting temperature data around cities by using mobile sensing platforms—such as mobile phones and personal weather stations—that are fitted with temperature sensors. This is a community-based monitoring initiatives and participatory sensing campaigns, which track temperature fluctuations locally and pinpoint UHI hotspots in their neighbourhoods (Diviacco, P et al., 2022).

Machine learning is the latest application method to estimate urban heat island intensity. It approaches data analysis methods and machine learning algorithms to analyse big amount of temperature data to identify regional trends and pattern of UHI (Hou, H., et al., 2023) which can reveal interactions between land use, temperature, urban features etc. These methods use for fusion of satellite imagery as required (Nguyen, T et al., 2020).

2.6.2 Land Use Land Cover Classification Methods

There are different LULC classification methods which can be employed to map and classify various LULC types in designated areas. These techniques categorise and identify different forms of land cover by using computer algorithms and software in conjunction with a variety of data sources such as aerial photographs, satellite imagery, and datasets from field surveys. Following are a few popular techniques for classifying LULCs.

Visual Interpretation: This method involves satellite imagery or aerial photos to identify and classify different land cover types. It requires to draw manual polygon and differentiate land cover based on colour, pattern, form, and texture (Sun, X., et al 2022). This process is time consuming.

Supervised classification: Select sample pixels or polygons illustrating landcover types and training a classification algorithm with them. Maximum likelihood supervised classification, Random Forest, Neural networks these methods are standard to classify land cover types. The method classifies land cover types using spectral signature which obtained from remote sensing data. After training, the algorithm categorises the image or the study area (Lu et al., 2007; Salah, M. 2017).

Unsupervised classification: This method does not use specific training samples. However, this method automatically creates groups/segments with comparable polygons or pixels, based on spectral equivalency and then analyse and produce different classifications for land cover (Kulkarni, G et al., 2020). This method is less labour oriented, but its reliability is not accurate.

Change detection methods: It is another way to identify changes of landcover over time. Image differencing, Image rationing and post classification methods are used to classify images (Chughtai et al, 2021) with this type of methods.

Machine learning: Deep learning and programming is the recent invention which can automatically learn the hierarchical features from satellite or other remotely sensed datasets and identify landcover accurately (Talukdar, S et al.,2020). Convolutional Neural Networks

(CNN) and other methods of deep learning and machine learning are commonly used to detect land use and landcover types.

2.7.2. Identified Knowledge Gap

According to the literature review, some areas have not focused or studied within the research area which require further research in future. The following research gaps are identified for the study area, Dhaka:

- Most of the research cited in the review concentrates on short-term assessment of UHI dynamics and changes of LULC. Longitudinal studies that examine these changes over various decades are rare. Longitudinal research would offer important new perspectives on the patterns of LULC changes over time, then intensification of UHI and the efficiency of mitigation techniques.
- Although the study addresses a different method for UHI estimation and LULC classification, more integrated or data fusion from several sources are required. Assembling data from remote sensing, computational models, and ground-based observation can enhance the precision and reliability of UHI estimation and provide a thorough comprehension of the basic mechanisms and drivers.
- The review underscores the significance of mitigating strategies like expanding green-infrastructures, there is little empirical data on how well these approaches work to reduce the effects of urban heat islands (UHIs), especially in the setting of rapidly developing cities like Dhaka. Subsequent investigations may concentrate on assessing the effects of certain measures on lowering temperatures, strengthening urban resilience, and improving air quality.
- Furthermore, there is a shortage of research evidence in Dhaka about the relationship between mitigation strategies like urban greening and transforming land use and cover (LULC), which presents a significant study opportunity. Although greening has shown promising results (Kruize et al., 2019) in decreasing urban heat island (UHI) impacts, research has shown that the specific characteristics of the metropolitan area such as its size, structure, neighboring land use, and climate may affect how successful these efforts are. Given the extremely rapid population growth in Dhaka, the city's urban environment can experience both rapid and subtle changes in terms of urban transformation. To fully understand how these factors interact with the city's urban growth, more academic research over both short and long time periods is needed.

3. CHAPTER THREE

DYNAMIC LANDUSE AND LAND COVER CHANGES IN DHAKA FROM 2011 TO 2022: ALARMING TRENDS FOR GREEN SPACES

3.1 Introduction

Urban sprawl across the globe has resulted in an era of significant transformation influencing the way we work, live, and interact with the environment surrounding us. As the population becomes increasingly urbanized worldwide, it is important to understand the interrelationship between population dynamics and urban expansion. World population has already reached to 8 billion on 15 November 2022 (UNFPA 2023; Jain et al., 2023). At the world's largest biodiversity conference, municipal leaders from 15 cities around the world urged to provide extra financial support to assist community for conducting substantial greenspace and ecological restoration actions project held in Montreal on 10 December 2022 (UNEP,2022); Dhaka was one of those 15 cities. According to the Global Livability Index 2023 published by the Economic Intelligence Unit (EIU) of Economist, Dhaka has been identified as one of the least livable cities in the world and positioned seventh. Unplanned urbanization and increasing congestion of transport are causing various challenges in the city. Environmental pollution rates are significantly rising in Dhaka. Waterlogging, air pollution, and deforestation are becoming more prevalent issues. Additionally, a range of socio-economic problems are also on the rise in this region. The study has employed both Census datasets and spatial imagery to assess the correlation between urban expansion and population dynamics. Population and housing census of Bangladesh for 2011(BBS) and 2022 (BBS) has been utilized to determine the demographic changes over the period. This paper investigates the evolution of the land use patterns in Dhaka considering the potential role of green spaces enhancing the city's livability.

3.2 Background

Incorporating urban green spaces, urban forest and urban infrastructure into an urban setting is an important step to achieve sustainable development goals (SDG 11.7.1) (UN,2017). An investigation of the temporal changes in land use and land cover (LULC) across a given area is critical for effective resource management, promoting sustainable development, and facilitating extensive procedure of regional planning and decision making. Urban recreational

activities, urban farming, gardening is some of bioeconomic activities (Kang et al., 2021). These initiatives not only support to the ecosystem but also enhance economic development.

Green spaces serve as a city's lungs (Jones et al., 2018; Jim et al., 2006), which involve in air filtration, control temperature, and managing stormwater. UNEP recommends, there should be 25% of greenspace in a city (UNEP,2010; Cobbinah, 2021). These green spaces influence in shaping the economic environmental, social elements are shaped in a city (Aronson et al., 2017). Green space is one of the major components which driving better human settlement, and well-being (Gaston, 2010; Wang, J et al 2018). It could give fewer benefits in compared to other market products, but they are able to contribute to environmental sustainability, aesthetic development, recreational activities, social and health benefits. By mitigating pollution and enhancing overall environmental quality, green spaces contribute to creating healthier (Almeida et al., 2022) and more sustainable urban habitats (MacKaye, 1990). Greenspace is an essential and common tool to measure the agricultural and other vegetation conditions. Changes in temporal and spatial trends of greenspaces have significant impacts on cities architectural structure, development, and activities (Liu et al., 2020). Anthropogenic activities and climate change are two major drivers of land use and land cover (LULC) changing (Assede, E. S et al, 2023; Qu, S. et al., 2020). LULC change act as an important role (Zaldo et al., 2021) to determine the extent of human contributions for socio- economic conditions and biodiversity (Aronson et al., 2017).

According to (Allan et al., 2022), LULC is related to human activities which include deforestation and urbanization. Land cover is the type of land which indicates physical characteristics such as forests, built-up infrastructures, grasslands, or bodies of water (Yadeta et al.,2019). Turner, B.L et al, (1994) indicated about human and land use linkage and a recent study focused that there are various types of human activities which considered for land use, such as timber extraction, farming, preserve area, construction, town expansion, mining, residential buildings (Yadeta et al.,2022) which have impact on environment from local, regional, and global level (Huang et al.,2022). On the other side, land cover defined as agriculture, swampy land, woodland, and other feature types (Arafaine et al., 2019). Climate change, air composition, ecosystem, water and sediment, condition of soil all are represented (Turner, B.L et al, 1994, 2009). Anthropogenic influence on vegetation cover is well studied and found that woodland devastation, urban development, restoration of grassland contributes to the loss of biodiversity (Huang et al., 2022).

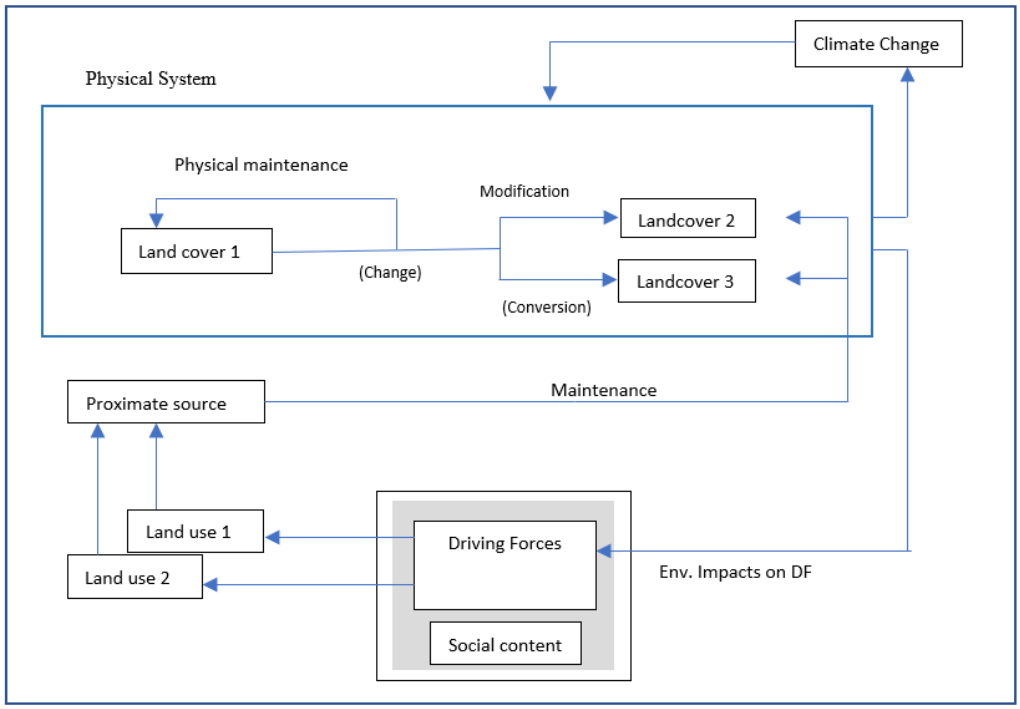

Figure 7: Linkage between human driving forces, land use land cover (Turner, B.L et al,1994)

Figure 7 illustrated that LULC is a continuous and complex process impacted by various factors. Physical, proximate sources and social factors play a vital role (Liu et al., 2020) in changing of LULC over time. Climate change can directly modify or preserve land cover by various actions like erosion/weathering, vegetation growth and deposition. For instance, melting of glacier (Romshoo et al.,2022) is a climate change that has an impact on available water and vegetation patterns. Normally land cover changes are mostly affected by human activities (Feng et al., 2022) and proximate sources such as urbanization, deforestation, and practices in agriculture. Deforestation could be a result of agricultural methods and lead to changes in water availability and soil quality (Peplau, T, et al, 2023). Socio economic factors, such as government policy, economic growth, increased in population can also influence land use and landcover changes. These could increase the demand for resources and accessibility of technology. Another essential aspect of this concept is interaction between human driving forces and LULC are highly context specific and varies across different spatial and temporal scales. What exactly drives the land use change may not be the same that works in the other region. Sometimes the impacts of land use change can appear over in immediate or long-term periods.

3.3 Population Dynamics

In accordance with UN projections, countries with low and middle income like Bangladesh, will be responsible for more than 90% of the predicted urban population size. Furthermore, Dhaka, Bangladesh's main city, is anticipated to become the world's fourth most populated metropolis by 2030, trailing only Delhi, Shanghai and Tokyo (UN, 2022).Seraj et al, (2013) reported, Dhaka has emerged as one of the rapidly developing megacities, with forecasts indicating that the city is going to become one of the world's most populous capital cities by 2025, joining the ranks of other prominent cities worldwide such as Mexico City, Tokyo, Beijing, Shanghai, and New York City. Bangladesh's urban population grew by 31.22% in 2011 and reached at 39.72% increasing in 2022. This corresponds to an overall increase of 8.51% during a 12-year period (BBS). This increase in urban residents necessitates a bigger allocation of land resources for urban residential needs. Human activity's extensive extension of developed areas is referred to as urban growth. (McDonald et al, 2020 ; Qin et al., 2022). The financial condition of Dhaka's neighboring regions is mostly dependent on agricultural, but Dhaka's metropolitan area is primarily concentrated on industry (Roy, S. et al.,2021).

It is worth noting that Dhaka receives a considerable inflow of immigrants each year, with roughly 2000 people moving to the city in pursuit of work and for a variety of other reasons (DNCC, 2023). Dhaka's urban region has several possibilities for employment in areas including production, textiles, apparel, pharmaceuticals, construction, and services. Such economic attraction, along with the desire for better work opportunities and greater quality of life, draws a significant amount of people from the neighboring rural areas and other parts of the nation. (BBS,2011). Built areas are the most dominant land cover classes in Dhaka, according to an analysis of Land use and land cover (LULC) maps. The maps visually depicted the variations in the number and size of different thanas between two census periods. Thana is the name of administrative areas in Bangladesh that serve as a district sub-unit and the second lower tier of regional administration. Thanas are larger than wards and have their own administrative boundaries. In 2011, there were 41 thanas in Dhaka, however by 2022, the number grew to 53 but the geographical area remained the same. The makeup of the thanas, on the other hand, has changed. Some thanas were dissolved, and new thanas were added, resulting in a shift in the overall feature classes.

Over the years, there has been a notable transformation in the landcover patterns. The total area of built-up land cover in Dhaka expanded significantly from 8992.1 ha to 16784 ha from 2011 to 2022 (CEGIS , Figure 16) which denotes the demand of more houses for the increased

population. In 2011, these increases are predominantly concentrated in the middle east part of the city and the highest population was 596,835 in Pallabi thana. Mirpur and Khilgaon consisted of 113750 and 113273 respectively. The lowest populations were in Biman Bandar thana (10626) which changed in 2022 with its boundary and population also decreased to 7424. There is a visible change in population in Turag thana from 2011 to 2022 which was reached by 266064 from 157316. Turag's major source of earnings was agriculture (BBS,2001); nevertheless, the neighborhood has begun to shift because of the building of housing complexes and its closeness to the Metro rail project's (Raj et al., 2022) starting platform. This infrastructural development has drawn individuals to the region, who have relocated to take jobs in such industries (Hossain, 2017).

Pallabi, Mirpur, and Jatrabari are still within the comparable range. Pallabi and Mirpur are two thana's with a high concentration of middle-class residents. The cheaper cost of living in these places (Raj et al., 2022 ; Chowdhury et al., 2023) contributes significantly to their attraction to this demographic. Furthermore, the presence of clothing industries in these locations has aided their rise. Mohammadpur thana has had a substantial growth in population since 2011, when it was ranked lower in terms of population density. On the other hand, Badda thana is now divided into two thanas, and the population of the former Badda thana has declined. Maps showed (Fig 8) that the population transferred towards eastern to western locations over the research period. Darus-Salam, Hazaribagh, and Uttar Khan are all displaying a rising pattern. The population of Kamrangirchar thana in Dhaka's southwest has grown by a factor of four since the previous census in 2011. Its population was 93,601 in 2011, but it is expected to expand to 372302 by 2022. This is an astounding 300% increase. Dhaka's growing population has resulted in a massive spike in the need for housing. This has put a strain on the city's infrastructure since there is inadequate space to handle the rising population. Because of this, many individuals have been forced to live in slums or informal settlements, which are frequently congested and lack basic facilities.

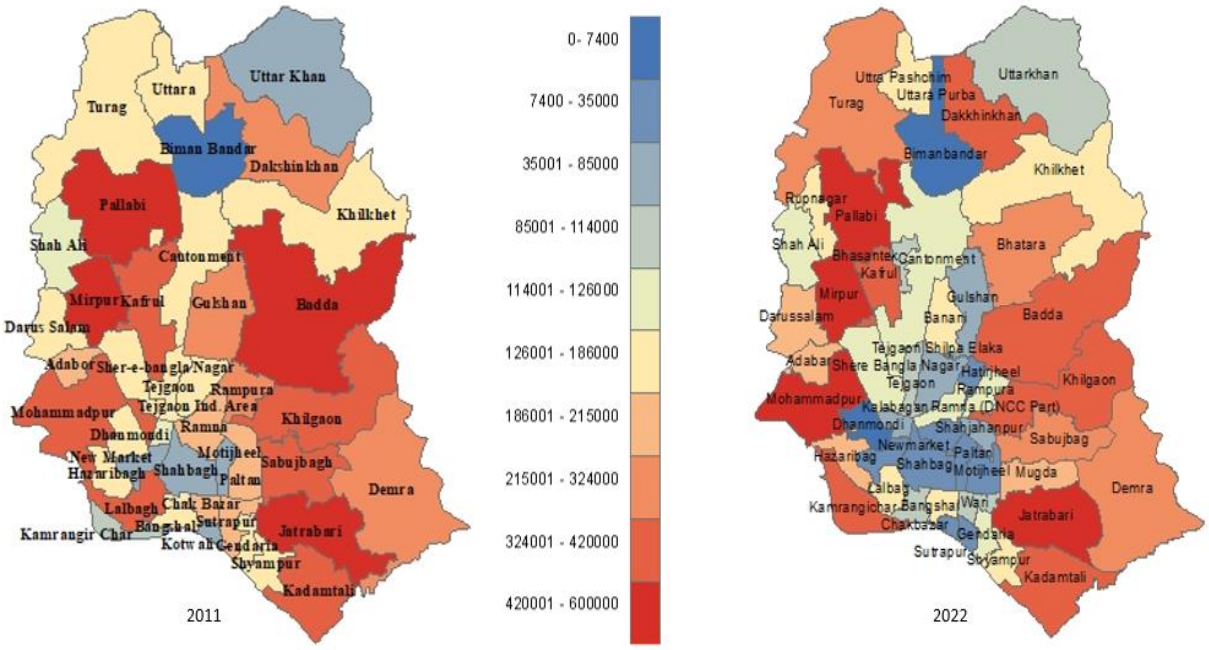

Figure 8: Population changes from 2011(left) to 2022(right) . The figure also showing the transformation of new thana boundary of Dhaka (Source: BBS, 2011 and 2022)

3.4 Methodology

The primary objective of this study is to investigate the transformation in land use patterns in Dhaka and their association with population changes in the city. Based on two recent population and housing census of Bangladesh for 2011 to 2022, there has been a significant and noteworthy shift in land use within the city. A national census is typically conducted every 10-year period in Bangladesh. It is a complete and official count of a country's population that offers vital demographic, sociological, and statistical information for a variety of reasons such as government planning, resource allocation, and policymaking. Several measures were taken to appreciate the magnitude of this transition. Hard classifiers like supervised Maximum Likelihood Classification (MLC) have been applied for the LULC detection using four feature classes. However, NDVI, NDBI, MNDWI used to measure such other vegetation, built areas and water bodies of the study area. Overall transformation and a thana scale green index of Dhaka city has been calculated for the study period.

3.4.1 Datasets

Table 1: Datasets

Dataset	Scale	Date/year	Source	Used for
Landsat 5 TM, Level 2 Path/Row:137/44	30 m	2011	USGS Earth Explorer	Land use land cover map for 2011 and NDVI, NDBI, MNDWI
Landsat 9 OLI/TIRS, Level 2 Path/Row:137/44	30m	2022	USGS Earth Explorer	NDVI, NDBI, MNDWI
Sentinel 2A	10 m	2022	ESA Copernicus Open Access Hub	Generate land use land cover map for 2022.
Boundary Shapefile datasets of Dhaka	1:100,000	2011 and 2022	Centre for Environmental and Geographic Information System (CEGIS), LGED	Delineation of study area to maintain spatial consistency

3.4.2 Data pre-processing, processing, and analysis

3.4.2.1 Landcover classification to produce landcover map for 2011 and 2022 using hard classifier.

This research employed an extensive range of satellite imagery to produce LULC maps for the study period of both 2011 and 2022. For the generation of maps, a classification method has been utilised which was proposed by Ahmed et., al (2013). Table 2 described the land cover classes that used in the classification process. This classification is based on some previous research (Parvin et al., 2017 ; Ullah et al., 2019) and local knowledge of the research area. To digitise training pixels for each feature class, ArcMap 10.7 software tools have been utilised

and employed Maximum likelihood classification (MLC) method for land use land cover (LULC) map production.

Very high resolution (VHR) imagery from Google Earth and archives has been used for digitised the vector polygons for each of the four feature classes of LULC (Table 2). Area of interest (AOI) formed by the digitisation of vector polygons and exported to the satellite imagery (Landsat 5TM for year 2011 and Sentinel-2 for year 2022) to acquire the spectral signatures for using the training of LULC classification.

By using high VHR imagery from Google Earth, the study was able to evade the difficulties of drawing AOIs on a Landsat 5 TM 30m spatial resolution imagery or the Sentnel-2 10m spatial resolution. Figure 9 shows the distribution of AOIs used in the collection of training spectra.

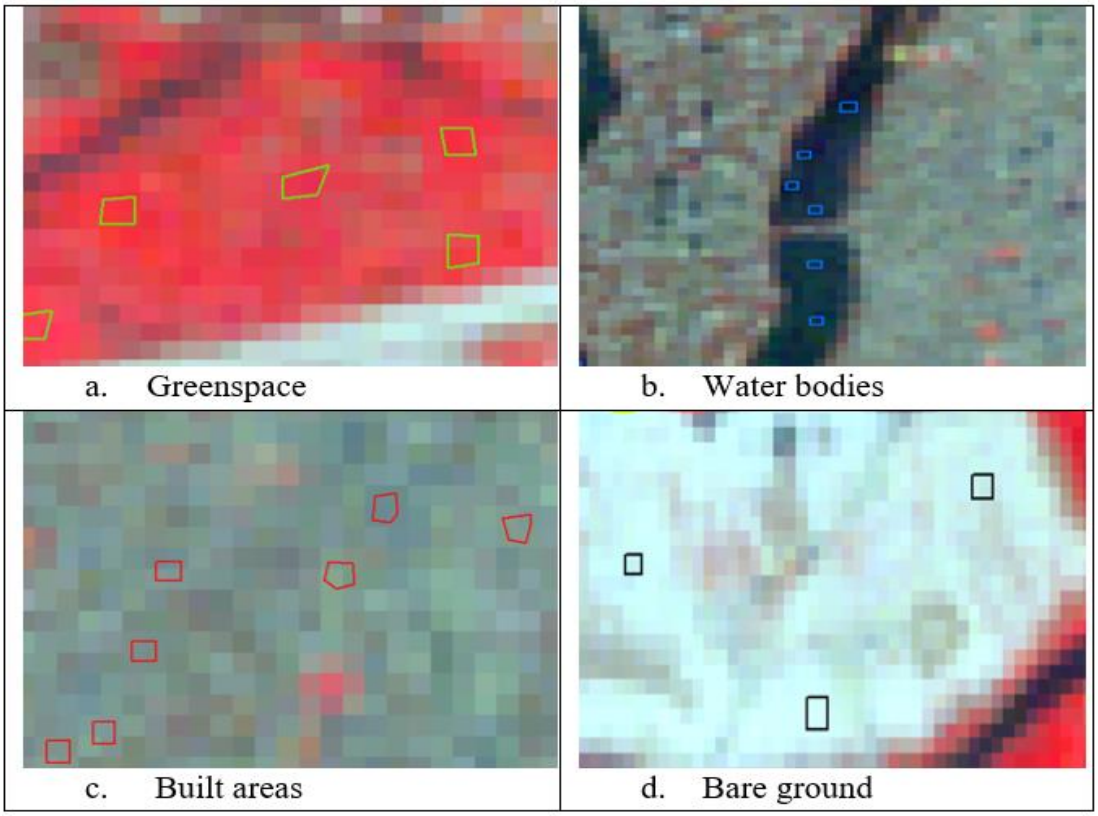

Figure 9: AOI collections for each feature class.

To train the MLC algorithm, 250 pixels were used for each class of the training data. Areas such as water, which has limited extent in the study area provided fewer training pixels as compared to other dominant LULC classes such as built area or green spaces. The 2011 and 2022 images were trained and classified separately because they have different spatial

resolutions. Training was done recursively by increasing or decreasing the number of input training pixels from the many AOI polygons. This allowed for refinement as the output of each training set was evaluated using statistical outputs such as examining the histogram.

Subsequently, each of the 2011 and 2022 images were ran a supervised Maximum Likelihood Classification (MLC) method using the trained algorithm. MLC is one of the supervised classification methods which according to Lu and Weng, (2007) produces superior results due to its strength in minimising misclassification error. It depends on the assumption that statistical data for each feature class from each band have been distributed uniformly and determines the probability of a particular pixel belong to a particular class.

The resulting classified LULC map for 2011 was at a 30m spatial resolution while for 2022, the results followed Sentinel's 10m spatial resolution. To ensure spatial resolution uniformity for analysis and comparison purposes, the 2011 LULC map was resampled using Nearest neighbour tool within ArcGIS, from 30m to 10m to match the spatial resolution of Sentinel-2 images used in 2022 LULC map production. Nearest neighbour tool is the most accurate way to converting or resampling one resolution to another without affecting its original resolution (Wang et al., 2020). This approach of up-scaling is supported by (Forkuor et al., 2017).

To determine the changes that occurred from each land cover class from 2011 to 2022, the study utilised the ArcGIS pro built in change detection tools (Basheer, S, 2022). The toolset provide flexibility is determined in the LULC changes such as provisioning continuous change detection or specific calculations of absolute, relative, categorical, or spectral difference in the two LULCs. The obtained results are in Table 12 and Figure 11.

Table 2: Classes used for land cover classification, Source: Ullah (2019) & Ahmed (2013)

Classes	Description
Bare ground	Fallow land, earth, and sand land in- fillings, construction sites, developed land, excavation sites, open space, bare soils, and the remaining land cover types.
Built areas	All infrastructure- residential, commercial, mixed use and industrial areas, villages, settlements, road network, pavements, and man-made structures.
Green spaces	Trees, natural vegetation, mixed forest, gardens, parks and playgrounds, grassland, vegetated lands, agricultural lands, and crop fields.
Water bodies	River, Permanent open water, lakes, pond, canals, permanently/seasonal wetlands, low-lying areas, marshy land, and swamps

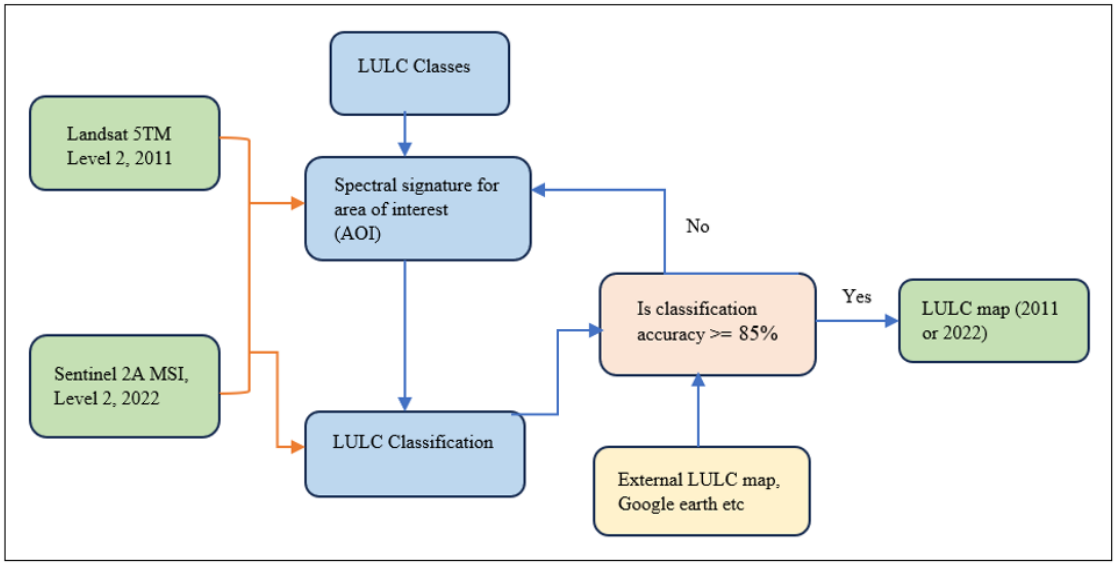

Figure 10: LULC map creation steps.

Figure 10 summarises the steps followed to generate the LULC map of the study area for 2011 and 2022 respectively. Landsat 5 TM and Sentinel 2A imagery were obtained at surface reflectance level, already atmospherically and radiometrically corrected for any cloud pixels and geometry errors. Sentinel -2 consists with 10-meter spatial resolution (Kaplan et al., 2017) which is for classification useful (Nguyen, H et al., 2020) of images for land cover and land use. Sentinel-2 image was used for 2022 LULC classification and Landsat 5TM for 2011. Sentinel -2 consists of 12 spectral bands (Tavares et al., 2019) and bands 2,3,4, and 8 have been used for this classification. Landsat 5 TM has 7 spectral bands and bands 1,2,3 and 4 were stacked for composite and to then classify for LULC mapping. Landsat level- 2 datasets are atmospherically corrected and produce more accuracy than level-1 datasets. Landsat-9 OLI/ TIR and Landsat 5 TM are therefore used in this analysis to calculate different spatial index such as NDVI, NDBI and MNDWI.

Table 3: Landsat 5 and 9 bands spectral band, Source: USGS.

Landsat Spectral bands	Wavelength(μm)	Resolution (m)	Landsat 5 TM	Landsat 9 OLI/TIR
Coastal/aerosol	0.43 - 0.45	30m	X	Band 1
Band 2-Blue	0.45 - 0.51	30m	Band 1	Band 2
Band 3-Green	0.53 - 0.59	30m	Band 2	Band 3
Band 4-Red	0.64 - 0.67	30m	Band 3	Band 4
Band 5-Near infrared	0.85 - 0.88	30m	Band 4	Band 5
Band 6- Shortwave infrared (1)	1.57 - 1.65	30m	Band 5	Band 6
Band 7-Shortwave infrared (2)	2.11 - 2.29	30m	Band 7	Band 7
Band 8-Panchromatic	0.5 - 0.68	15m	X	Band 8
Band 9-Cirrus	1.36 - 1.38	30m	X	Band 9
Band 10-Thermal wave infrared (1)	10.6 - 11.19	30m		Band 10
Band 11-Thermal wave infrared (2)	11.5 - 12.51	30m	Band 6	Band 11

Table 4: Sentinel spectral bands, source: USGS.

Sentinel-2 Spectral Bands	Central wavelength(μm)	Resolution (m)
Band 1 -Coastal aerosol	0.443	60
Band 2- Blue	0.490	10
Band 3- Green	0.560	10
Band 4-Red	0.665	10
Band 5-Vegetation Red Edge	0.705	20
Band 6- Vegetation Red Edge	0.740	20
Band 7- Vegetation Red Edge	0.783	20
Band 8-NIR	0.842	10
Band 8A-Vegetation Red Edge	0.865	20
Band 9- Water vapour	0.945	60
Band 10-SWIR cirus	1.375	60
Band 11-SWIR	1.610	20
Band 12-SWIR	2.190	20

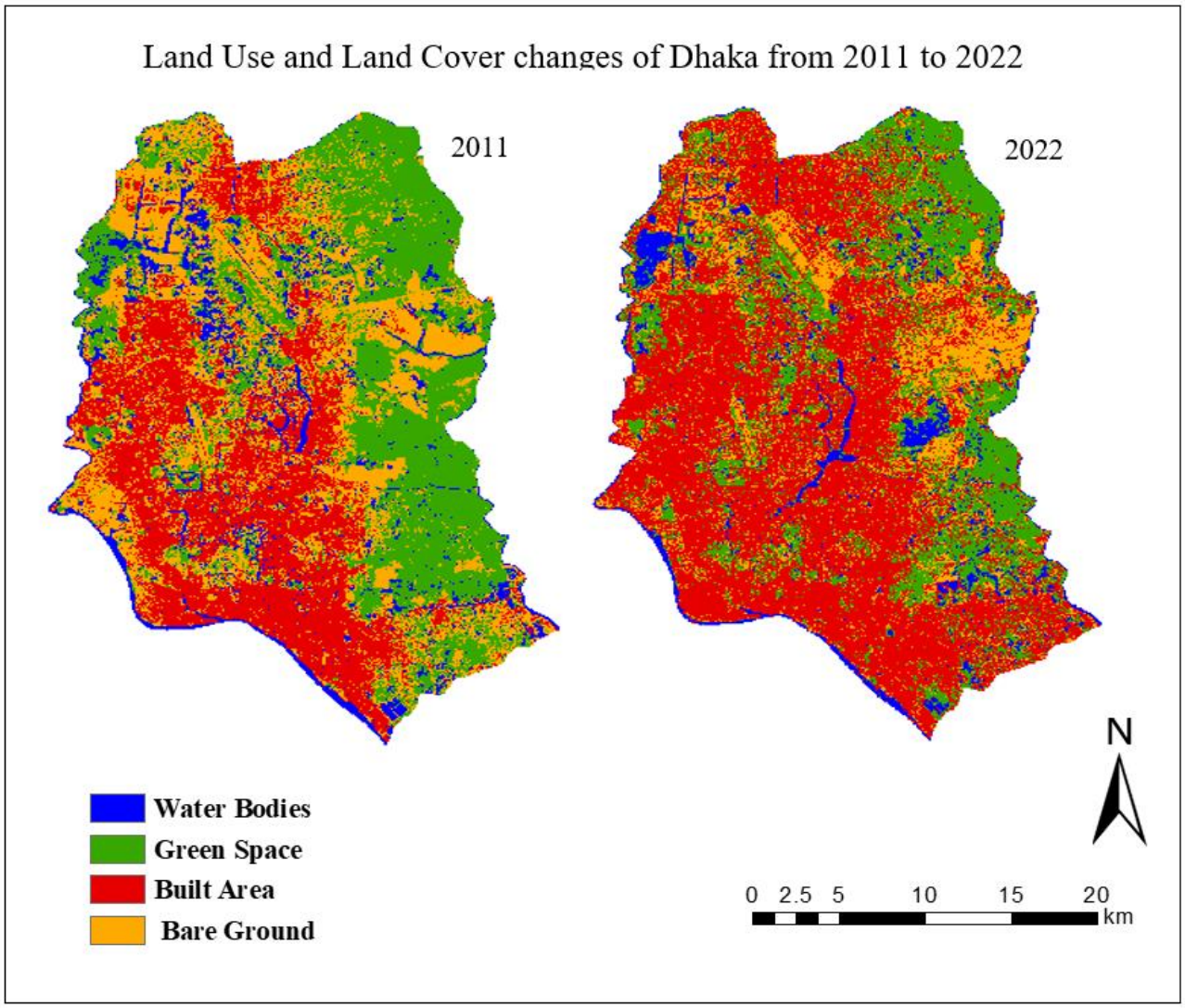

Figure 11: Dhaka's land use land cover (LULC) map for the years 2011 and 2022.

3.4.2.2 Land cover classification using Normalized difference vegetation Index (NDVI)

The Normalized Difference Vegetation Index (NDVI) is an important parameter for quantifying the level of greenness in vegetation and can provide insights into vegetation density and changes in plant health. It is calculated using spectral reflectance measurements in ArcGIS pro platform in the red and near infrared bands. The NDVI values ranges from -1 to +1, with lower values typically indicating light or dark soils (usually between 0 and 0.2), while higher values indicate denser vegetation. NIR reflected by plants leaves when chlorophyll absorbs. The calculation of NDVI can be performed using the following formula (Hussain, S. et al., 2020; Alademoni, A. et al.,2022)

For Landsat 5, NDVI = (Band 4 (NIR)- Band 3 (IR))/ (Band 4 (NIR) +Band 3 (IR)) (2011)
For Landsat 9, NDVI = (Band 5 (NIR)- Band 4) (IR)/ (Band 5 (NIR)+ Band 4 (IR)) (2022)

One of the challenges for indices-based classification such as NDVI-land cover mapping, is the identification of what NDVI range corresponds to different land cover classes. NDVI varies throughout periods (Idrees et al., 2022) and location to location (Jin. H et al., 2021). For Dhaka mega city, the NDVI categorization or class ranges for each of the four land cover classes (see Table 5) considered in this study in 2011 and 2022, is not available in the literature. Therefore, this study tested the possibility of a two-stage classification to identify the acceptable NDVI class ranges for each of the four land cover classes. Firstly, Land cover classification was performed for 2011 and 2022 using a supervised Maximum likelihood classification (MLC) as detailed in Section 5.2.1.

Secondly, the NDVI image (fig: 12) and the MLC classified image (fig: 11) were compared to identify acceptable NDVI class ranges for each of the four land cover classes. This was done using the Reclassify and Raster calculator tools within the ArcGIS. Reclassify operations were used to presence and absence of each of the four classes. The reclassify output were then subjected to a multiplication operation within Raster Calculator to obtained NDVI class range for the specific LULC class considered. The importance of utilizing LULC from the vegetation indices (NDVI) is that it avoids the over generalisation problem which is very common with hard classifiers such as MLC. NDVI ranges allows for detailed examination of a land cover (Szabo et al., 2016). For instance, the green space LULC class considered by this study can be further examined within smaller administrative boundaries of thana (parish) level, as considered in this study. To the best of our knowledge, thana scale NDVI of Dhaka has not been studied. Therefore, the study conducted post classification of greenspaces using ArcGIS-Pro, to observe the status of green areas and vegetation patterns throughout every thanas in Dhaka (Figure 15). Three sample thana have been examined because they exhibit a changeable pattern as the population grows.

Table 5: NDVI range for Dhaka , (2011 and 2022. Fig. 12)

Feature class	NDVI ranges (2011)	NDVI ranges (2022)
Water bodies	-0.075 - 0.035	-0.053 - 0.04
Built area	0.036 - 0.076	0.041 - 0.1
Bare ground	0.077 - 0.143	0.101 - 0.147
Green space	0.144 - 0.449	0.148 - 0.404

Table 6: Classified vegetation value in NDVI index (2011, 2022) (Figure 12a, b)

Vegetation types	NDVI ranges (2011)	NDVI ranges (2022)
No vegetation	-0.0753 -0.143	-0.053 -0.147
Low vegetation	0.144 - 0.165	0.148 -0.165
Moderate vegetation	0.166 - 0.224	0.166 -0.224
Dense vegetation	0.225 - 0.449	0.225 - 0.404

NDVI classification at thana scale for 2011 and 2022

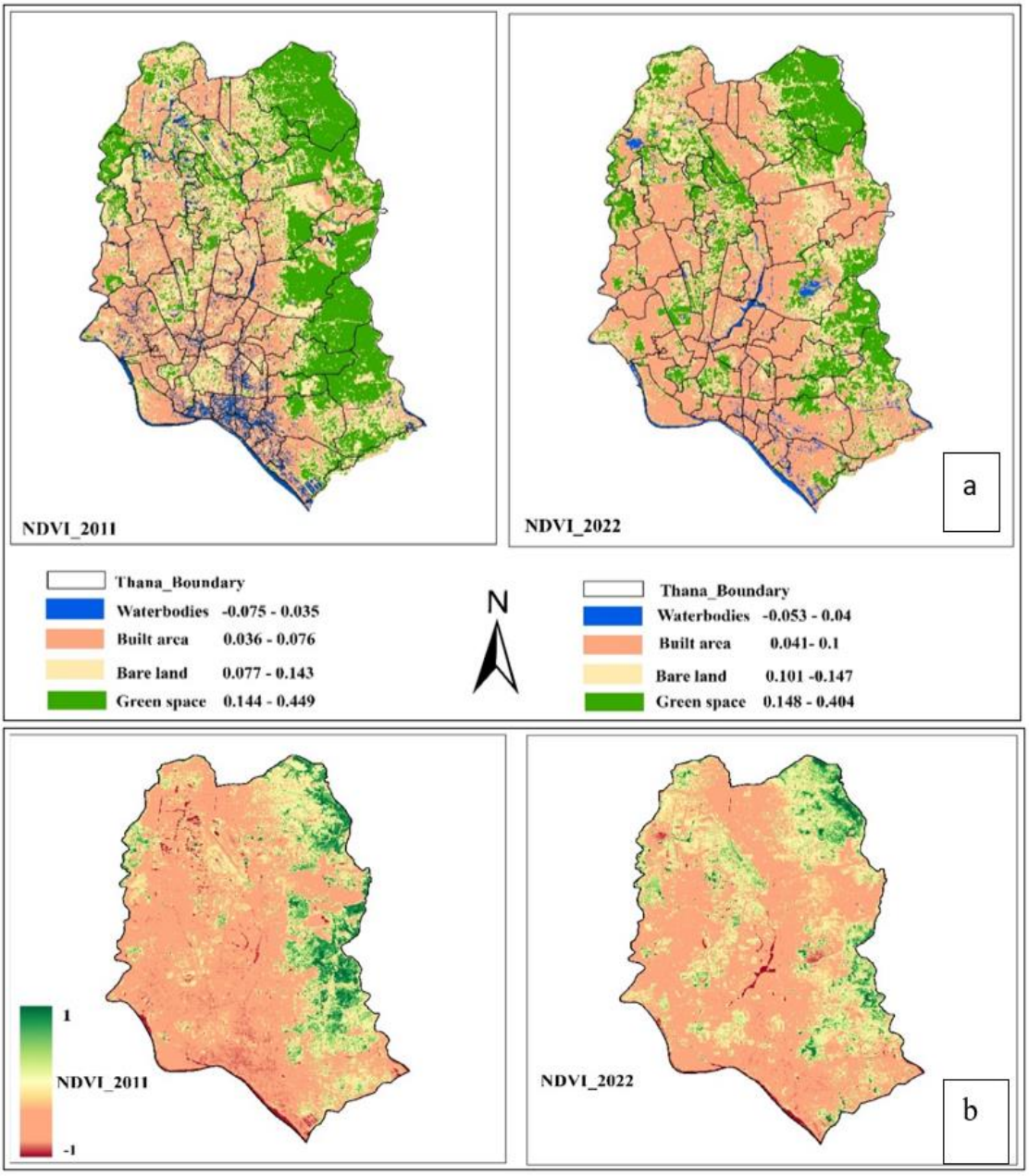

Figure 12: a. NDVI value for Dhaka, for 2011 and 2022. b. Compare with same legend.

3.4.2.3 Normalized different built-up index.

Built-up areas and bare soil have a higher reflectance in the Short-Wave Infrared (SWIR) region compared to the Near- Infrared (NIR) region. Water bodies, on the other hand, do not exhibit significance reflectance in the infrared spectrum. The NDBI values ranges from -1 to +1. Negative values indicate water bodies, while higher positive values indicate build-up areas. Vegetation typically has low NDBI values. (Hussain, S et al, 2020; Alademomi, A et al, 2022).

For Landsat 5, NDBI = (Band 5 (SWIR)- Band 4 (NIR))/ (Band 5(SWIR) + Band 4(NIR))
And Landsat 9, NDBI = (Band 6(SWIR)- Band 5(NIR))/ (Band 6(SWIR) + Band 5(NIR)).

NDBI classification for thana scale for 2011 and2022

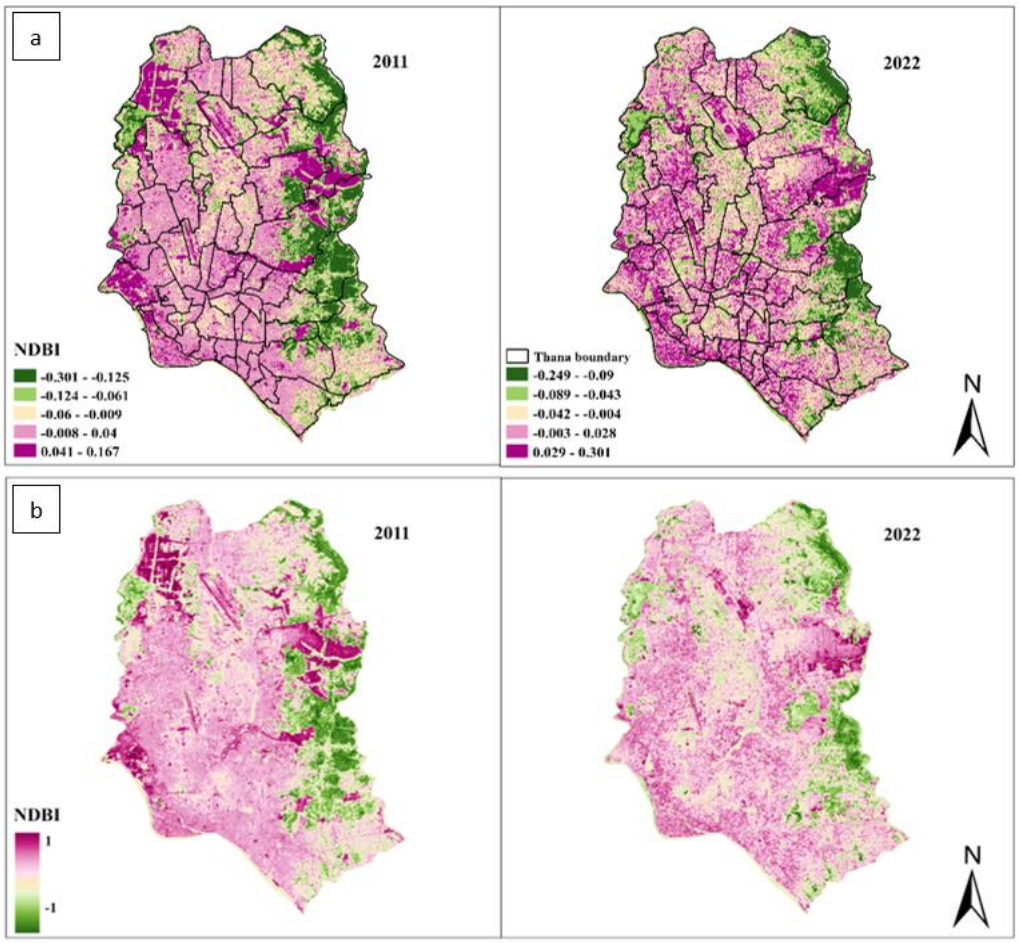

Figure 13: a . NDBI value for 2011 and 2022 b, comparison of two years using same legend.

3.4.2.4 Modified normalized different water index.

MNDWI is a remote sensing satellite-based indicator which used to analyse water and urban area differentiation. Its values range from -1 to +1, where negative and low values suggest land/urban area and high values are for high volume of water or depth of water. This spatial index utilizes the Green and shortwave infrared (SWIR)bands of satellite imagery. Clear water has a tend to the highest reflectance in blue of the visible spectrum which give a blue appearance. Formula used to calculate MNDWI (Laonamsai, 2023) is as follows,

MNDWI = (GREEN - SWIR)/ (GREEN + SWIR)

For Landsat 5-7 imagery, MNDWI = (Band 2(GREEN) -Band 5(NIR))/ (Band 2(GREEN) + Band 5(NIR))

For Landsat 8-9, MNDWI = (Band 3(GREEN) -Band 6(SWIR))/ (Band 3+ Band 6(SWIR))

MNDWI classification for thana scale for 2011 and2022

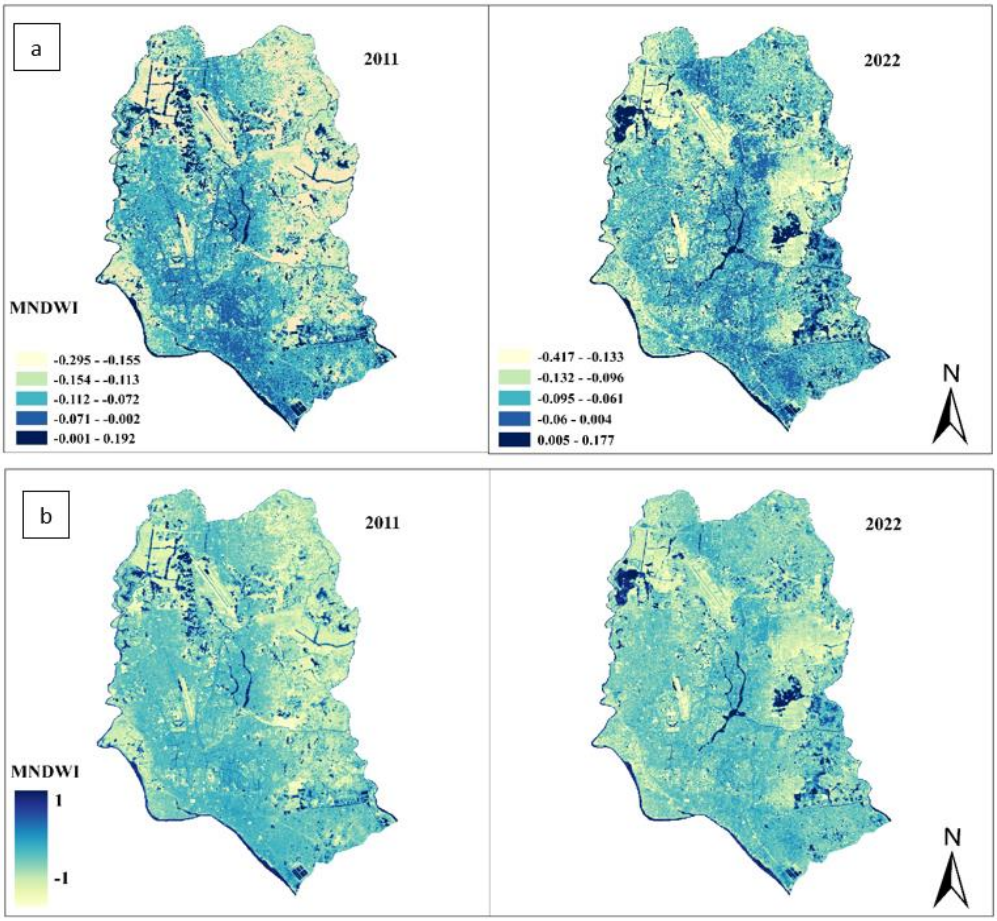

Figure 14: a, MNDWI values in 2011 and 2022. b, comparison of two years using same legend.

The normalised difference vegetation index (NDVI) can be useful in identifying and assessing the existence of living vegetation that is green. It may be used to determine the density of green on a piece of land by utilising satellite data to explain the difference between visible and near-infrared reflectance of plant cover. Tepanosyan, G. et al., 2021 further said that the NDVI has been widely employed in numerous environmental monitoring systems including surface urban heat and the yearly change in plant cover using satellite-derived imagery. Considering surface urban heat is created by the transformation of vegetation to other constructed buildings, monitoring surface temperatures and vegetation change from urban regions have been critical topics in this work.

Table 7: NDVI, NDBI, MNDWI values of year 2011 and 2022.

NDVI	Low	High	Mean	Standard Deviation
2011	-0.076307	0.448818	0.1862555	0.371319448
2022	-0.0540436	0.403808	0.1748822	0.323749971
Change (Δ)	-0.0222634	-0.04501	-0.0113733	
	2%	-5%	-1%	
NDBI	Low	High	Mean	Standard Deviation
2011	-0.301925	0.167183	-0.067371	0.331709448
2022	-0.250214	0.300667	0.0252265	0.389531691
Change (Δ)	0.051711	0.133484	0.0925975	
	5%	13%	9%	
MNDWI	Low	High	Mean	Standard Deviation
2011	-0.296235	0.191568	-0.0523335	0.344928809
2022	-0.417863	0.176744	-0.1205595	0.420450642
Change (Δ)	-0.121628	-0.014824	-0.068226	
	-12%	-1%	-7%	

The calculations of NDVI, NDBI and MNDWI for a specific pixel consistency yield values ranging from -1 to +1 (Topaloğlu et al, 2022). Analysed the data, it is visible that there have been minimal changes in the water bodies but significant decrease in green spaces and notable rise in built areas. Transformations that detected in land use patterns for the study period relate to significant development projects and in both the north-western (Diyabari) and north-eastern (Bashundhara residential area) region of Dhaka. These areas witnessed the establishment of housing societies, construction of multiple flyovers, 7.8 miles long Purbachal express highway and the construction of the Metrorail project. These infrastructure developments have caused a substantial effect in shaping the land use changes, including the increase of built-up areas and consequence decrease in vegetation. Table 7 illustrated the changes of three spatial indices over the study periods. In 2011, the low NDVI value was -0.076307 and the high value was 0.448818, which has since changed to -0.0540436 at low and 0.403808 at high in 2022. From 2011 to 2022, the high value declined by -5%, while the low value also decreased by 2%. Dhaka city's dense vegetation area has covered only in north-east region (Uttarkhan) of the city in 2022, however there were dense vegetation cover in the eastern part of Khilgaon, Badda, Dakhinkhan, Uttarkhan, Khilkhet in 2011.

Value of NDBI ranged from -0.301925 to 0.167183 in 2011, while in 2022 it ranged from -0.250214 to 0.300667. The investigation revealed that NDBI grew by 13% between 2011 and 2022, indicating an increase in building/built areas. MNDWI also decreased in both high and

low levels between 2011 and 2022. It has low values of -0.296235 and 0.191568 in 2011 and high values of -0.417863 and 0.176744 in 2022. Lower numbers, as determined by MNDWI, indicate built-up or land areas. Lower levels of MNDWI raised by -0.121628 between the year 2011 to 2022, reflecting a -12% decline in water bodies/blue areas.

3.4.2.4 Quantification of Green Spaces at Thana scale

2011	2022
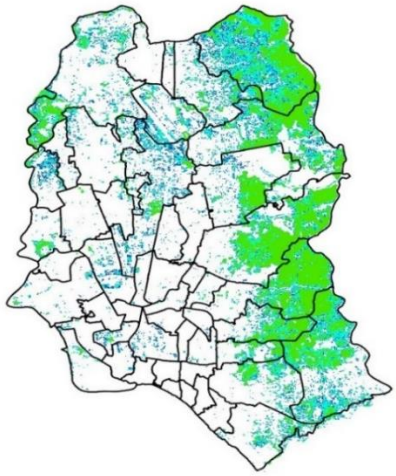	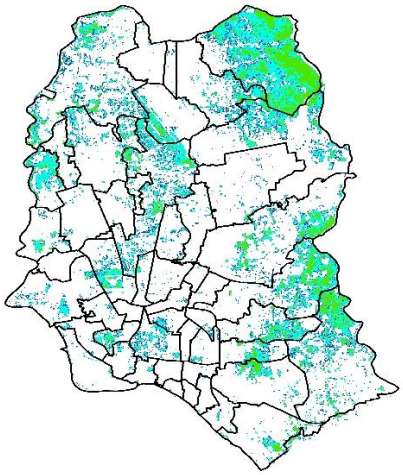
a. Pattern and distribution of vegetation at thana scale	b. Pattern and distribution of vegetation at thana scale
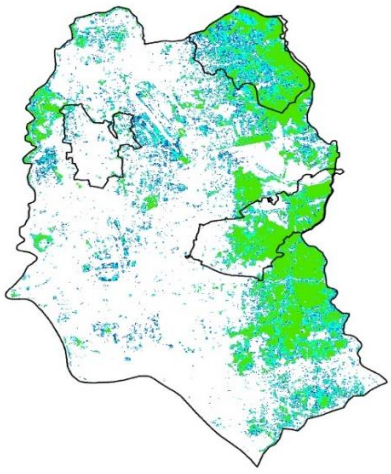	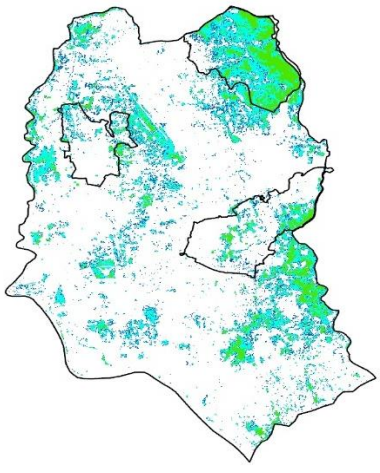
c. Location of 3 sample thana	d. Location of 3 sample thana

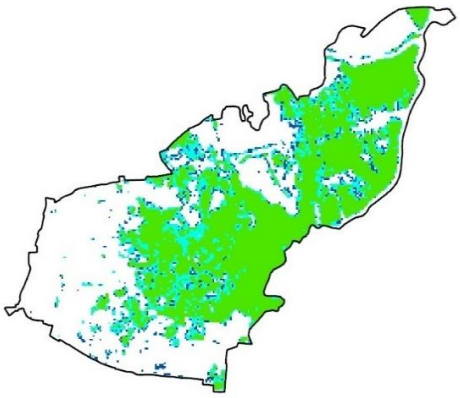

e. Badda thana

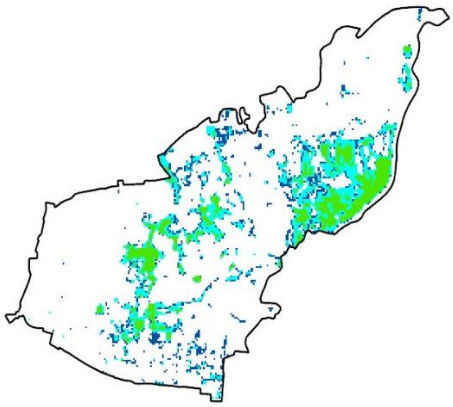

f. Badda thana

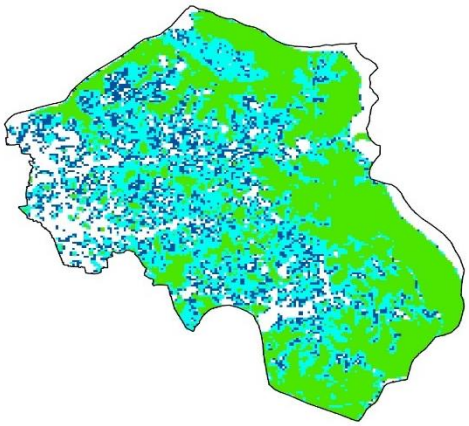

g. Uttarkhan thana

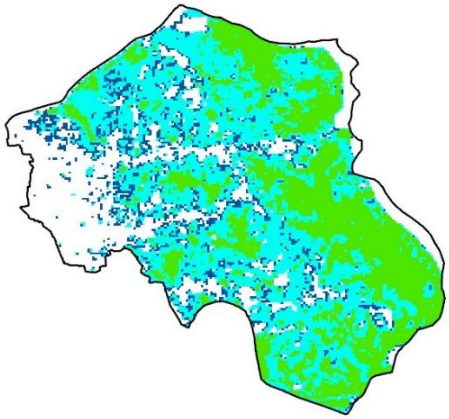

h. Uttarkhan thana

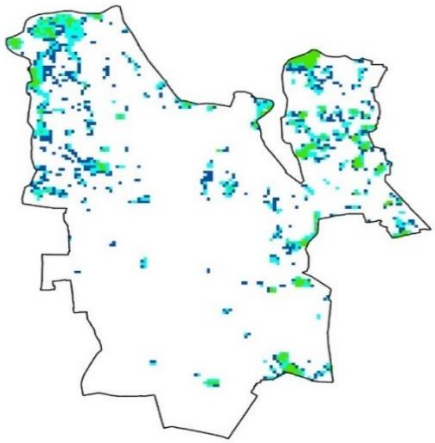

i. Pallabi thana

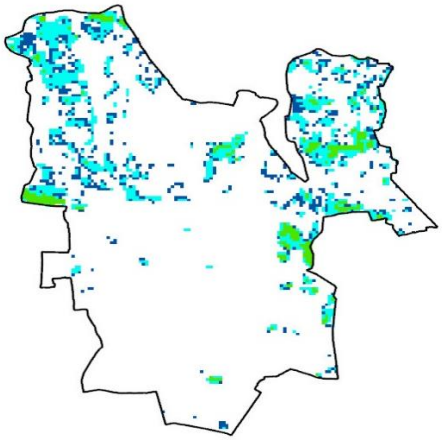

j. Pallabi thana

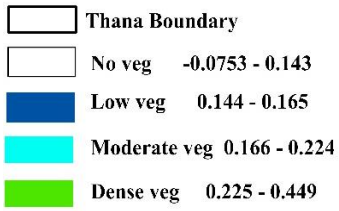

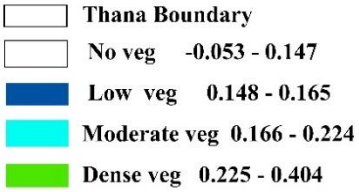

a, b: Vegetation pattern and distribution at thana scale for 2011 and 2022 in Dhaka

c, d: Sample thana location

e, f: Badda thana

g, h: Uttar khan thana

i, j: Pallabi thana

Figure 15 : Comparison between 2011 and 2022 vegetation pattern and distribution at 3 different thana in Dhaka.

3.4.2.1 Accuracy assessment of land use and land cover mapping

The accuracy of the classification process was checked using the confusion matrix (Lovell et al, 2022). The method upholds a statistically valid assessment of thematic accuracy by providing an estimate of the proportion of pixels in each class that are correctly or incorrectly classified against a reference data, indicating the overall accuracy, accuracy for individual classes, and the extent to which individual classes are confused with one another (Kappa statistic). Previous studies (Eskandari et al., 2020 ; Abebe et al., 2022) shared that five sampling strategies have used to acquire reference data/assess accuracy: (1) systematic sampling (2) cluster sampling (3) stratified random sampling (4) simple random sampling and (5) stratified, systematic, unaligned sampling. The study used a combination of previous LULC maps of the area, and Google Earth imagery as the reference data. A stratified random sample selection method was adopted to select at least 250 pixels per LULC class (1000 in total), per the given year. As detailed in Lovell et all (2022), confusion matrix (Table 9) shows the counts of a classifier's predictions in response to a set of reference with known classes. From the counts, a fixed total count can be obtained that will represent the performance of the classification. For instance, considering binary class representation, the total count or overall accuracy (N) can be obtained as shown in formula (i) (Foody, G. et al., 2023). The study considered an accuracy threshold of 85% because it is widely accepted for remote sensing-based classification as a benchmark accuracy threshold (Hussain et al., 2022).

$$N = TP + FP + FN + TN \quad \text{----------(i)}$$

Table 8: **Representation of a confusion matrix**

Generated LULC map	Reference data		
	Positive	***Negative***
Positive	True Positives (TP)	False Positives (FP)
Negative	False negatives (FN)	True negatives (TN)

The precision evaluation of Land Use Land Cover Classification can be accomplished by utilizing high-quality imagery from Google Earth (Abineh et al., 2015) which allows for a thorough comparison of individual points. To achieve this, a total number of 1000 equal startified random sampling points for each year were produced using ArcGIS within the region of interest, and their respective values are determined through the aid of Google Earth.

Green space, built area, water bodies, bare land water bodies were the land use and land cover classes used in the study. For each class in classified LULC map, 250 randomly stratified points were generated, resulting into a total of 1000 points for each year .The spatial analyst tool in ArcGIS was used to generate the 1000 points, which were then used to check for classification accuracy using the high-resolution imagery (Yadeta et al., 2022) from Google Earth. The generated points were converted to KML (Keyhole mark-up language) format that is suitable for viewing in Google Earth. KML format is used (Tilahun et al., 2015) in two-dimensional maps and three-dimensional Earth browsers to describe geographical information and visualisation. Layer to kml conversion tool within ArcGIS was used to convert points to kml and then import kml to Google Earth to check and validate each feature classes with original land uses. Given that the land cover class of each point is known prior, the corresponding landcover class in the Google Earth is then confirmed and recorded in the confusion matrix (Abineh et al., 2015) to perform the accuracy assessment.

Accuracy assessment was performed based on calculating the user accuracy, the producer accuracy, and the overall accuracy of the classification. The User accuracy is calculated using the formula 1. This shows the confirmation rate of what the user identified in the LULC classification and is confirmed in the Google Earth data. On the other hand, formula 2 was used

to determine the producer's accuracy. This tests the confidence level in the classification system itself checking the confidence on the ground-truth (Google Earth data).

Kappa co-efficient formula (Rwanga et al., 2017; Helmer et al., 2000) applied for the accuracy assessment (Jalal ,2022). In 1960, Kappa coefficient was introduced by Cohen (Vieira et al., 2010) as a statistical measurement tool and it is used by remote sensing users to estimate the precision of an image classification algorithm used to generate a themed map (Foody, 2020). The overall classification accuracy was tested using an error matrix for the two years that were taken into the study, yielding an overall accuracy of 94.7% in 2011 and 96.3% in 2022, with the Kappa coefficients of 0.93 and 0.95, respectively (Table 10 and 11). The Kappa statistics provides a statistical measure of the performance of the classification process including the confidence in the data spatial and radiometric properties used in the classification process. Several research (Ukrainski P, 2019 ; Chughtai et al, 2021) have found that if the kappa coefficient is 0, there is no concordance in between the reference image and the categorised image and. When the kappa coefficient is 1, it indicates that the categorised picture and the ground truth image are identical. As a result, the higher the kappa coefficient value, the more accurate the categorization (Vieira et al., 2010). The associated Kappa statistics of 0.93 and 0.95 for each sensor indicate a significant level of agreement between observed and projected classifications, supporting the suggested standard accuracy of 85-90% for LULC mapping tests (Dewan et al, 2009; Anderson et al,1976 ; Foody, G. et al., 2023). The study found the Landsat -5 TM was lower in accuracy than to Sentinel- 2, which may be for their spatial resolution.

Formulas used for accuracy assessment were proposed by (Abineh et al., 2015 ; Subedi et al., 2022)

$$\text{User accuracy} = \left(\frac{NP}{TP(RT)} * 100\right) \quad \text{..... (1)}$$

Where,

[NP = Number of correctly classified pixels in each category,
TP = Total number of classified pixels in that category,
RT = Row total]

$$\text{Producer accuracy} = \left(\frac{NP}{TP(CT)} * 100\right) \quad \text{..... (2)}$$

Where,

[NP = Number of correctly classified pixels each category,

TP = Total number of classified pixels in that category,

CT = Column total]

$$\text{Overall accuracy} = \left(\frac{TP(D)}{TP(R)} * 100\right) \quad \text{..... (3)}$$

Where,

TP(D) = Total number of correctly classified pixels

TP(R) = Total number of reference pixels

Kappa Coefficient (T): Formula

$$T = \left(\frac{(\text{TS}*\text{TCS}) - \sum(CT*RT)}{TS^2 - \sum(CT*RT)}\right) * 100 \quad \text{..... (4)}$$

This equation as proposed by Foody, 2020. Where,

[TS = Total Sample, TCS = Total Correctly classified sample

CT = Column total, RT = Row total]

For this study,

Overall accuracy for 2011= 947/1000 x 100 = 94.7

Overall accuracy for 2022 = 963/1000 x 100 = 96.3

Table 9: Error matric for accuracy assessment of land use and land cover classification in 2011.

	Reference Data 2011							
	Feature classes	Water Bodies	Green Space	Built Area	Bare Ground	Total	User Accuracy (%)	Commission Error (%)
Classified LULC Map 2011	Water Bodies	222	14	11	3	250	88.80	25.01
	Green Space	1	242	3	4	250	96.80	4.02
	Built Area	0	2	247	1	250	98.80	2.00
	Bare Ground	1	6	7	236	250	94.40	7.03
	Total	224	264	268	244	1000	---	---
	Producer Accuracy (%)	99.11	91.67	92.16	96.72		Kappa Coefficient	0.93
	OmissionError (%)	1.00	16.02	14.03	7.00		Overall accuracy (%)	94.7

Table 10: Error matric for accuracy assessment of land use and land cover classification in 2022.

	Reference Data 2022							
	Feature classes	Water Bodies	Green Space	Built Area	Bare Ground	Total	User Accuracy (%)	Commission Error (%)
Classified LULC Map 2022	Water Bodies	246	2	1	1	250	98.4	3.00
	Green Space	1	249	0	0	250	99.6	0.00
	Built Area	3	2	240	5	250	96	5.02
	Bare Ground	0	7	15	228	250	91.2	7.06
	Total	250	260	256	234	1000	---	---
	Producer Accuracy (%)	98.4	95.77	93.75	97.44		Kappa Coefficient	0.95
	Omission Error (%)	1.01	4.03	1.06	1.02		Overall accuracy (%)	96.3

3.5 Change detection

Thana boundaries of Dhaka has significant changes between 2011 and 2022. In 2011, there were 42 thanas, but by 2022, this number had increased to 53 covering different wards and areas under DNCC and DSCC. Certain thanas were dissolved as part of this expansion, and new boundaries have been established at their stead. The assessment of post-classification change detection was carried out using ArcGIS, which generated change maps to determine the geographical variance in patterns across years.

A notable observation is highlighted in the study's (Figure 15). In compared to Badda and Uttarkhan, Pallabi thana has seen a significant growth in population. For example, Badda Thana has been divided in to two, with one half called as Bhatara Thana. The abrupt change in floral patterns inside Badda thana during this study period is noticeable. Dense vegetation has shifted to no vegetation areas and a loss of greenspaces observed in entire thana (Figure 15). Lowest populated thana is Biman bandar (Figure 8).

Biman Bandar Thana is an airport zone, with most of the area utilised for aeroplanes, runways, and other associated concerns. As a result, there are few opportunities to create residential areas in this thana, and the only green space in Bimanbandar thana is for aesthetic purposes. From 2011 to 2022, Pallabi thana lost certain territory that were acquired by new Rupnagar thana and some parts of Cantonment. Pallabi population remains increasing in 2022, although Pallabi thana has gained some vegetation. Defence officer housing society (DOHS) is a new residential neighbourhood that contributes to the expansion of green areas in the surrounding region (figure 15.i, j). The population of Uttarkhan Thana was in the range of 35000- 85000 and it grew and changed to the range of 85000 - 114000. Uttarkhan Thana was the most densely vegetated area in 2011 and is expected to progressively transition from dense to moderate vegetation by 2022.

Table 12 indicates the significant LULC conversions, or 'from-to' data, that occurred during the research period. As previously stated, a large portion of the urban area has been obtained by transforming previously land used for agriculture, vegetation, water bodies, or low-lying regions, meaning that natural resources in Greater Dhaka are under increased pressure to meet the growing demand for urban space. Based on the study, Dhaka's growth in urban areas has been very rapid (Byomkesh et al., 2012), resulting in extensive environmental degradation. The study also found that the process of urban growth varied significantly between 2011 and 2022. The entire land cover changes in Dhaka are the product of three sectors: private, public, and

private residence. The development of real estate in Dhaka has increased dramatically. Developers have constructed on wetlands and agricultural regions without addressing the environmental consequences (Dewan et al, 2009).

The Sankey chart (Figure 16) shows that the total area of Dhaka is 61636.88 ha where built-up areas rose significantly from year 2011 to 2022. Built area increased from 8992.1 ha to 16784 ha, which shows 12% of growth rate of the total built area in the city. Waterbodies declined from 2608.84 ha to 1896.03 ha with 1% change, greenspaces decreased from 9988.42 ha to 7717.81 ha indicates 3% decline, and bare ground decreased from 9226.18 ha to 4422.85 ha represent 8% disappearing in open bare ground. The study also revealed the spatial conversion of one feature class to other feature classes. Table12 and Figure 17 shows the areas changed from one class in 2011 to another in 2022.

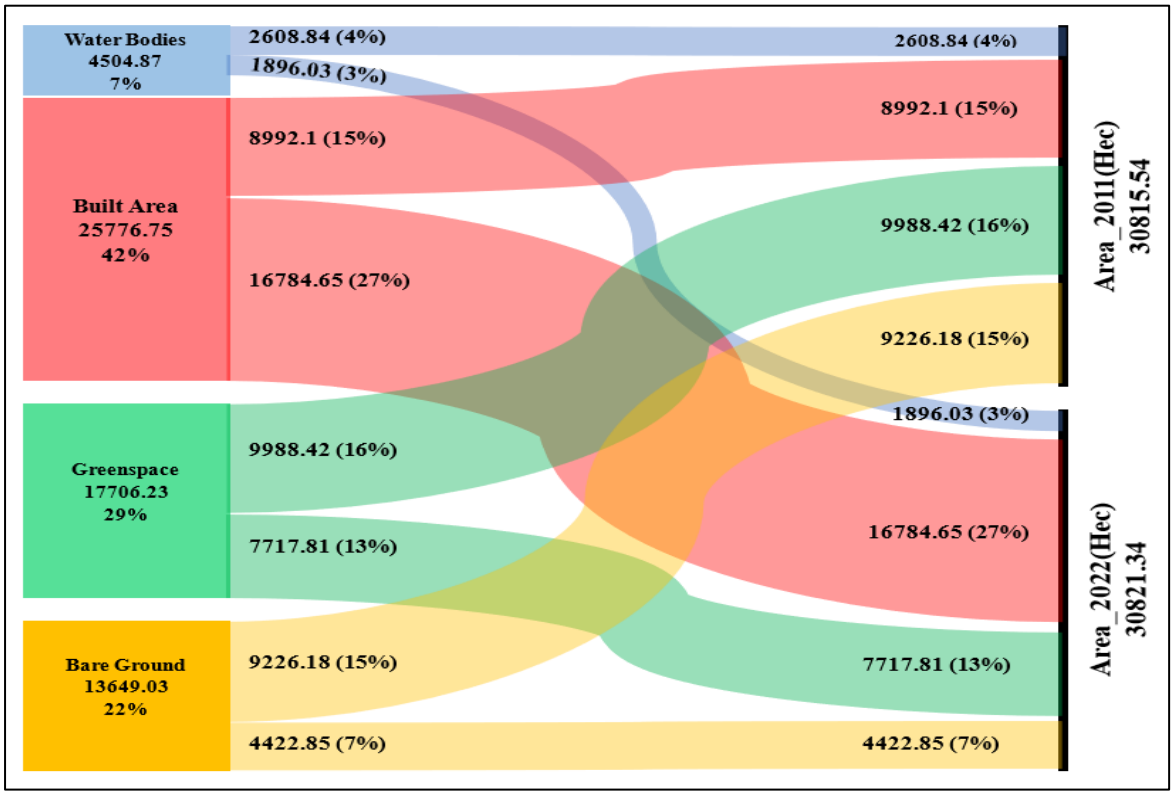

Figure 16: Sankey Chart showing the area (in hectares and percentage) transformation in Dhaka from 2011 to 2022.

Table 11: Dhaka's land use land cover (LULC) conversion for the years 2011 and 2022.

From class	To class	Area Changed (Hectare)
Bare Ground	Bare Ground	2069.28
	Built Area	5290.27
	Green Space	1773.07
	Water Bodies	92.71
Built Area	Bare Ground	416.03
	Built Area	8268.63
	Green Space	208.36
	Water Bodies	98.01
Greenspace	Bare Ground	1601.92
	Built Area	2448.80
	Greenspace	5170.42
	Water Bodies	765.68
Water Bodies	Bare Ground	334.97
	Built Area	771.98
	Greenspace	564.44
	Water Bodies	919.04

From one feature class to other feature class land use transformation

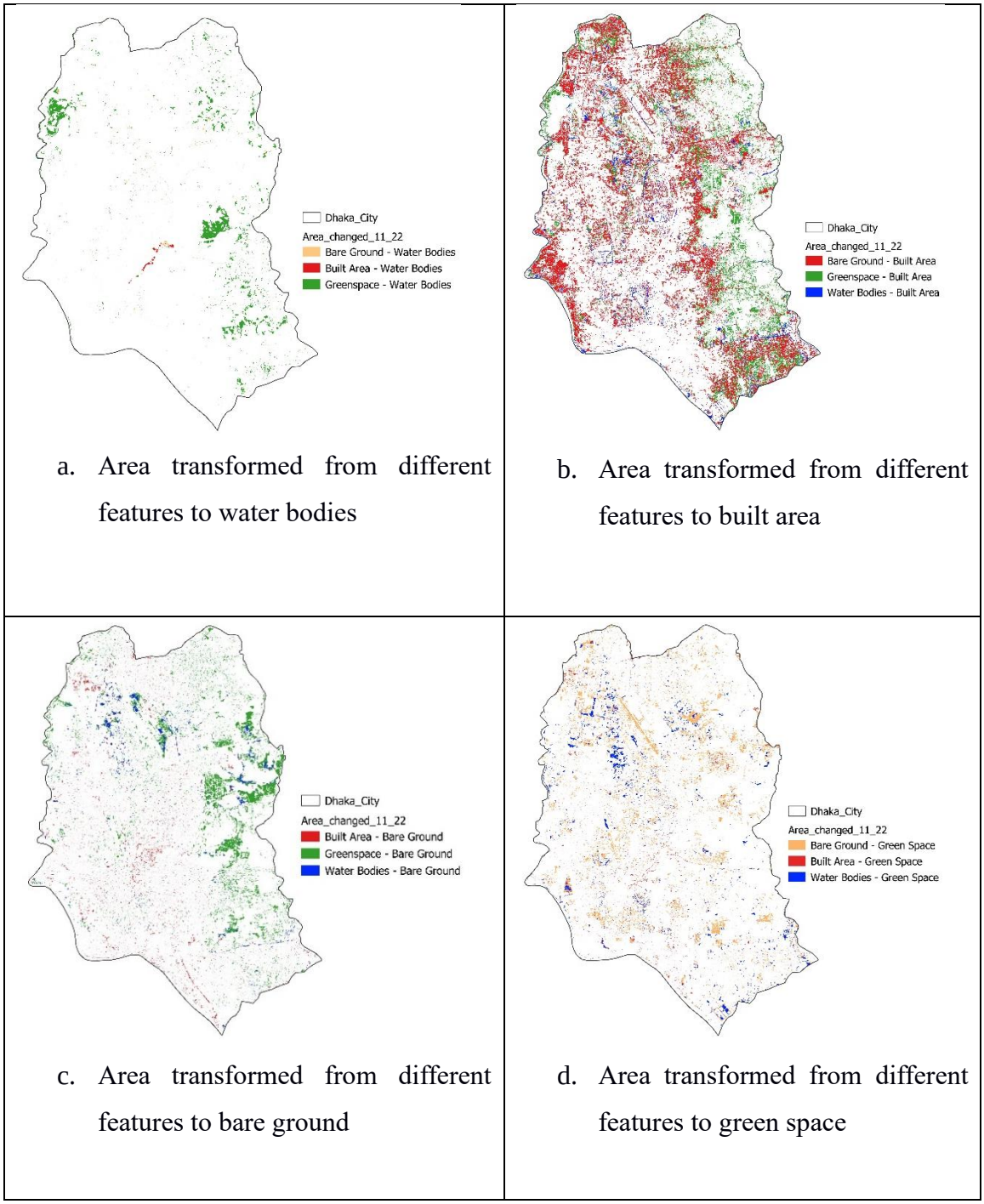

a. Area transformed from different features to water bodies

b. Area transformed from different features to built area

c. Area transformed from different features to bare ground

d. Area transformed from different features to green space

Figure 17: Conversions of different feature classes (from one class to other class) in Dhaka from 2011 to 2022.

Figure 17 (a) illustrated that an area in the middle of the city converted from bare ground to water. According to the knowledge about the city, this is Hatirjheel lake. Few greenspaces transformed to water in western part of the city. Diabari Lake, located in the northwest corner of Dhaka, was established as a leisure space for the newly constructed residential area, also

converted from green space to waterbodies. Figure 17(b) shown that most of the feature classes has converted to built area from 2011 to 2022. According to the Census 2022 (BBS 2022), Dhaka's population has increased 47% from 2011 (6,970,105) to 2022(10,278,882). Due to this huge addition of the residents in the city, built infrastructure developed a significant number. Noticable transformation observed from bare ground and green spaces to built areas. Huge amount of waterbodies/ blue spaces declined (17c) which have been converted to either bare ground which have been filled up for building infrastructure development or recreational areas. It is also illustrated that some areas also transformed to green spaces (17d) which is a little amount but it is for the beautification of the city. Few areas from built-up to water bodies converted within the study period. Few areas from built-up to water bodies converted within the study period and Hatirjheel -Begunbari (figure 11) is one of the significant of them. This area was covered with slum till 2009.

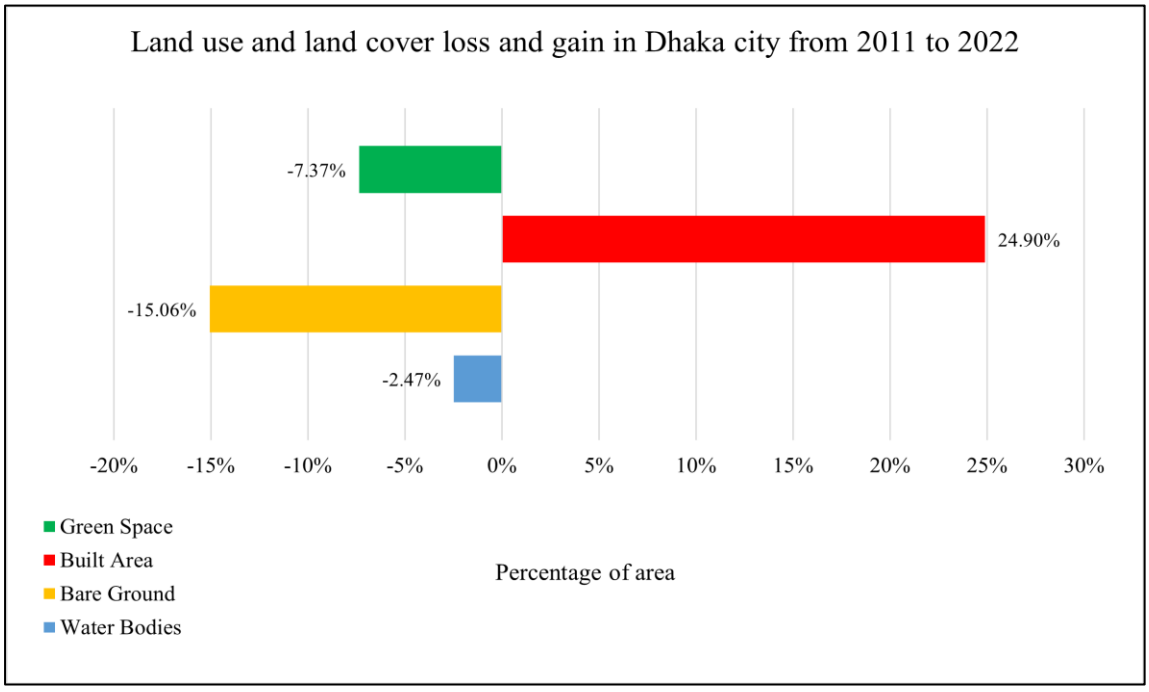

Figure 18: Percentage of gain and loss of LULC in Dhaka

3.6 Land use land cover variation of Dhaka city

The conversion of several green spaces within Dhaka city into affordable housing units, as well as the conversion of open fields into parking lots for shopping malls and low-lying areas such

as ponds and lakes into reclaimed built-up lands, has resulted in a scarcity of available open spaces. Unfortunately, the city's citizens' physical and emotional well-being has suffered because of this lack of open space (Nawar et al, 2022). The maximum likelihood supervised classification approach was used to create a land use land cover (LULC) map for Dhaka. Figure 11 illustrated the LULC maps of 2011 and 2022 respectively. Examining figures 17 a, b, c and d, shows significant losses of all LULC classes except for Built areas. Bare ground areas suffered the worst loss at 15.06%while built areas made the biggest gain at 24.9% of the total area. Greenspaces lost 7.37% and waterbodies which are the blue spaces of the city, decreases by 2.49% Some of the unpaved roads, and open areas in 2011 were converted to built-up areas as urbanisation increased in Dhaka city. The significant loss of greenspaces to built-up areas poses serious concern to the climate and ecology of Dhaka. This is also leads to resurgence in UHI effects and confirms previous studies that reported the existence of UHI in Dhaka.

To meet the demands of the capital's constantly growing population size, the most obvious alteration has been the transformation of land used for agriculture into both residential and commercial zones. Urban sprawl has resulted in the loss of wetlands, agricultural land, bare ground and green areas, exacerbating environmental problems such as increasing air pollution and decreased water storage capacity. In addition, the development of infrastructure such as roads and highways, metro rail, elevated expressways, as well as the development of business districts, has transformed Dhaka's land use pattern. This has not only aided economic growth, but it has also resulted in environmental issues such as traffic congestion and degradation of habitats.

There are very few reserved greenspaces in Dhaka. The national Botanical Garden, Ramna Park, and some part of the University of Dhaka. Covering an area of around 205 acres, the National Botanical Garden of Bangladesh is an ecological reserve and the country's largest plant conservation site. It is in Mirpur, sharing the same boundary of National Zoo in Dhaka. The Botanical Garden is an important reminder of the necessity of preserving green spaces in a fast-urbanising metropolis like Dhaka, emphasising the importance of biodiversity and sustainable development. Ramna Park is 74.13 acres in size and is located immediately east of the University of Dhaka campus. It contains a variety of plant types, including different size and shapes of canopies, and herbs and shrubs. Both of this area contains waterbodies such as ponds and lakes. Dhaka's canopy cover has been decreasing (Figure15) because of to the constant clearing of vegetation and trees. Urbanisation has led in the entire disappearance of

forests within the city, which might be home to a variety flora and fauna, giving balance to the environment and aesthetic elegance.

Water bodies of the city has similarly indicated concerning patterns. Built-up areas have consistently taken over the city's water bodies. Development of Purbachal's residential area has been replaced by massive water bodies since 2009 (Mowla. Q et al., 2011). To provide a place for housing or other infrastructures, many ponds, swamps, lakes have been filled out over the study periods. In Dhaka, river encroachment is an inevitable and serious problem. A study focused that Turag, Buriganga and Balu, have been severely affected by human activities (Hossain, 2017). The study also investigated that. Riverbanks are progressively being taken up by developers and other companies. Housing, sand depots, brickfields, sand sales centres, cremation centres, mosques, rice mills, stone sales centres, and other industries are constantly changing the land use of the riverbanks, however, these rivers formerly served as the city's economic and biological lifeline.

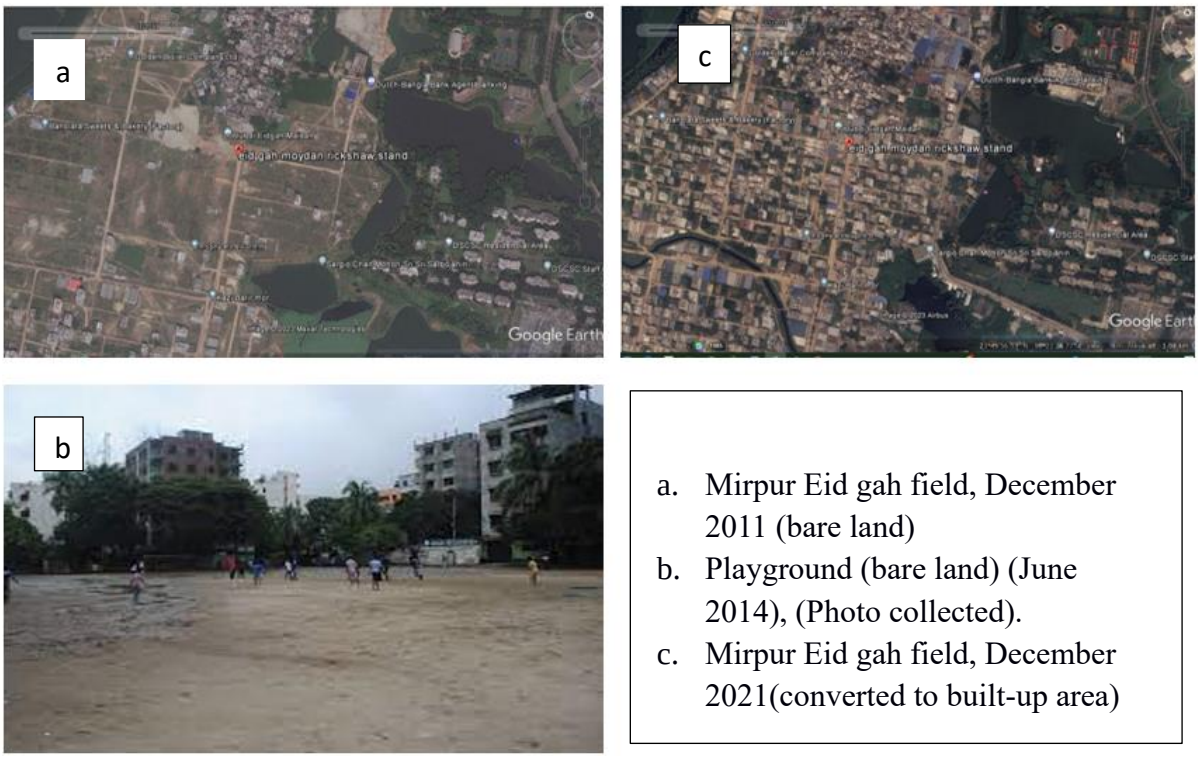

a. Mirpur Eid gah field, December 2011 (bare land)
b. Playground (bare land) (June 2014), (Photo collected).
c. Mirpur Eid gah field, December 2021(converted to built-up area)

Figure 19: Land conversion in Dhaka city (Source: Google Earth, accessed on 15 May 2023).

3.7 Chapter Conclusion

The analysis of spatiotemporal changes in land use and land cover change in greater Dhaka has indicated a disturbing pattern of fast loss in green areas, bare land, and water bodies. This suggests that the region's green lands and other natural areas are shrinking with time. Dhaka's urban infrastructure is currently under tremendous strain because of overpopulation, with over 10 million people residents in the metropolis and the city has only 2% of healthy vegetation (Nawar et al, 2022). Furthermore, the population continues to grow by hundreds of thousands each year as migrants flood to the city in quest of work and better economic possibilities.

The pressure on green spaces forces them to be invaded and converted into structures and other facilities which expands the area that is urbanised. This construction adds even more to the city's deficit of green spaces. Urbanisation is a major and potent driving force (Wang et al., 2018) underlying changes in land use and land cover in Dongguan, China (Han, D. et al., 2023). Land use and land cover (LULC) changes in cities are mostly determined by the process of urbanisation. Establishment of law is one of the key factors which impacting the development and management of urban green spaces.

Urban landscape is increasing because of these policies' significant effects on the quantity, standard, and connectivity of green spaces inside the infrastructure of city. Several aspects of well-being have been positively correlated with the presence of outstanding blue-green infrastructure, according to earlier research. Rural to urban migration and financial growth and lack of knowledge among the policy maker and inhabitants drives (Feng, C. et al, 2022; Vidal et al, 2022) the population increases and change the LULC of the city.

Furthermore, additional variables exacerbating the circumstances include the use of political power to regulate illegal park conversion and leasing, insufficient rules, and regulations to protect urban green spaces, and inadequate fund allocations for effective management and maintenance of these green areas (Feng, X. et al.,2022). Considering the ratio of conversion of different feature classes to build-areas (Figure 18), Dhaka could be greatly benefitted by establishing a greenbelt around the city. It would help the city to reduce carbon footprint, controls of temperature, allow sheds with oxygen supply, restore the green spaces. MacKaye, (1990) given an in-depth analysis of the diverse uses for urban green belts, focusing on several important targets: effective control of growing urban areas, building environmentally friendly and conservation, promoting the expansion of a satellite towns and cities, and providing recreational spaces for the city residents. The Greater London Regional Planning Committee's

suggestion of a "green girdle" (Amati, 2016). Following World War II, the green belt become one of the most common growth management methods in a variety of socioeconomic and geographical circumstances (Ignatieva et al., 2020).

These elements all lead to the continued deterioration and loss of urban green areas. The importance of land use cannot be overlooked in understanding the significant impact of human activities on environment. Future studies must address how human activities change the plant cover since the underlying surface has a significant impact on it. To achieve the goals of SDG 11.7.1, innovative and effective urban forestry policies and plans (Nitoslawski et al., 2019), and programmes must be implemented to increase vegetation cover and develop urban green areas. The study also recommends preservation of the environmental activities (Kruize et al., 2019) in Dhaka to minimise the disappearance of green spaces. This may be accomplished by implementing community-based participatory programmes aiming at protecting urban green areas which are still moderate and low vegetated area. The study suggests, in compared to population growth, greenspace and other feature classes should maintain a balance land use. Such efforts contribute to the promotion of SDG goals.

4. CHAPTER FOUR

FUSION OF LANDSAT AND MODIS SATELLITE IMAGERY TO DETERMINE LAND SURFACE TEMPERATURE OF DHAKA

4.1 Introduction

The climate in urban and rural places differs. This is due to the modification of the urban landscape and its surface which affects the humidity, temperature, wind intensity and speed. In 1833 British chemist and meteorologist, Luke Howard first observed and documented that city area are often warmer than its neighbouring areas which he mentioned as 'external heat' (Gartland, 2012). Ting (2012) stated that Emilien Renou (1855, 1862, 1868) also described about the same condition in Paris and later, Oke (1976) defined this as urban heat island (UHI) by the temperature variations between itself and its surroundings. UHI varies seasonally and in relation to space and time. It is important to understand UHI as the urbanisation is an increasing process in the world. UHI has various effects such as, in which the average temperatures in densely populated cities tend to be higher than in rural areas, is one of the environmental issues (Maharajan, M. et al., 2021).

Despite natural climatic variability, human-made global warming, particularly a rise in extreme events, has resulted in significant negative consequences, losses, and damage to environment and humans (IPCC, 2022).

The growing hazard of heat and heat waves is considered the most serious concern for human health in Europe. A recent example is the summer of 2022, which witnessed a considerable increase in excessive mortality throughout Europe because of severe temperatures and extended heat waves. According to projections, heatwaves are expected to occur more often, linger for longer periods of time, and reach higher intensities in the next decades. At the same time, demographic changes, such as an ageing population, and the continuing trend of urbanisation, increase the population's vulnerability (EEA, 2022).

Extreme temperatures in cities become more severe by the urban heat island (UHI) effect.

The canopy layer UHI, which is most important for human health, delineates the temperature disparity between urban street canyons at 1-3 metres from the surface and rural temperatures at the same height (Stewart, 2011). Southeast Asia (SEA) is characterised by a dense population and diverse topography, and it is an area that is generally vulnerable to global warming. The

Asian-Australian monsoon system has a significant influence on the climate of the SEA area (Sun X. et al., 2022).

The heat island effect is exacerbated by anthropogenic heat sources such as industrial activity, unplanned infrastructure, air conditioner, closely spaced buildings, and transport emissions. Dhaka's subtropical weather, which is marked by substantial humidity and harsh temperatures, exacerbates the problem even more. UHI trends are complicated by Dhaka's distinct urban structure, which is characterised by a blend of informal settlements and facilities with cutting-edge technology (Abrar et al., 2022). To accurately computing LST, time series photos from satellites that span a whole year, month, or season are crucial, as are methods like statistical assessment, atmospheric correction, and temporally averaging data.

In addition, Huang et al. (2013) suggest that combining data from multiple sources and sensors might help overcome the deficiencies of individual datasets. This study also attempts to draw comparisons with other research that used one or more satellite images for analysis to show how the urban heat island (UHI) of Dhaka is affected.

4.2 Background

To estimate land surface temperature, satellite imagery is continuously applied. They have been used to identify hotspot throughout the timeframe for any particular UHI related investigations. They can produce accurate outcomes across large geographic locations while giving quick and effective findings. (Deilami et al., 2018). A common shortcoming in many studies is to focus on the use of single satellite imagery for a single period (Abrar et al., 2022), or the use of two or more satellite imagery over short periods of time (Ahmed, et al., 2013; Rashid, et bal, 2022). An attempt at exploring the use of extensive datasets for UHI estimation such as the case of Birmingham city UK (Tomlinson, et al, 2012) have shown LST results that are a compromise with the ground-based measurements because there are no available spatial air temperature data at comparable resolution and study extent. The study required climate data for surface network in Dhaka and this type of data didn't exists. As a result, satellite imagery is the only feasible approach to explore UHI in Dhaka.

In Wuhan, China, Shen et al. (2016), despite integrating series of summer-based satellite imagery over a 26-year period observed accuracy problems associated with temporal aggregation of different viewing angles of different satellite sensors. By adopting fewer

sensors, Kamali et al. (2021) was able to work with seasonal imagery with similar viewing angles from Landsat and MODIS to improve the results of season UHI monitoring. In Amiens France Qureshi and Rachid (2022), the study notes that due to climate dynamics, heat episodes during summer days are not uniform and therefore identification of extreme events will require near-hourly datasets. The study recommended use of near-hourly datasets as compared to datasets for daily isolated data in a month for accurate characterisation of UHI effects. The use of extensive datasets further increases the reliability of UHI models in supporting decision making. The feasibility of using more than two satellite imagery each month to assess UHI vulnerabilities in Dhaka city is still unknown. To the best of our knowledge, the use of multi-temporal and multi-spatial remote sensing for UHI estimation over seasonal scale in Dhaka is novel.

To account for local scale variations of LST, Landsat's 30m imagery is sufficient. However, it is not possible to obtain more than three Landsat imagery in each month. Therefore, there was need to exploit the MODIS's high temporal resolution with Landsat's high spatial resolution to synthesize a high spatiotemporal imagery (HSR). This was achieved by using the Spatial and Temporal Adaptive Reflectance Fusion Model (STARFM) first proposed by Gao et al (2006). STARFM is a widely used model for Landsat and MODIS fusion because of its flexibility of being adjusted to adapt to different scenarios (Singh et al., 2011 and Emelyanova et al., 2013). This have been demonstrated by Walker et., al (2012) in forest phenology studies, Xu et., al (2020) for monitoring crop water content, and Liu and Weng (2018) for LST prediction. Since MODIS's thermal bands 31 and 32 have similar centre wavelengths with Landsat's thermal bands 10 and 11 respectively, it is possible to exploit the statistical information in the corresponding bands, to predict a new HSR band. Masek et., al (2006) showed that MODIS and Landsat demonstrate consistent surface reflective properties, despite their radiometric differences. Therefore, firstly, the study has been ensured uniform georeferencing and resampling of image and pixel sizes for both Landsat and MODIS and obtained base-pair imagery on the same day.

The study aims to assess the use of multi-temporal and multi-spectral satellite imagery for UHI vulnerability of Dhaka city from 2011 to 2022. The selected years correspond the respective censuses of 2011 and 2022. Dhaka's summer seasons usually run from February to June annually with few variations. The study adopts the season approach of characterising UHI as demonstrated in Wuhan, China (Shen et al. 2016), Tehran, Iran (Kamali et al. 2021) and Amiens France (Qureshi and Rachid, 2022). The seasonal approach allows for proper

characterisation of extreme heat episodes within the summer season and ensures hotspot identification for frequent monitoring. The study demonstrates the utility of fusing multi-temporal datasets from MODIS, and Landsat 5/9 to obtain imagery with both high spatial and temporal resolutions necessary for accurate UHI estimation. Ground climate datasets about Dhaka city provided the surface air temperatures for comparison and accuracy assessment. The study results will assist policy makers, urban planners, and the community to effectively monitor UHI and related public health hazards and contribute to the UN's Sustainable Development Goals 11 and 13.

4.3 Methodology

Considering no geographical variations or exceptions in atmospheric correction, it is reasonable to predict that LST readings obtained from various satellite imagery recorded on the same day will be similar and exhibit a relationship in a homogenous geographical region.

This section describes the procedures that were performed, such as the datasets and data sources, preliminary data processing in the Google Earth Engine (GEE) cloud computing environment, and predictions of Landsat synthetic imagery from MODIS utilising the STARFM fusion algorithm, as well as the procedures utilised to calculate Dhaka's UHI.

4.3.1 **Datasets**

Following datasets have been used to analyse the fusion of different satellite imagery. MOD11A1 of MODIS, Landsat 5 and 9, Weather data from the ground station of Dhaka and boundary map used to processing and analysing the fusion process and produce syntetic Landsat imagery.

Table 12: Datasets for the study

Dataset	Scale	Date	Source	Used for
MODIS daily land surface temperature (MOD11A1)	1 km	2011, 2022	USGS Earth Explorer	Fusion to produce synthetic Landsat images and deriving LST and

Landsat 9 OLI-2/TIRS-2	30 m	2022	USGS Earth Explorer	related indices (Landsat only).
Landsat 5 TM	30 m	2011	USGS Earth Explorer	
Weather data	3-hourly	2011 - 2022	Bangladesh Meteorological Department (BMD)	Air temperature, accuracy assessment of LST
Boundary datasets	1:100,000	2022	Centre for Environmental and Geographic Information System (CEGIS),	Delineation of study area to maintain spatial consistency

4.3.1.1 MODIS Satellite Data

MODIS satellite data has two LST products that use different ways to obtain LST with a 1Km-spatial resolution. Both items are issued by NASA and can be obtained daily at a global scale. Both product's compute LST using different approaches, and whether way produces better results depending on local factors. The generalised split-window algorithm underpins the MOD11A1 product. This method determines emissivity using a landscape classification technique. To account for atmospheric effects, two distinct longwave bands are employed. This approach is especially useful in situations when most of the surface is assumed to have the same emissivity (Wan, 1999).

The thermal emissivity separation (TES) technique is used by the newest MOD21A1 devices, which were introduced in 2018. This approach is based on a surface reflectance fluctuation-based emissivity concept. (Hulley et al., 2016).

Literature supported that MOD21A1 products gives better results than MOD11A1 products in arid regions and similar outcomes in all other locations (Hulley et al., 2020). MOD11A1 product was regularly used to LST observation (Liu et al., 2012; Huang et al., 2013; Weng et al., 2014, Li et al., 2016) and therefore this study also intend to use the same. However, the study site Dhaka is not situated in arid region where MOD21A1 could show significant results.

The MODIS satellite imagery for this study was obtained from USGS Earth Explorer. At the initial stage, raw data was multiplying by the scale factor of 0.02(table 14) to convert to Kelvin. After that, values of LST in Kelvin were converted to Celsius by subtracting 273.15 from Kelvin values. MODIS LST user guide was used to address the calculation of the transformation (Emelyanova et al., 2013; Frimpong et al., 2023).

4.3.1.2 Landsat Satellite data

Landsat 5 and Landsat 9 satellite imagery of level 2 and collection 2 products were utilised which includes LST products. This extensive dataset contains essential elements which include surface temperature, surface reflectance, intermediate bands used for LST calculations, and quality evaluation masks. The surface temperatures in this dataset are generated from the Collection 2 Level 1's thermal infrared Sensor (TIRS) band 10, using a single-channel technique. Landsat data is organised into paths and rows according to the satellite's orbit. In Landsat imagery, Path and Row for Dhaka are 137 and 44 respectively.

Thematic Mapper (TM) sensor on Landsat 5 enables it to record pictures in various spectral bands, giving vital information to monitor changes in land cover, vegetation health, and other environmental aspects. Landsat 5 was retired after over two decades of duty because to technical concerns, including a malfunction in its solar matrix drive mechanism. However, this study used Landsat 5TM for 2011, because this was in operation on that period.

Landsat 9 began operations in September 2021 to continue and improve on its successors' data-collecting capacities. The satellite is equipped with two primary sensors: the Operational Land Imager 2 (OLI-2) and the Thermal Infrared Sensor 2 (TIRS-2). This equipment records pictures and data in a variety of spectral bands, allowing scientists and researchers to examine land usage, changes in land cover, vegetation health, and other environmental variables.

Each day, Landsat acquisition starts from North to South and they pass through the equator between 10am to 10.25 am at local time. For study are Dhaka, Landsat acquire imagery at about 10.30 a.m. local time (GMT+6). According to (Hussain et al, 2023; Corner, R.J., et al. 2014; Raja et al., 2021) , Landsat's path and row for Dhaka is 137 and 44 respectively. From January to May of 2011 and 2022, all imagery were obtained from the "USGS Earth explorer" (USGS, 2022). The data has been multiplied by 0.00341802 (Multiplicative scale factor) and an additive offset of 149 (table 14) was applied to convert it from Band 10 to Kelvin (USGS, 2022).

4.3.2 Data pre-processing, processing, and analysis

In all cases, datasets were clipped to the study extent of Dhaka city, and spatial consistency maintained by projecting the datasets to UTM Zone 46 N projection system, with raster datasets interpolated to 30m spatial resolution and vector datasets scaled to 1:100,000 map units. To model a near-daily climate phenomenon, cloud cover was not factored in the choice for the imagery. Changes in the amounts of clouds and moisture, for example, can have an effect on the balance of radiation at the surface. Surface temperatures can be impacted by clouds that either increase or impede incoming solar energy. STARFM is primarily concerned with combining reflectance and radiance values from several sensors to create a dataset that is consistent across time and space.

4.3.3 Fusion process of Landsat and MODIS satellite imagery

Landsat 5, Landsat 9 (hereafter referred collectively as Landsat), and MODIS were processed in the Google Earth Engine (GEE) proposed by Gorelick et al (2017). GEE provides an open-access cloud-based computing environment with several ingested imagery archives, and code-based processing environment, allowing for custom python or JavaScript codes and a faster-processing cycles. The study developed a custom JavaScript code (Abudu, et al., 2022) for processing both Landsat and MODIS in GEE for the required summer seasons of 2011 and 2022 respectively. Figure:19 summarises the processing steps following in the GEE environment.

For MODIS of each year (2011 and 2022), all LST bands of each year were combined into one single image. Some bands had null pixel values, which affects estimation of UHI. To address this, an interpolation was conducted by considering neighbouring pixel values of 30 images with future dates from the considered date and 30 images with previous dates to improve the accuracy of the interpolation. The resulting MODIS composite imagery consisted of 150 LST bands for 2011 and 2022 respectively without any null pixel values. This approach was adopted for the Landsat imagery as well resulting into Landsat composite imagery of 150 bands to match the dates and number of bands of MODIS. An exception was that not all the bands in the Landsat composite had non-null values, because MODIS has daily imagery while Landsat has a 16-day repeat cycle. It was important to have the same number of bands in Landsat as that of MODIS for the application of STARFM algorithm. On application of STARFM algorithm, the synthetic out image replaces the corresponding null-valued bands in Landsat.

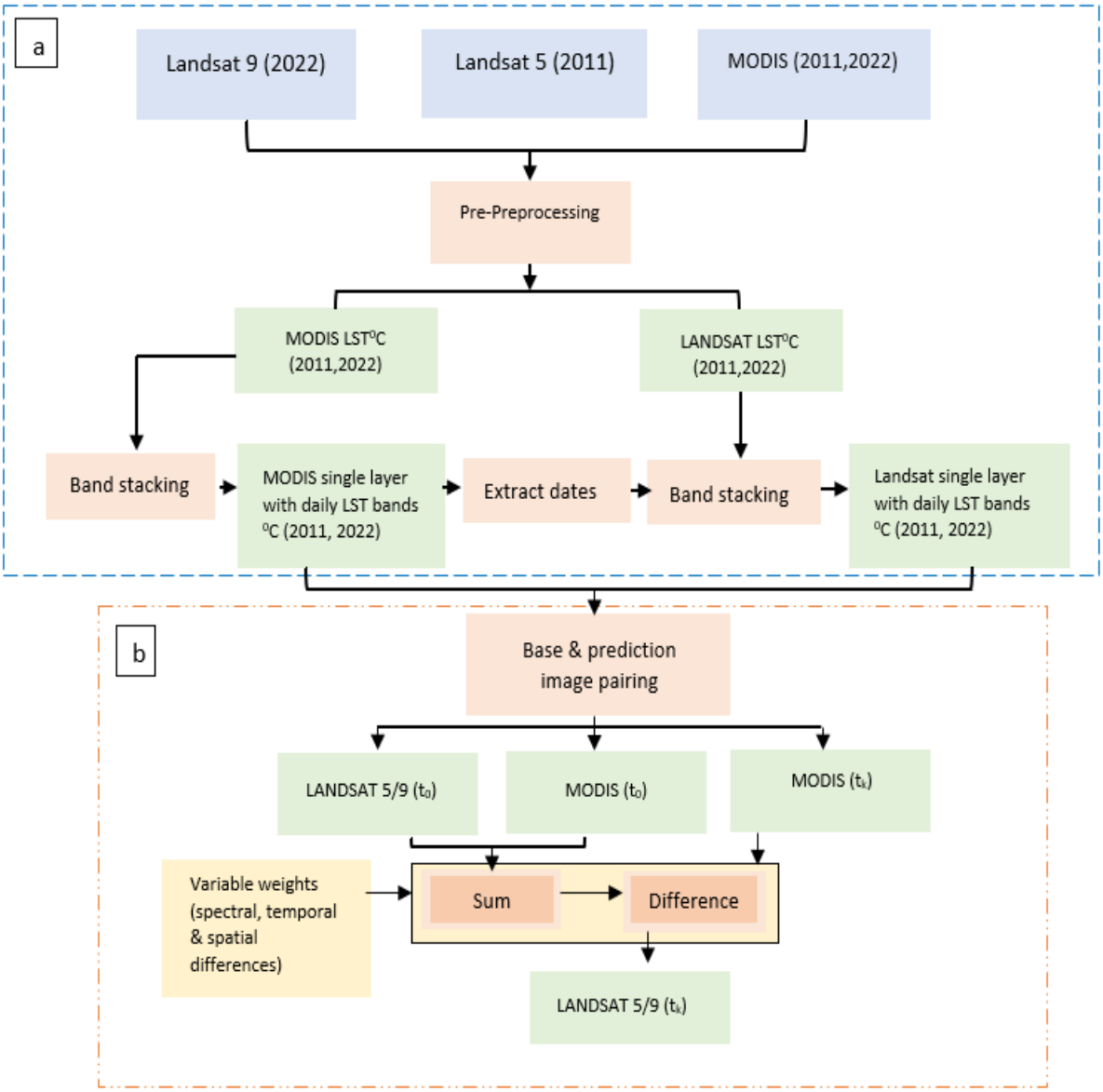

Figure 20: a. Google Earth Engine (GEE) cloud computing environment, LST, b. STARFM implementation on PC Python environment.

The daily MODIS land surface temperature (LST) data are provided as unscaled digital numbers (DN) format in GEE for both day and night times. The study selected daytime datasets to correspond to the Landsat imagery which are taken at about 10.30 am local time (GMT+6). One of the main downside of MODIS data is the frequency of empty pixels over tropical areas due to extreme weather patterns. The study addressed this problem by assuming a minimal temperature variation within a seven-day period. Using a custom gap-filling algorithm

developed in GEE, twelve-day temperature values from six days preceding and succeeding the missed pixel date, respectively were averaged to fill the gap. Then converted the DN to temperatures in degree Celsius (^{0}C) using equation 1. The processed daily MODIS datasets were then stacked into one single imagery with each band corresponding to respective LST days, for easier data download and further processing.

$$I_c = (I_{DN}) * (f_1) + (f_2) - (k_0) \quad (1)$$

Where, I_c is the output image in ^{0}C, I_{DN} is the unscaled input image in DN, f_1, f_2 and k_0 are sensor specific and provided in Table 14.

Table 13: **Sensor properties used in the scaling Landsat and MODIS imagery.**

Product	**Scale factor1 (f_1)**	**Offset/Scale factor2 (f_2)**	**Absolute temperature in ^{0}C (k_0)**	**Source**
Landsat Level 2 collection 2	0.00341802	149.0	273.15	USGS
MODIS Level 2	0.02	0	273.15	ERI-UCSB

Similarly, each of the Landsat land surface temperature (LST) bands provided in GEE were scaled to degree Celsius (^{0}C) using the equation 1 and stacked into a single image ready for download and processing. Given that Landsat has a 16-day revisit cycle, several days corresponding to MODIS dates were unavailable. An empty band (a band with null values) was created in the Landsat composite imagery to correspond with the MODIS dates for which Landsat had not data. This was done to ensure, the number of bands of MODIS corresponds with that of Landsat to enable automatic calculation of synthetic Landsat imagery using the custom python script described in Section 4.3.4.

4.3.4 STARFM Fusion process

To account for local scale variations of LST within Dhaka, Landsat's 30m imagery is sufficient. However, it is not possible to obtain more than three Landsat imagery in each month. Therefore,

there was need to exploit the MODIS's high temporal resolution with Landsat's high spatial resolution to synthesize a high spatiotemporal imagery (HSR). This was achieved by using the Spatial and Temporal Adaptive Reflectance Fusion Model (STARFM) first proposed by Gao et al (2006). STARFM is a widely used model for Landsat and MODIS fusion because of its flexibility of being adjusted to adapt to different scenarios (Singh et al., 2011 and Emelyanova et al., 2013). This have been demonstrated by Walker et., al (2012) in forest phenology studies, Xu et., al (2020) for monitoring crop water content, and Liu and Weng (2018) for LST prediction. Since MODIS's thermal bands 31 and 32 have similar centre wavelengths with Landsat's thermal bands 10 and 11 respectively, it is possible to exploit the statistical information in the corresponding bands, to predict a new HSR band. Masek et., al (2006) showed that MODIS and Landsat demonstrate consistent surface reflective properties, despite their radiometric differences. Therefore, firstly, we ensured uniform georeferencing and resampling of image and pixel sizes for both Landsat and MODIS and obtained base-pair imagery on the same day.

STARFM represented in equation 2, produces synthetic Landsat imagery for the dates that MODIS imagery exist. The model assumption is that the difference between MODIS and Landsat observed in the same day is constant, meaning that we can predict Landsat data for days where MODIS data has been observed and vice versa (Gao et al., 2006). For each Landsat and MODIS corresponding pixels (x_i, y_j), at an initial time t_0, the resulting (error resulting from system and pixel properties) can be applied to a new MODIS data at time t_t, to predict Landsat imagery at t_k. Given that the error is constant at both t_0 and t_t, the algorithm should consider only three other properties in the prediction namely, the pixel's spectral differences, the pixel's temporal difference and the centre pixel's spatial Euclidean distance from its neighbours. In this study we constructed a moving window of size 5x5 over the imagery to reduce computational complexities without compromising the accuracy. We accounted for the three properties by applying a variable weighting factor w_{ij} over the neighbouring pixels. This improved the accuracy of the synthetic Landsat imagery ($\mathrm{Landsat}_p$) at $(x_{w/2}, y_{w/2}, t_k)$. Using Mileva, N. et., al (2018)'s Python program for Sentinel-2 and -3 fusion, this study developed a custom script for MODIS and Landsat fusion using STARFM model (Abudu & Parvin, 2022).

$$\mathrm{Landsat}_p = \sum_{i,y,=1}^{w} w_{ij}[\mathrm{modis}(x_i, y_j, t_k) + \mathrm{landsat}(x_i, y_j, t_0) - \mathrm{modis}(x_i, y_i, t_0)] \qquad (2)$$

Where, w is the size of the moving window. Weighting function was used to incorporate more information from neighbouring coarse and good resolution image pixels. (Gao et al, 2006; Walker, J. et al, 2012).

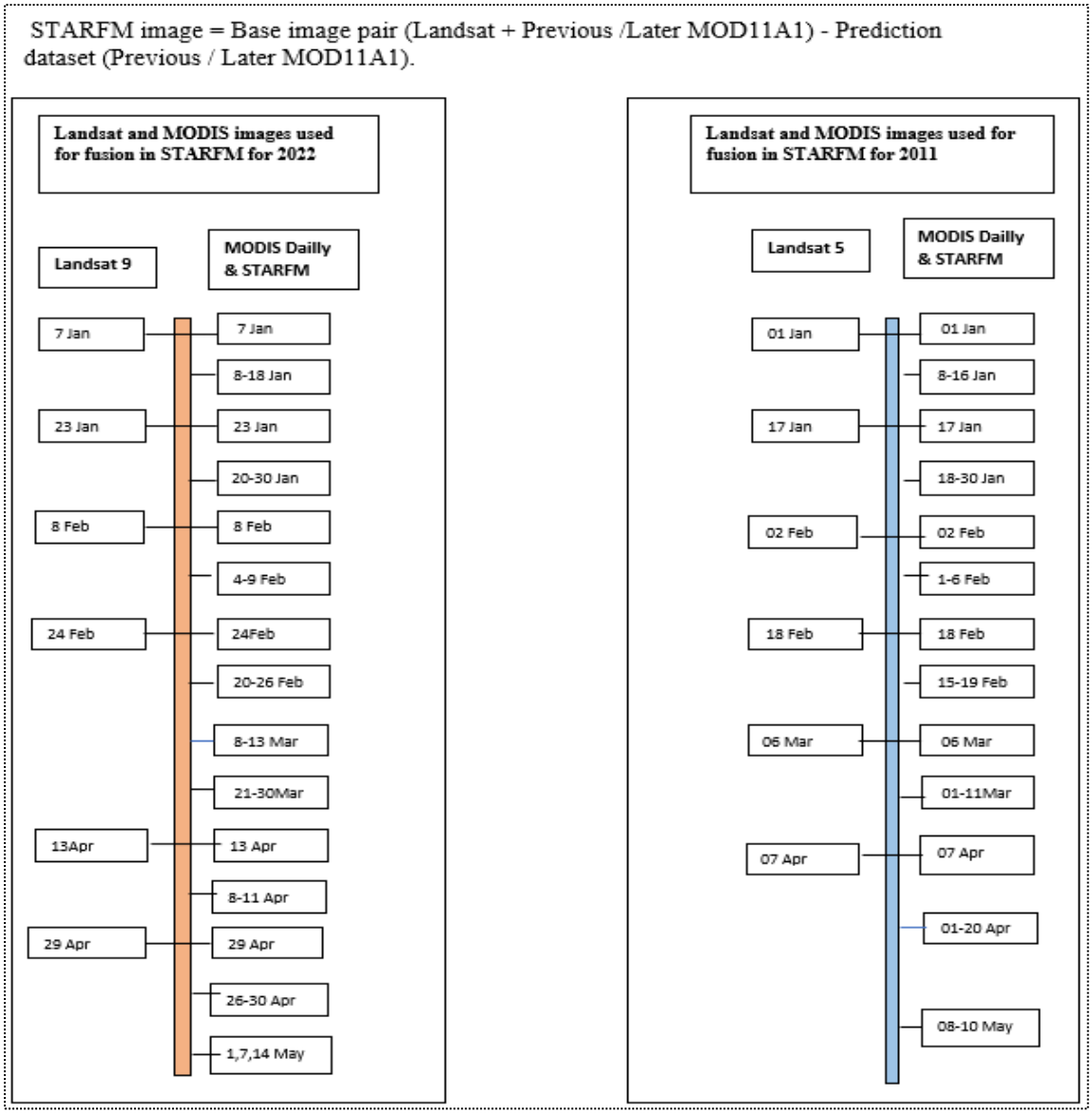

Figure 21: Landsat and MODIS images used for the Fusion process.

4.4 Accuracy of the fusion process

Several studies have confirmed the STARFM based fusion processes as accurate, reproducible, but sensitive to thematic focus (Walker et al., 2012; Emelyanova et al., 2013; Singh et al., 2011). Weng et., al (2014) for example, evaluated the accuracy of STARFM based fusion of Landsat and MODIS using comparison of ground-based point weather datasets and synthetic

LST. In this study, ground weather stations data from only one station in Dhaka were employed, thereby influencing decision to evaluate the accuracy of synthetic Landsat imagery against the real imagery obtained on the same date. Walker et., al (2012) applied a similar accuracy evaluation approach in their forest phenology study. The study predicted Landsat imagery for dates that have existing Landsat scenes and then performed pixel-wise comparison of the two imageries. Due to the size of the imagery, it was used a randomly sampled 10% pixels per imagery pair.

4.4.1 Processing of weather data

The obtained ground-based weather data contained rainfall and air temperature information necessary to account for both land surface and air temperatures contribution to UHI effects. Rainfall dataset provided insights that are complimentary to the air temperature data. The air temperature data provided a metric for comparison with the estimated LST for preliminary accuracy check. The study considered weather data from January to May of 2011 and 2022 respectively. January was considered to show winter to summer transition. Using the inbuilt Microsoft Excel plugins, extract weather data for each day of each month, and then use an excel automatic technique to get the average temperature for each month for each year (Figure: 21). Daily temperature estimates were extracted for the selected years, then geocoded in ArcGIS software with location data from the geometrically corrected imagery and finally pre-processed into either a vector point-temperature or raster air temperature datasets over Dhaka city. Figure 21 provides a seasonal trend of the temperature for each year, 2011 to 2022. Heat map (Table: 15) shows that Dhaka's monthly average temperature for the summer months of January to May, generally varied between 17 and 31 degrees Celsius since 2011 to 2022. May was the hottest month in 2011 whereas April become the warmest month in 2022.

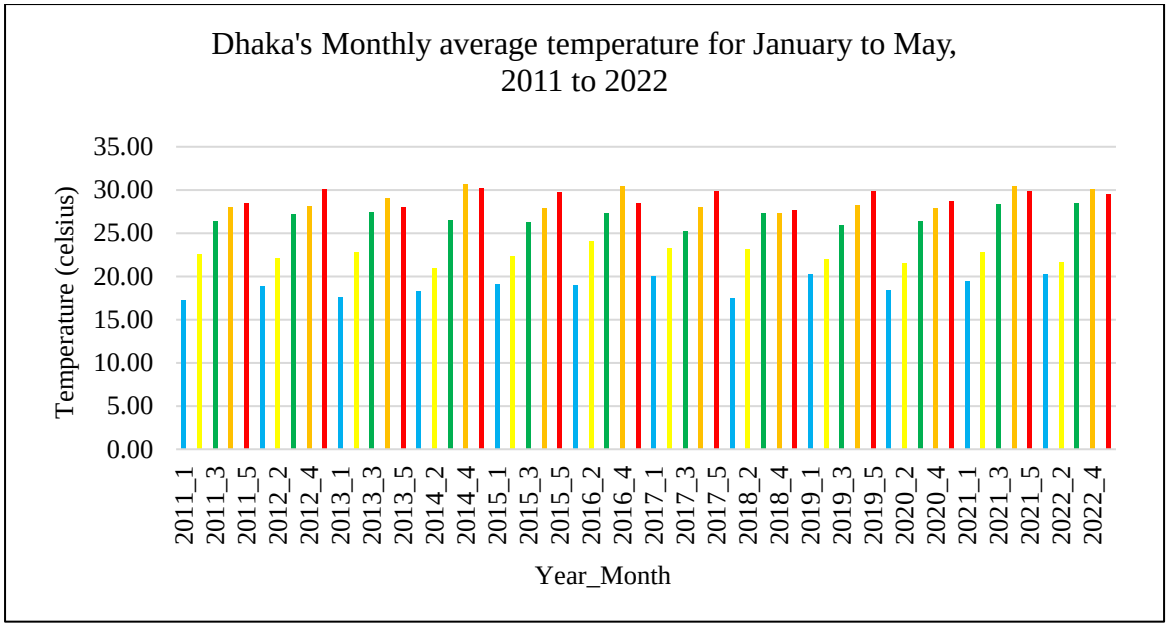

Figure 22: Average temperatures of every five months from year 2011 to 2022.

Average temperature of Dhaka for the study periods (Degree Celsius)

Table 14: Heat map of Dhaka from January to May monthly average temperature (Source: BMD, 2022).

Year	January	February	March	April	May
2011	17.27	22.55	26.38	28.02	28.42
2022	20.24	21.62	28.47	30.04	29.47

4.5 Satellite imagery availability and synthesis of high quality spatio-temporal imagery

Table 13 shows the satellite imagery used in the study. Daily MODIS imagery was available for both 2011 and 2022 at 1km spatial resolution. However, Landsat imagery (Landsat 5 and Landsat 9) was obtained at higher spatial resolution of 30m but with a poor temporal resolution (16 day repeat and no imagery in some months) compared to MODIS. Therefore, using STARFM algorithm, synthetic imagery with high spatial and temporal resolutions were created and samples shown in Figures 22 and 23. Using Landsat and MODIS image pairs shown in the

figures, near-daily images were created for each of the five months consider for both 2011 and 2022.

It should be noted the study could only obtain one Landsat 9 base imagery to use to produce synthetic imagery for both April and May for year 2022. To minimise error, the study ensured that the matching MODIS pair were used to the corresponding synthetic image on the same date as MODIS. Additionally, from the figures 23 and 24, there are patterns of cloud cover in months of March and April in 2022, and May in 2011. Due to the presence of cloud cover, the study used imagery from April as the base of the month of May. Despite this cloud cover, the study involved several imagery because its objective was to simulate exact scenario on the ground. As a result, the land surface temperature trend seen by MODIS images was very slightly impacted by cloud patterns. The similar trend displayed between Landsat, Modis and synthetic imagery is an indicator of the reliability of fusion process.

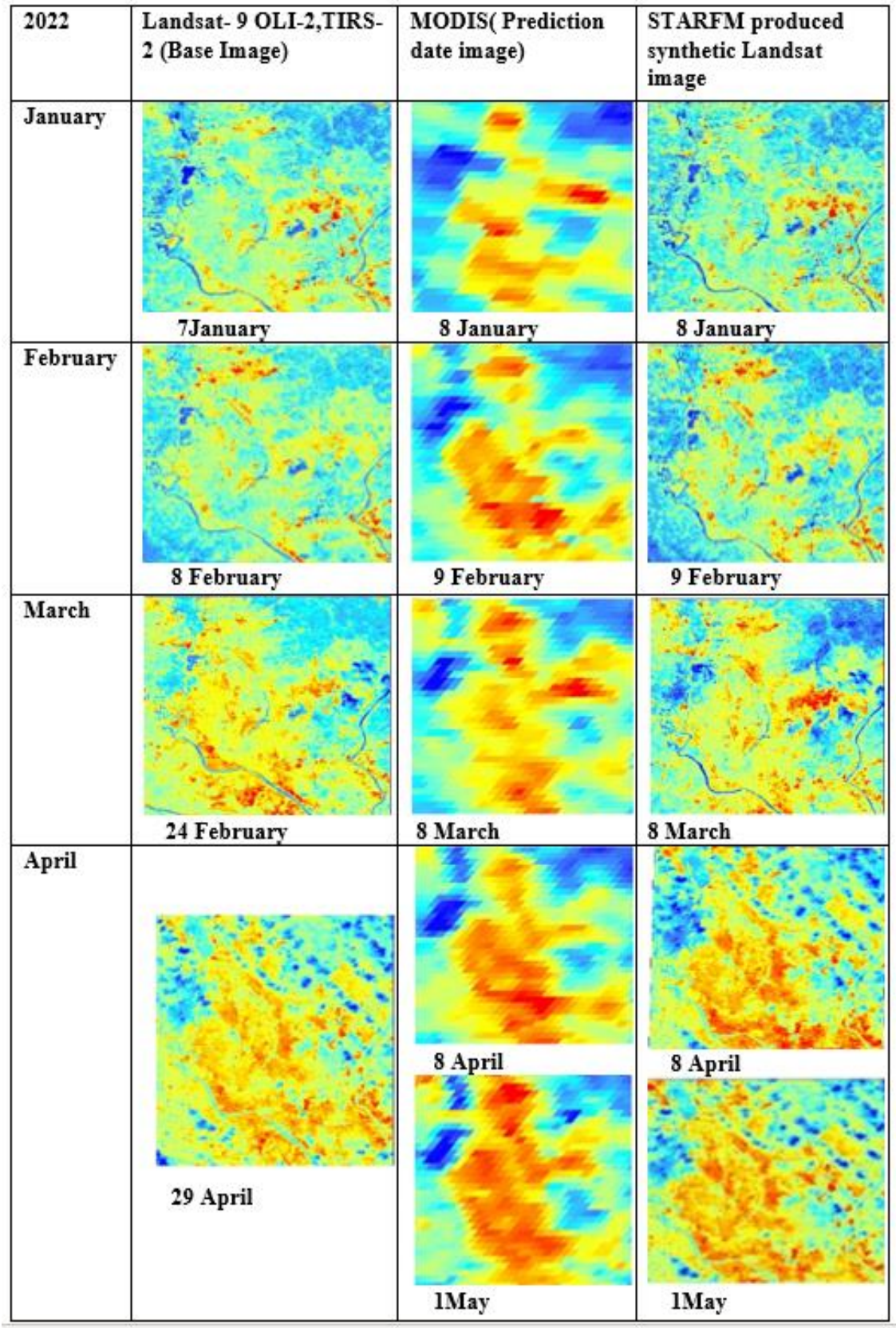

Figure 23: Sample base and predicted pairs of 2022 Landsat-9 and MODIS imagery used to create synthetic images using STARFM algorithm.

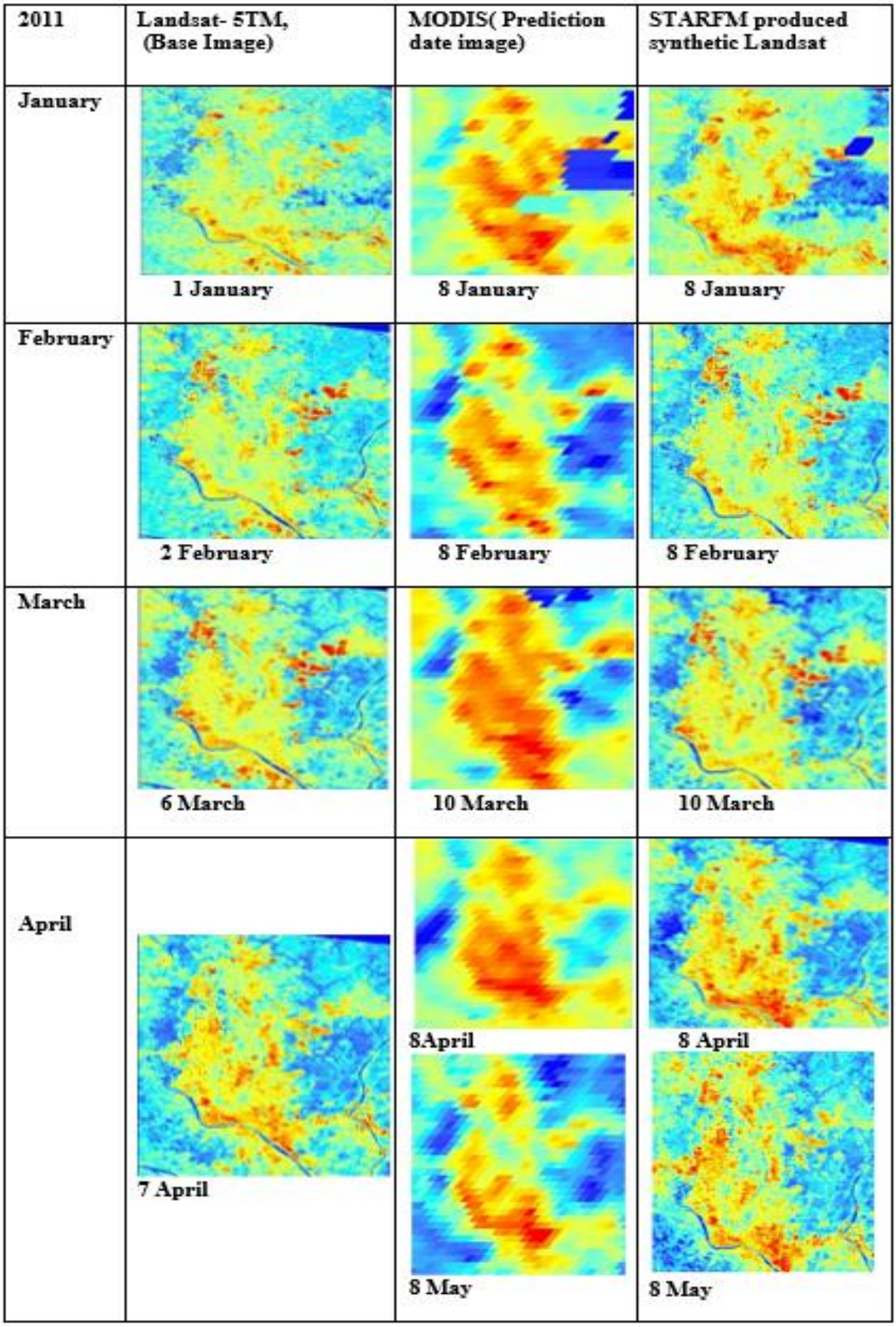

Figure 24: Sample base and predicted pairs of the 2011 Landsat-5 and MODIS imagery used to create synthetic images using STARFM algorithm.

4.6 Estimation of land surface temperature using synthetic imagery

The average seasonal land surface temperature (LST) for 2022 and 2011 respectively. In 2022, the average maximum LST of Dhaka was 39.75^{0}C, compared to 37.06^{0}C in 2011.On the other hand, minimum LST for the study years were 20.27^{0}C and 23.84^{0}C respectively. This is approximately more than two degrees Celsius increment over the twelve-year period in both minimum and maximum temperature. However, a close examination of Figure 25, shows the spatial distribution of the increasing LST over Dhaka city and indicates small pockets of heat islands in 2011 as compared to the distribution of heat islands in over 75% of the Dhaka city with few exceptions in the tips of northeast and northwestern regions. In fact, in 2011, the heat islands reported in small areas around northwestern and eastern areas were due to the construction of large buildings in the area at the time. Areas with the centre and southwest are covered by city centre's predominantly built-up infrastructures. The existence of UHI in Dhaka city has exacerbated over the twelve-year period to a point where there are limited areas with temperatures below 30^{0}C.

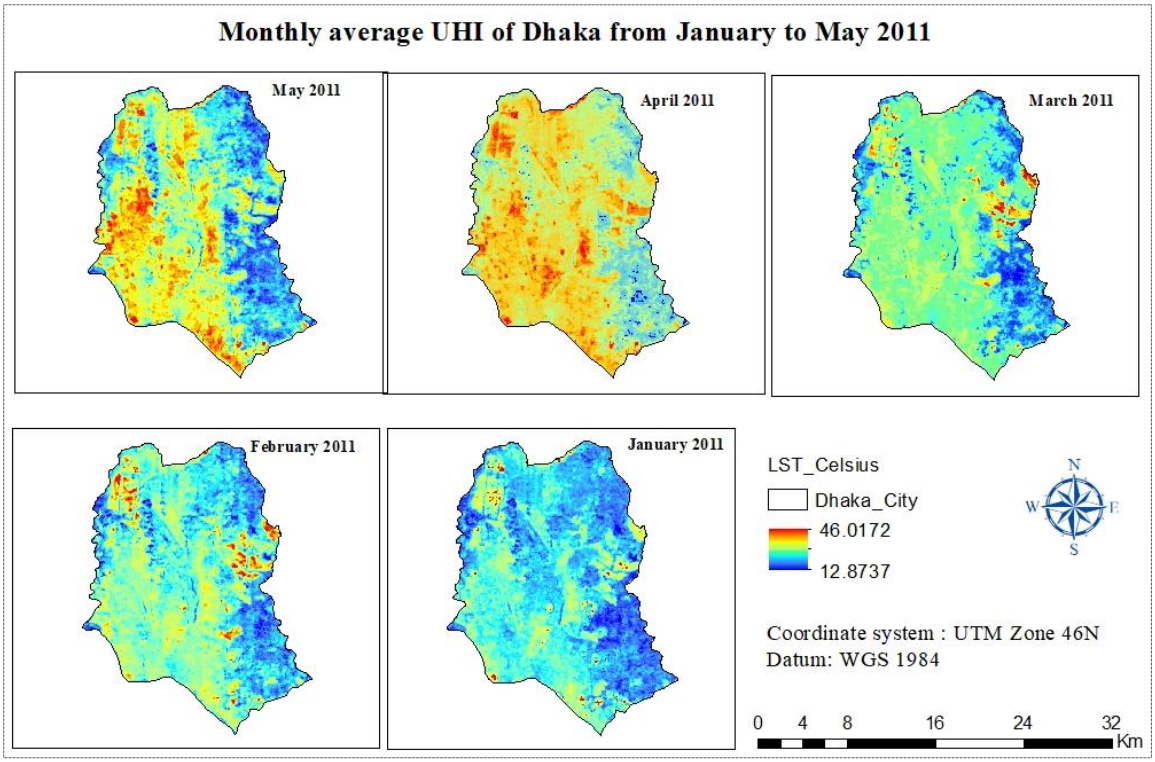

Figure 25: Monthly average LST of Dhaka from January to May 2011 produced with fused images.

As Qureshi and Rachid (2022) noted in their work, a single summer imagery is insufficient to fully represent the UHI complex and dynamic interactions with climate, and landcover, among others. As a result, the study investigated the impacts of UHI throughout the summer season

using monthly average LST as shown in figure 25 for 2011 and figure 26 for 2022. Despite average seasonal temperatures climaxing at 39.75^{0}C for 2022 and 37.06^{0}C for 2011, monthly average temperatures reached 46.18^{0}C and 46.01^{0}C in 2022 and 2011 respectively. The hottest and coldest months were April and January in 2022, May and January in 2011 respectively.

According to local knowledge of Dhaka, temperatures are expected to increase from January to May as the city transitions from winter to summer. However, this trend was observed only in 2011. In 2022, temperatures increased from January to April as expected, but dropped in May. This drop in temperature can be accounted for by examining both (Figure 3 and 5) where the city received high amounts of rainfall throughout the month of May 2022. These heavy rains were attributed to nor 'westers – a localised rainfall and thunderstorm events common in India and Bangladesh which occurred during the months of May 2022 (BDNews24, 2022). Despite April already being the hottest, examining (figure 26) further shows that the occurrence of the cyclonic event on 20th April 2022 contributed to slight decrement of the April's temperature which could have shot beyond the current highest level of 46.18^{0}C.

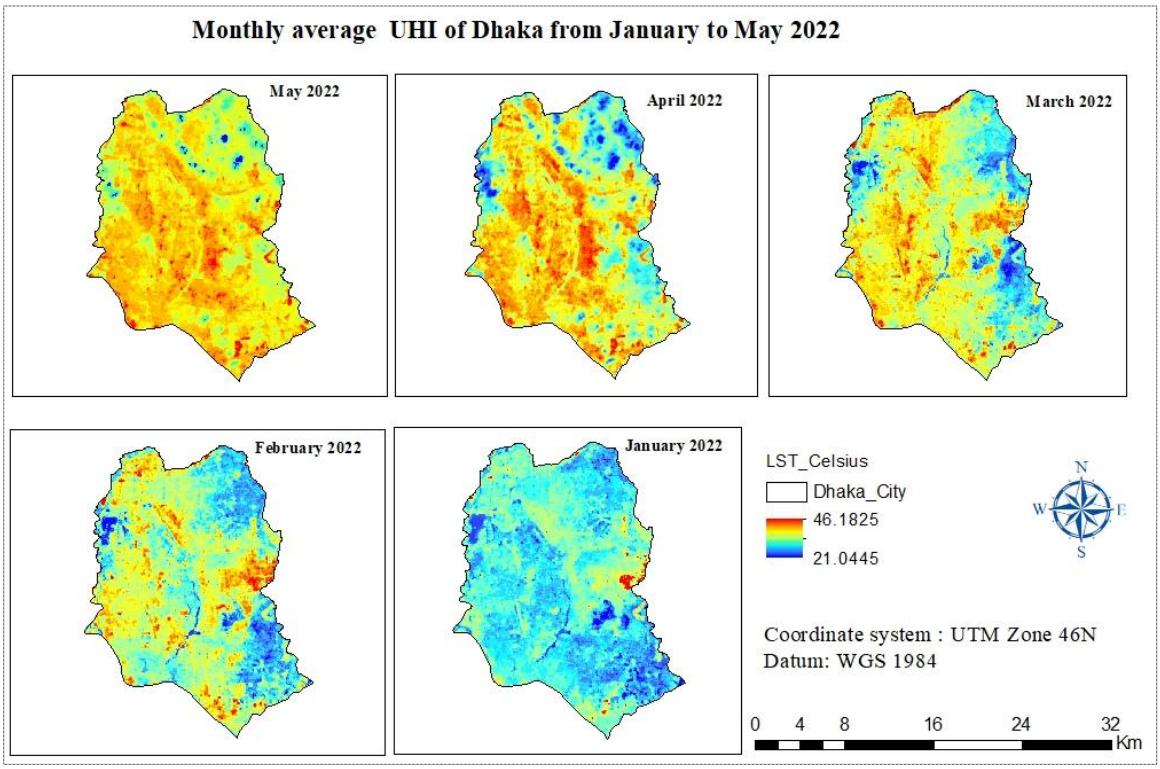

Figure 26: Monthly average LST of Dhaka from January to May 2022 produced with fused images.

Furthermore, small cold patches observed in several LST results such as in May 2011, March, April, and May 2022 are due to the cloud cover presence in the original Landsat and/or MODIS imagery. The cloud cover's effect on the study results could be in numerically minimal and systematic, given that the pattern obtained from LST maps (Figure 27) are similar with the temperature pattern observed from air temperature datasets shown in figure 22. This therefore supports this study's objective of utilising supplementing Landsat with MODIS daily datasets to produce a higher spatio-temporal imagery that can produce LST's with near semblance to ground based temperature.

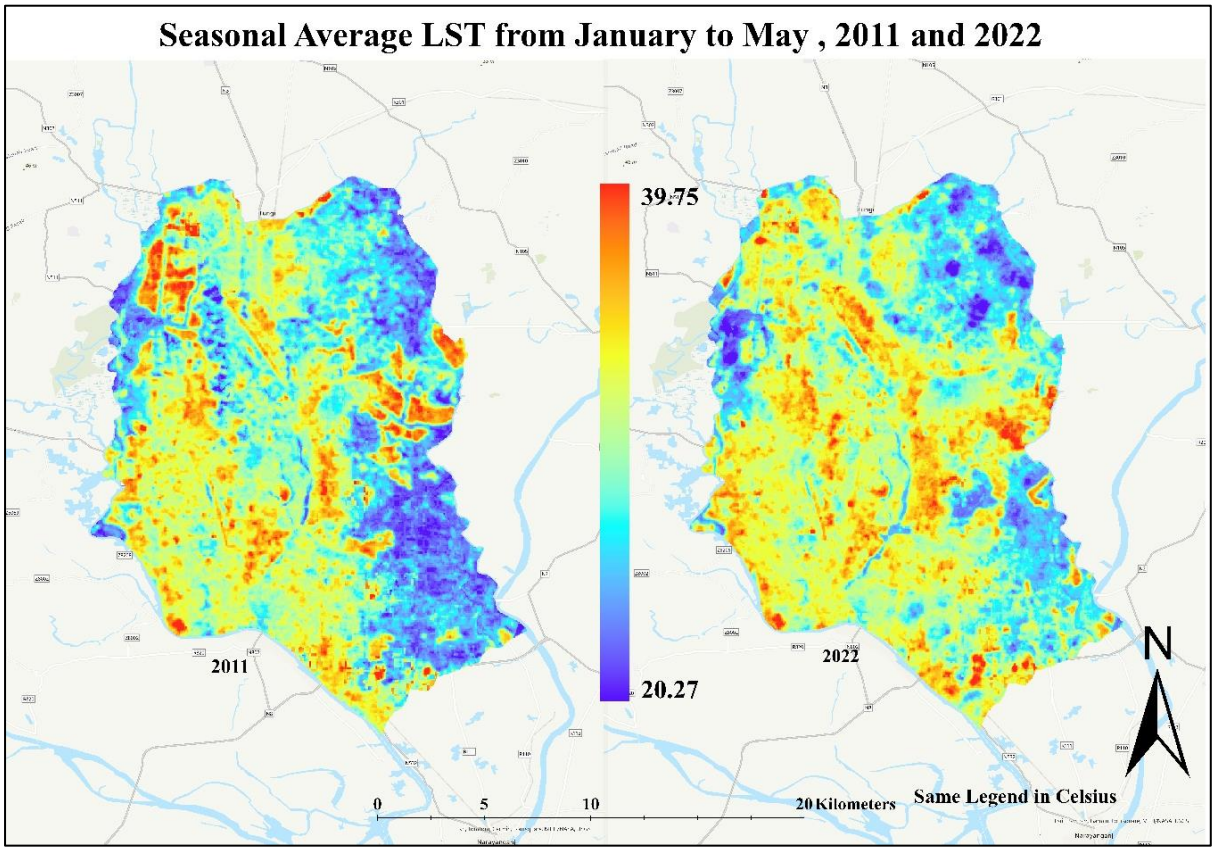

Figure 27: Comparison of Seasonal average LST (STARFM produced image) of Dhaka from January to May for 2011 and 2022 using same legend.

4.6.1 Comparison of different sensor generated LST.

The comparison of seasonal average LST (land surface temperature) between several satellites and STARFM (spatial-temporal adaptive reflectance fusion model) image sensors is shown in the graph.

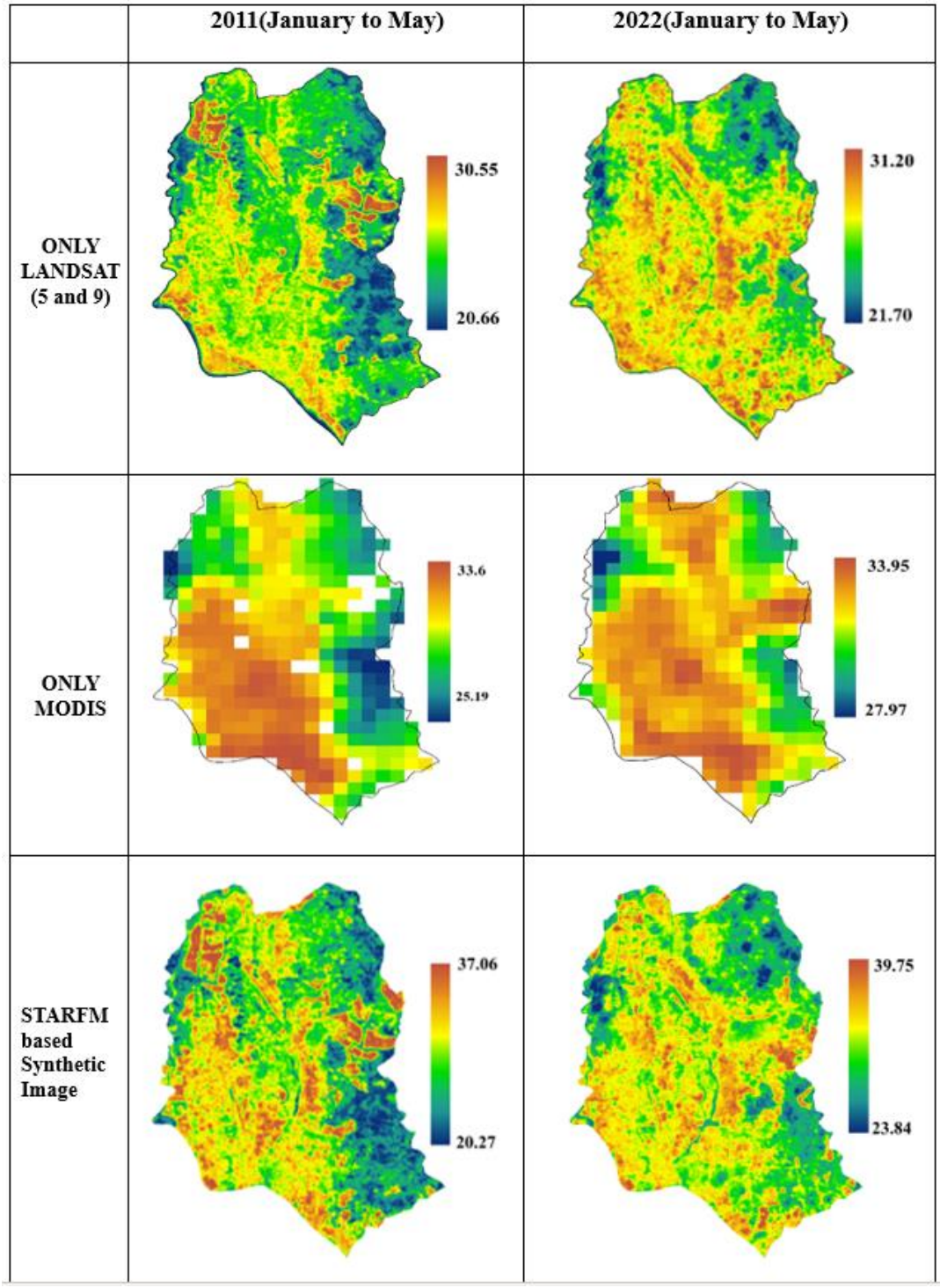

Figure 28: Seasonal average LST comparison between different satellite sensors and STARFM generated imagery for 2011 and 2022. Landsat 5(2011) and Landsat 9(2022).

Integrating various satellite imagery could produce a higher range of values because of capturing data in different spectral bands with different resolutions. By fusing those imagery, they are combined with their strength which could increase spatial resolution, temporal coverage and spectral bands. This fusion often resulted in an intensive dataset which may not be captured by single satellite imagery.

Figure 28 illustrates that all three sensors have comparable seasonal average LST values. In 2011, Landsat 5TM produced LST's were 30.55^0C, MODIS 33.60^0C, and synthetic Landsat, which was merged by combining Landsat and MODIS, resulted 37.06 ^{0}C. On the other hand, in 2022, the trend shows the same temperature in several satellite sensors. The average LST of Landsat 9 was 31.20^0C, MODIS was 33.95^0C, and fused imagery was 39.75^0C.

Single Landsat and MODIS generated LST were lower than synthetic Landsat basis LST. It's possible that combining the imagery enhanced resolution to both and resulted in a more accurate temperature without missing pixels from the specific area. Only MODIS in 2011 showed some missing pixels which are present in fused synthetic Landsat imagery (Figure 28) due to added pixels and increased the intensity of the temperature for the area. In 2011, STARFM based synthetic imagery illustrated more widespread and intensity than only Landsat and only MODIS. However, in 2022, only Landsat represented some widespread in 2022 but more intense in synthetic imagery.

4.7 Comparison of the estimated Land Surface Temperatures with Ground Temperature.

Comparing the air temperature data shown in Figures 22 and table 15 with the temperatures estimated from satellite imagery (Figures 25 and 26) shows similar increasing trends. However, the air surface temperatures are generally lower than the satellite estimated LST.

Ground-based air temperature measurements (Figures 22 and table 15) reveal a consistent upward trend in temperatures over the past 12 years. These measurements, combined with satellite-derived temperature estimates (Figures 25 and 26), provide valuable insights into the urban heat dynamics of Dhaka city. Although, the air temperatures are generally lower than the estimated satellite LST, analysis shows a similar trend between ground-based and satellite-derived temperatures, indicating the reliability of satellite data for monitoring temperature trends in urban areas. Both the air temperature and LST has increased from winter to summer for the respective years.

Furthermore, Dhaka's inadequate number of weather stations may be the reason for the lower values seen in the air temperature readings taken from the ground. Based on the total area of Dhaka city, one weather station is not enough for coverage the spatial resolution of daily temperatures. More than one ground stations are time demand for the study of complex characteristics of Dhaka's weather.

A spatial investigation of temperature patterns in Dhaka reveals the immense magnitude of the UHI impact on the city's thermal environment. It is essential to examine the influence of the UHI effect, due to Dhaka's high population density and substantial urban growth are causing local warming relative to neighbouring rural areas.

Satellite imagery shows higher surface temperatures when comparing less developed or forest-covered regions in the northeast and southeast to more inhabited areas and metropolis corridors. These findings show how man-made heat sources, such as building materials, manufacturing activities, and vehicle emissions, contribute to urban warming and support empirical evidence. Nighttime temperatures data from a similar study by Bohnenstengel et al. (2014) demonstrated that high temperatures remain in urban areas, raising the heat stress for inhabitants, particularly during heat waves and prolonged periods of high temperatures.

Despite the challenges caused by the UHI effect, satellite-based temperature observation is a useful instrument for understanding urban climate patterns and directing mitigation efforts in Dhaka. When governments and urban planners combine satellite imagery with ground-based indicators, they may develop specific plans to mitigate heat-related risks and enhance urban resilience. Cool roof technologies, developing green spaces, constructing building with proper ventilation may reduce the intensity of UHI. Therefore, more sustainable, and healthier environments can be available for the residents. It would also require monitoring and analysis of satellite imagery-oriented temperature to assess the effectiveness of the initiative for the long run.

4.8 Dhaka's LST variation in other studies

It was stated that one single image for a year or each month cannot provide a better resolution of land surface temperature. Seasonal changes in weather, diurnal and nocturnal cycles, and other temporal variables can cause considerable variations in land surface temperatures

throughout time. Using several satellite imagery taken at different periods could provide a more in-depth knowledge of temperature changes.

In general, seasonal fluctuations in plant growth, the amount of water, precipitation, and other variables impact land surface temperature (LST). However, Dhaka's LST trend changes for many reasons within the city. Dhaka is situated in a monsoon climatic zone which includes hot and humid summer, heavy rainfall, and a cooler winter. This kind of seasonal variation also affect LST in Dhaka. Dhaka's LST could also affected by solar radiation, land use changes, vegetation dynamics and atmospheric conditions as the study observed Dhaka has lost its green spaces substantially over the research period. Many studies show contradictory results when it comes to calculating LST of Dhaka. Using imagery from various months allows such variations to be considered for the LST estimations.

The accuracy of LST estimations can be increased by averaging data across time. This is especially crucial when interacting with unclear data or data that has been impacted by short-term irregularities.

Abrar, (2022) research used only one Landsat 8 imagery from 18 April 2021, which could not represent the actual scenario of a whole year. April is considered summer in Dhaka, and due to its geographical position, Dhaka is situated in a monsoon climate zone with at least three seasons of summer, rainy and winter (Corner, R.J., et al. 2014; Rahman et al., 2020). The LST generated by the imagery from April 18, 2021, is a summer-only reflection which would fail to accurately address the temperature variations in Dhaka throughout different climatic seasons. For Abrar, 2022 study, the LST range is from 19.44^{0}C to 32.98 ^{0}C for Dhaka in 2021 (Figure 29a).

Kafy A. (2021), used Landsat 8 image of 15 April 2020 as summer representation and 09 November 2020 for winter. In Dhaka, hot summer starts from March and continue to till May whereas winter comprises the month of November to February (Corner, R.J., et al. 2014). In this study, LST generated from 15 April 2020, illustrated that the minimum LST was 23^{0}C and the maximum was more than or equal to 32^{0}C (Figure 29b). The study also mentioned 09 November 2020 imagery acquisition date as winter and used the only imagery for the calculation of the LST for winter. The study didn't consider other days or months to demonstrate the average temperature for the different seasons.

Hussain et al, 2023, employed three imagery for 2011 to calculate hot spot of Dhaka for three different seasons. Jan 17, 2011, for winter, May 09, 2011, for summer and Sep 30, 2011, for autumn. According to the study, summer temperature for September 30, 2011, was 39.28^{0}C for that specific day (Figure 29c). In Dhaka, June to October is monsoon wet season and a single day of September was not enough to illustrate all other days and study couldn't mention it's a seasonal UHI.

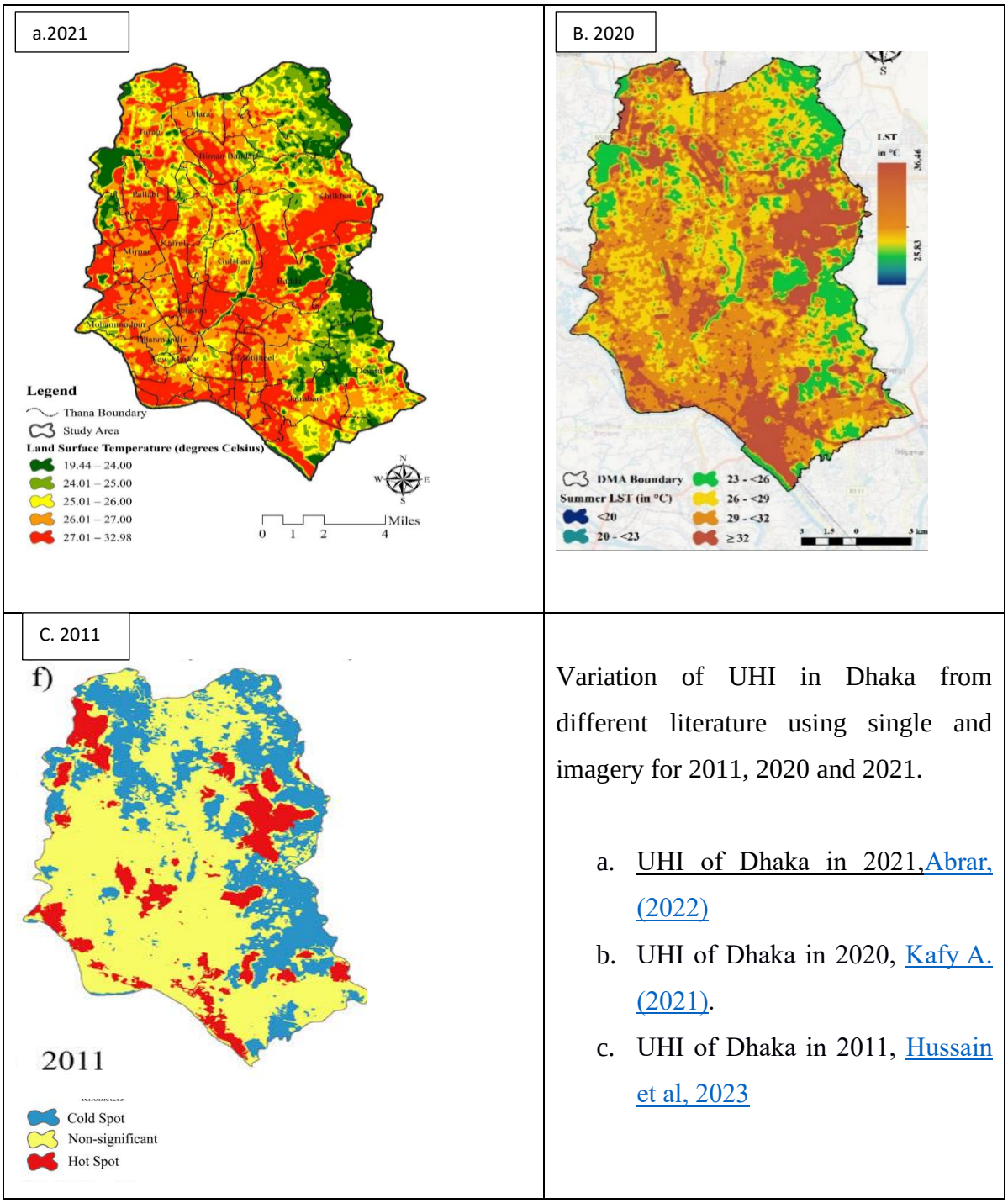

Variation of UHI in Dhaka from different literature using single and imagery for 2011, 2020 and 2021.

a. UHI of Dhaka in 2021,Abrar, (2022)
b. UHI of Dhaka in 2020, Kafy A. (2021).
c. UHI of Dhaka in 2011, Hussain et al, 2023

Figure 29: Examples of different trends of UHI in Dhaka from other studies.

The current study attempted to expose the outcome of integrated satellite images, which offered additional insight into spatial and temporal resolution, allowing the resolution of UHI to be adequately addressed (Figure 24, 25). There was no literature addressing the seasonal UHI of Dhaka in 2011 and 2022, thus this research focuses on the seasonal and winter to summer transitional phenomena of Dhaka's UHI using integrated satellite imagery. From above LST images from different studies, it is observed that Dhaka's temperature has been increased spatially from 2011 to 2022. Highest temperature shown in 2020 is >/32, however it increased almost 1C in 2021. Lowest temperature shown the similar trend for both years ranges 19.44C to 20C. In 2011 temperature was not widespread but its intensity was higher than 2021. According to the knowledge about Dhaka, there were some construction areas in the northeast and east part of the city which was covered with concretes or other materials which contributed to the temperature increasing. This study also focused on the relationship between LST and LULC.

4.9 Relationship between LST and LULC

One of the essential roles of land surface temperature (LST) is in evaluating the impact of landcover land use (LULC) changes in large geographical extents (Rahimi et al, 2021). Ting, 2022 evaluates this impact using correlation models of LST with LULC indicators such as NDVI and NDWI. Others (Walawender et al, 2014 and Connors et al, 2013) aggregate the LULC into two classes (vegetative and non-vegetative) to assess the LST impacts. This approach improves on (Rahimi et al, 2021), by using ArcGIS's zonal statistics tool to assess the impact of LST against each LULC class using minimum, maximum and average metrics shown in Table 17.

Table 15: Minimum and maximum land surface temperature of each landcover class in the hottest months, and hottest seasons of 2011 and 2022

	LST for May 2011		LST for Jan - May 2011		LST for April 2022		LST for Jan - May 2022	
LULC	Min	Max	Min	Max	Min	Max	Min	Max
Greenspace	12.87	44.29	21.44	37.52	21.04	44.61	23.38	38.91
Built area	15.51	46.02	22.29	38.39	25.92	46.09	23.56	39.26

Water	13.33	43.56	21.27	36.45	25.32	43.42	23.13	38.63
Bare ground	13.28	44.85	21.61	37.55	26.20	46.18	23.48	39.40

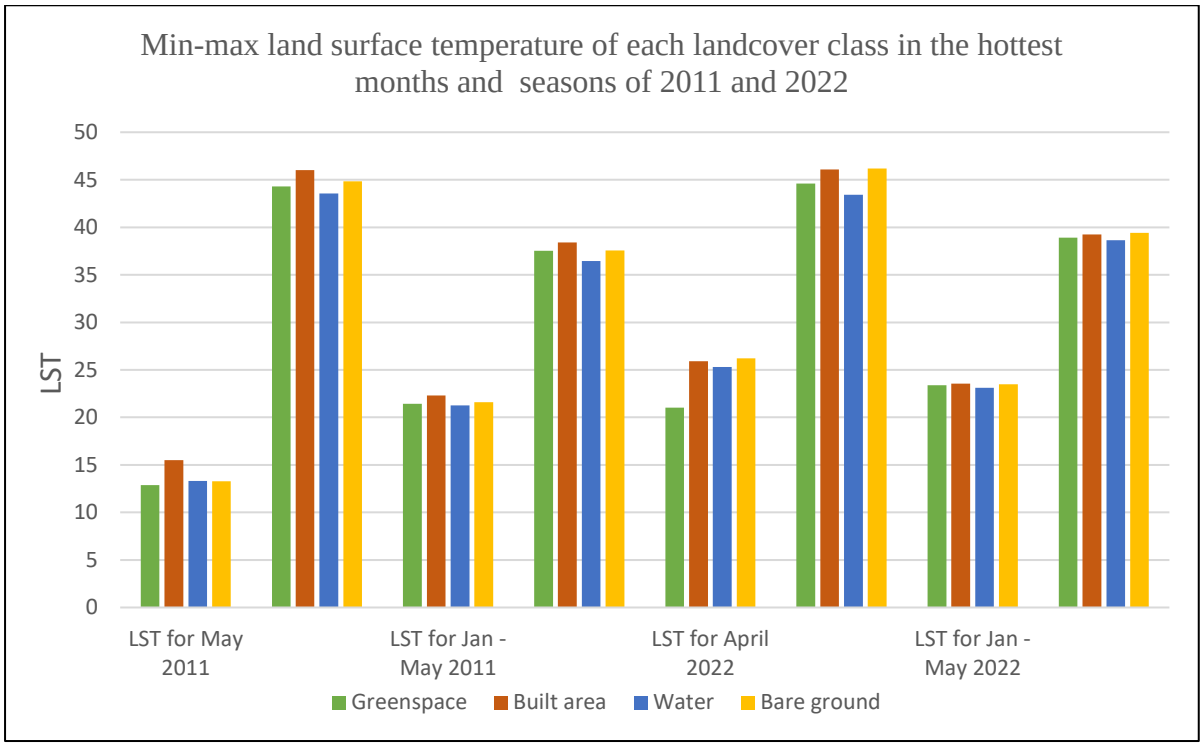

Figure 29a: Graphical representation of LST -LULC relationship for the hottest months and seasons of the study period.

The hottest month of 2011 was May and April for 2022, and the hottest seasons (January to May) in the years 2011 and 2022 respectively. It is evident that built areas emits higher LSTs, followed by bare ground, greenspaces, while water is the coldest. However, over the twelve year there is evidence in temperature saturation, where the difference between LSTs emitted by the different LULC classes becomes very small. For Dhaka, this is attributed to UHI effects due to increased urbanisation, population and built infrastructures such that there is very close proximity between low LST emitting classes (water and greenspaces) and the high LST emitters such as built areas and bare ground areas. Thereby increasing the LST of water and greenspaces. Following outcomes from the analysis are described below.

Built area:

2011: The minimum and highest LSTs were 15.51°C and 22.29°C and 38.39°C and 46.02°C, respectively.

2022: The minimum and highest LSTs were 23.56°C and 25.92°C and 39.26°C and 46.09°C, respectively.
Among all classifications, built regions continuously exhibit the greatest LSTs, underscoring the major heat input of metropolitan infrastructures. The lowest and maximum LSTs have both risen over time, suggesting an increase in urban heat brought on by elements like greater population density and increasing building.

Bare ground

2011: The minimum and highest LSTs were 13.28°C and 21.61°C and 37.55°C and 44.85°C, respectively.
In 2022, the minimum and highest LST values were 23.48°C and 26.20°C and 39.40°C and 46.18°C, respectively.
A further finding is that second only to developed areas, bare ground regions have high LSTs. The gradual rise in both temperature minimums and maximums points to more urbanisation and the baring of natural land.

Green spaces

2011: 12.87°C to 21.44°C was the minimum LST range and 37.52°C to 44.29°C is the highest LST range.
2022: The minimum and maximum LSTs were 21.04°C and 23.38°C and 38.91°C and 44.61°C, respectively.
The observation was that the cooling impact of green spaces is demonstrated by their lower LSTs when compared to developed areas and bare land. Still, there has been a discernible rise in both the maximum and minimum LSTs throughout time, maybe as a result of urbanisation and a decrease in vegetative cover.

Water

2011: 13.33°C to 21.27°C is the minimum LST range and 36.45°C to 43.56°C is the highest LST range.
2022: The lowest LST is between 23.13°C and 25.32°C, and the highest LST is between 38.63°C and 43.42°C.
Across all land cover categories, water bodies consistently have the lowest LSTs,

highlighting their cooling function. Despite this, LST has increased over time, demonstrating the impact of neighbouring high-LST regions (such as urban heat islands).

Considering the findings (Figure 29a), it is important to discuss how seasonal fluctuations have shaped Dhaka's surface temperatures. A persistent pattern of high LSTs during most of the study duration (January to May) supports this view. This has important policy implications as well since the study can help shape Dhaka's urban policy. In order to evaluate the heat-absorbing qualities of impermeable surfaces, for example, and to explore more environmentally friendly alternatives for building materials and short- and long-term greening projects, city planners can take use of the highest LST findings displayed by built-up regions. Greenery, or vegetated areas, helps keep temperatures lower next to bodies of water because they can absorb a lot of heat. Figure 11 illustrated that the planning authority has improved some water areas from 2011 to 2022. Hatirjheel lake has been expanded in the middle (Figure 11) of the city which enhanced aesthetic landscape of the city as well as managing the heat. Dhaka city corporations (both DNCC and DSCC) are working to encourage people to install green roof within the city.

4.10 Chapter Conclusion

For more than a century, UHI has been an increasing concern across worldwide. Considering the rising urbanisation of emerging nations, UHI evaluation continues to be an essential instrument for urban and environmental planning. The study demonstrated the utility of high spatio-temporal imagery for estimating UHI in Dhaka city and shown the existence of UHI in Dhaka city, that has been gradually increasing over the past twelve years. In demonstrating the UHI existence, land surface temperatures (LST) were derived from satellite imagery and compared with ground-based air temperature collected from a ground station in Dhaka city. Numerous previous literatures demonstrate Dhaka's LST, but they did not consider various satellite imagery for geographical and temporal resolution. Future research should consider the spatio-temporal resolution for an improved understanding of land surface temperature as well as urban heat islands to comprehend the zonal seasonal heat intensity in Dhaka as well as Bangladesh.

To summarise, this study demonstrates that the STARFM approach is appropriate for generating synthetic Landsat imagery for an urban area like Dhaka to gather additional

information about surface temperatures and this approach is still novel for Dhaka and Bangladesh too. The project's limitations were Landsat's 16-day return cycles and cloud cover in the study area. MODIS 1km spatial resolution was also unable to cover the correct pixels in this research region. However, while this research overlooked cloud coverings, it included minimal cloud covered imagery to analyse the LST of the cloud-based day as well. Another disadvantage was that the study area's Landsat acquisition period was during the day, but the research aimed to use nighttime images to prevent solar radiation and other physiological effects. As a result, daytime MODIS data has been combined with Landsat images. MODIS, on the other hand, has both day and night datasets available.

While the approach has certain limitations, the findings are satisfactory and may be used to compute the UHI on days without Landsat overflights. Cloud cover could have an impact on Landsat imagery, reducing the amount of cloud-free imagery. Because of STARFM's efficiency in creating synthetic data, UHI computations are possible even on cloudy days while imagery from Landsat is unavailable. There is an interval in time between successive overflights of Landsat satellites, due to specific revisit cycles. By combining data across the intended duration, STARFM can assist in filling up these temporal gaps and enable continuous UHI assessment over extended timeframes.

Improvements might be achieved by confirming the input imagery of Landsat and MODIS for the research region, especially by employing in real time data. Another enhancement in future research might be the use of higher-resolution data from unmanned aerial vehicles (UAV), such as drones, to learn more about the 3D structure of the city, as well as the integrating of fusion-based imagery to boost spatial resolution even more. Cloud pixel reconstruction techniques might potentially be used to improve temporal resolution.

5. CHAPTER FIVE - CONCLUSION

5.1 Thesis Conclusion

The thesis aimed to assess the urban heat island vulnerability of Dhaka city using multi-temporal and multi-spectral satellite imagery. First, a thorough, comprehensive study of the literature was carried out to assess the historical and contemporary urban heat island impacts in Dhaka. Next, using cutting-edge techniques, the study quantified the various land uses and land covers in the city during the study period, a twelve-year term, from 2011 to 2022.

Throughout the analysis, following objectives has been achieved and summarise below.

a. Quantify the land use land cover changes over Dhaka city from 2011 to 2022.

The research quantified various land use and land cover changes in Dhaka during twelve-year period from 2011 to 2022 which has been in details in chapter 3. The method utilised to address LULC determinations were the latest and sophisticated in that field. This method involved technology and scientific understanding. The results illustrated that the city is changing in its landuse and landcover which is gradually transformed to built up areas. This change has a significant impact on green spaces. This study's capacity to provide generalised vegetation indices (NDVI)for various LULC in Dhaka (thana scale) for the first time, as indicated in Table 5,6 would significantly enhance LULC categorization procedures in the future.

b. Estimate the urban heat island of Dhaka city and its change over time using multi-temporal satellite imagery, census, and ground weather data.

Using integrated satellite imagery to estimate UHI was another crucial objective of this study. Research estimated UHI utilised multiple datasets and identified that single imagery with high spatial or temporal resolution is not enough to estimate the accurate UHI intensity for the study area. Figure 27 shows the difference between single Landsat, MODIS and fused imagery based LST which is novel for Dhaka city and significant for future studies. Recent population census and city boundary map provided insights to analyse population dynamics and their density throughout the city at thana scales. Increasing population has influence on decreasing green spaces due to demand of housing and their activities which contribute to enhance urban heat. Ground weather data from Dhaka used to validate satellite produced temperature and understanding weather of the city.

c. Determine the significant land use land cover variables for heat vulnerability in Dhaka City.

The study utilised different LULC variables to justify heat vulnerability in Dhaka. Built area, green spaces, water body and bare ground, all these feature classes have their own correlation to the heat (Table 17). Green spaces often associated with lower temperature which has natural cooling effect to reduce heat vulnerability. Built areas and bare grounds have the capacity to reflect heat due to no vegetation. These influence increase urban heat.

In addition, the urban heat island (UHI) impacts inside the city and by LULC class were evaluated utilising a novel methodological approach for Dhaka that used integrated multi-spectral and multi-temporal Landsat (5 and 9) and MODIS (Terra) satellite images. Finally, the study analysed the influence of UHIs on the city's green spaces and other feature classes, comparing predicted land surface temperatures to ground-based temperatures to verify the accuracy of the methodologies implemented. Along with the assessment and analysis of UHI in Dhaka, the study's thorough examination into the dynamics of the LULC transformations has produced significant information into the intricate interactions between urbanisation, climate change, and environmental sustainability.

Novel analytical techniques of the research and thorough data analysis have illuminated important patterns and trends influencing the patterns of urban climate of Dhaka. Even though the study has significantly advanced our knowledge of urban heat mechanics and how they relate to land cover transformations, it is important to recognise both the study's limitations and strengths and recommend possible directions for further research.

The study's fusion of several remote sensing satellite datasets for UHI estimations and cutting-edge analytical methods, such as vegetation Indexes for green space identification and for LULC mapping using Maximum Likelihood Classification, are some strong points. This multi-dimensional approach has enabled the study to capture the spatial and temporal complexities of urban land cover dynamics and their implications for UHI intensity accurately. Additionally, the utilisation of data fusion algorithms, such as the Spatial and Temporal Adaptive Reflectance Fusion Model (STARFM), has enhanced the spatio-temporal resolution of satellite imagery, thereby improving the accuracy of seasonal UHI estimations and trend analysis, as the novel contribution for Dhaka city. Due to STARFM's efficiency in creating synthetic data, UHI computations were made possible even on cloudy days where imagery from Landsat is unavailable. Also, there is a sixteen-day interval in time between successive overflights of Landsat satellites, due to specific revisit cycles. By combining data across the intended duration, STARFM can assist in filling up these temporal gaps and enable continuous UHI assessment over extended timeframes.

5.2 Limitation of the study

5.2.1 Satellite data

Despite these strengths, the study met some limitations. The accuracy of UHI estimate and LULC categorization may be impacted by uncertainties relating to atmospheric conditions, spectral mixing, and sensor calibration that may be introduced by depending too much on satellite imaging and remote sensing data. By using reliable data from ground-based weather stations to precisely calibrate the satellite-based LULC and UHI estimate models, these uncertainties can be reduced. The study would be more feasible if the Landsat satellite imagery from nighttime would be available. MODIS has different temporal resolution, but Landsat for Dhaka was available for morning only. Since the research was aware that this may lead to a margin of error, an effort was undertaken to use datasets from the days and months when the study periods were most similar. In addition, the shadow effects cast by taller buildings on shorter structures can lead to misrepresentation in the recorded data because of the influence of building heights and materials with varying radiative properties, like glass and concrete, on the distribution of solar radiation in a typical urban area.

5.2.2 Meteorological data

Dhaka belongs to only one ground weather station situated in Agargaon within the metropolitan area which may influences the results that are collected. Moreover, though ground-based temperature observations offer significant validation, their accurate representation and application for larger-scale study may be limited by constraints in their temporal and spatial resolution. Also, the results may not be as suitable and applicable to other metropolitan city with distinct demographic and environmental features due to the study's particular emphasis on Dhaka.

5.3 Recommendations for Future Works

Within this study, the importance of fusing MODIS and Landsat to provide multitemporal and multispectral images has been researched to estimate land surface temperature (LST) and evaluate the impacts of urban heat islands (UHI) in Dhaka.

To enhance the precision of LULC categorization and UHI estimate at more precise geographical scales, future studies may investigate the use of high-resolution remote sensing data, such as LiDAR and hyperspectral images. Use of Unmanned aerial vehicles (UAV) with high resolution will also be a good choice. Furthermore, the integration of machine learning methods and spatial modelling methodologies may augment the prospective potential of UHI

modelling and accelerate scenario-based evaluations of forthcoming urban expansion and climate change consequences.

Further research efforts could expand the focus to include other components of UHI effect, like health vulnerability indices, are also crucial to improving knowledge of the complex correlation between urbanisation and climate relationships, and their impacts on public health outcomes. One potential way to highlight the health risks and socioeconomic inequalities caused by urban extreme heat is to integrate health vulnerability evaluations with UHI analysis. This assessment can enable future researchers to pinpoint Dhaka's populations at heightened risk of heat-related illnesses and mortality, shedding light on the complex interplay of socio-demographic factors, including age, income, and access to healthcare, within the urban landscape.

While this study represents a significant step towards understanding the complex interactions between urbanisation, land cover dynamics, and urban heat dynamics in Dhaka, continued interdisciplinary research efforts are needed to address collaborative research gaps in Dhaka amongst researchers, public health practitioners, urban planners, and policymakers. By integrating expertise from diverse fields, future studies can combine research outcomes with actionable case studies and innovative solutions that promote the health and well-being of urban populations in the face of climate change.

Study advises (Morabito, M et al., 2016; Pineo, H., 2022) local planning authorities to consider the impacts of LST on all facets of urban growth and implement strategies to control the ensuing repercussions on the environment and people, supports these findings. These impacts may be lessened by using and putting into practice various sustainable planning techniques, such as cool roofs, cool pavement, green roofs, and buildings with the best possible designs. While cool roofs are covered in white materials like polyurethane and acrylic, green roofs are covered with a variety of plants (EPA 2017). Cool roofs emit extremely little heat and can reflect up to 99% of solar radiation (Santamouris, M., 2014). By reducing heat through evapotranspiration, green roofs provide shade (EPA, 2014, 2017). A park with trees or a two-inch layer of grass might be covered by a green roof (Pineo, H., 2022). As of June 2018, there were about 8.5 million square feet of installed or planned green roofs in the United States, indicating the growing popularity of this trend (Santamouris, M., 2014). This kind of cool-city approach can be approved by the Dhaka city planning authority.

Advocating for policy interventions that prioritise the development of resilient and inclusive cities, including urban greening initiatives, improved access to cooling infrastructure, and enhanced social support networks, will be essential for mitigating the adverse health impacts of urban heat and fostering equitable and sustainable urban development. To comprehend the underlying implications of UHI in communities, this study concludes by recommending that future research take community engagement into account. It is crucial to include these impacts in the planning and modelling of UHI effects.

Appendices

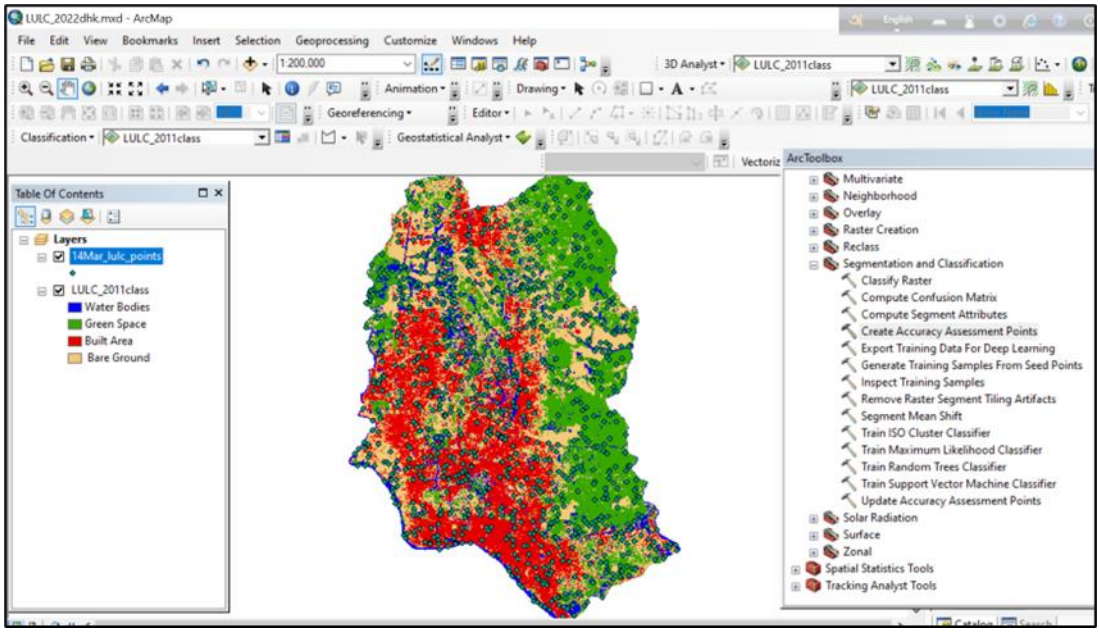

Figure 30: Creation of stratified random points.

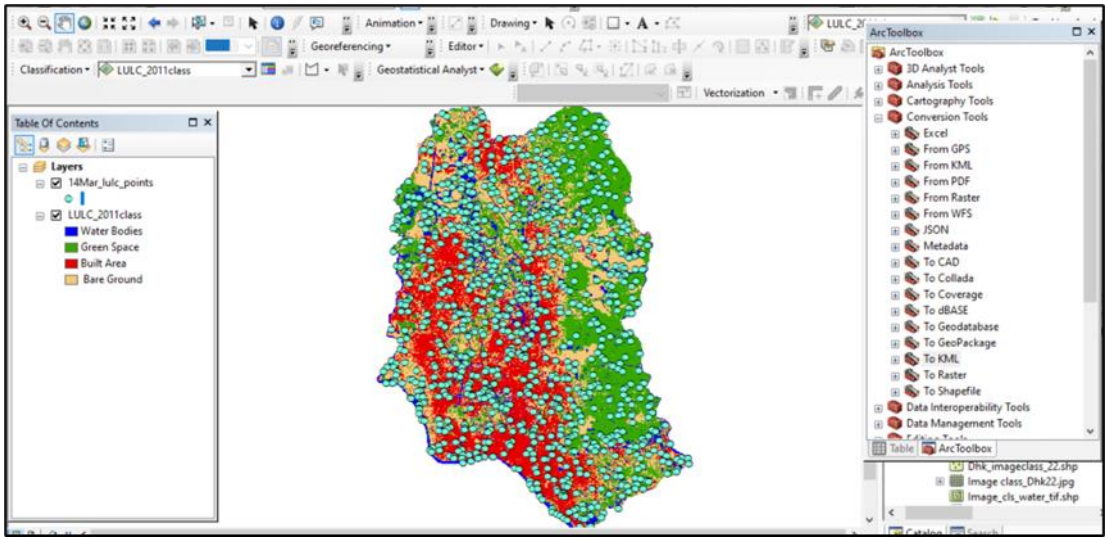

Figure 31:Converted points to Google's Keyhole Markup Language (KML) file.

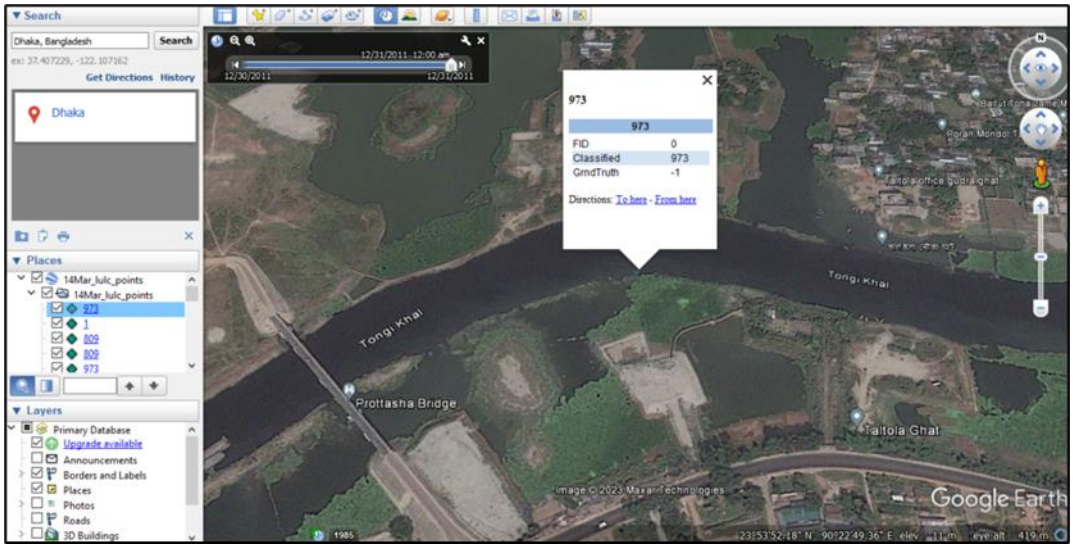

Figure 32: Checking the accuracy of each point.

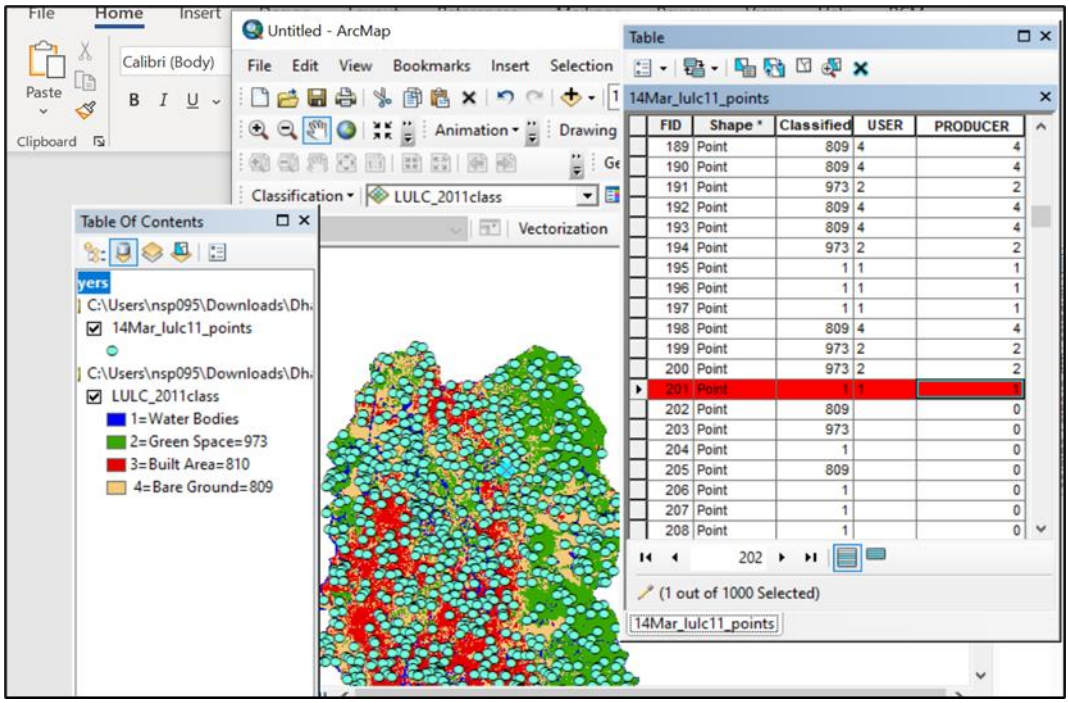

Figure 33:User and producer accuracy compare with the validation result from Google earth.

Java scripts for GEE codes

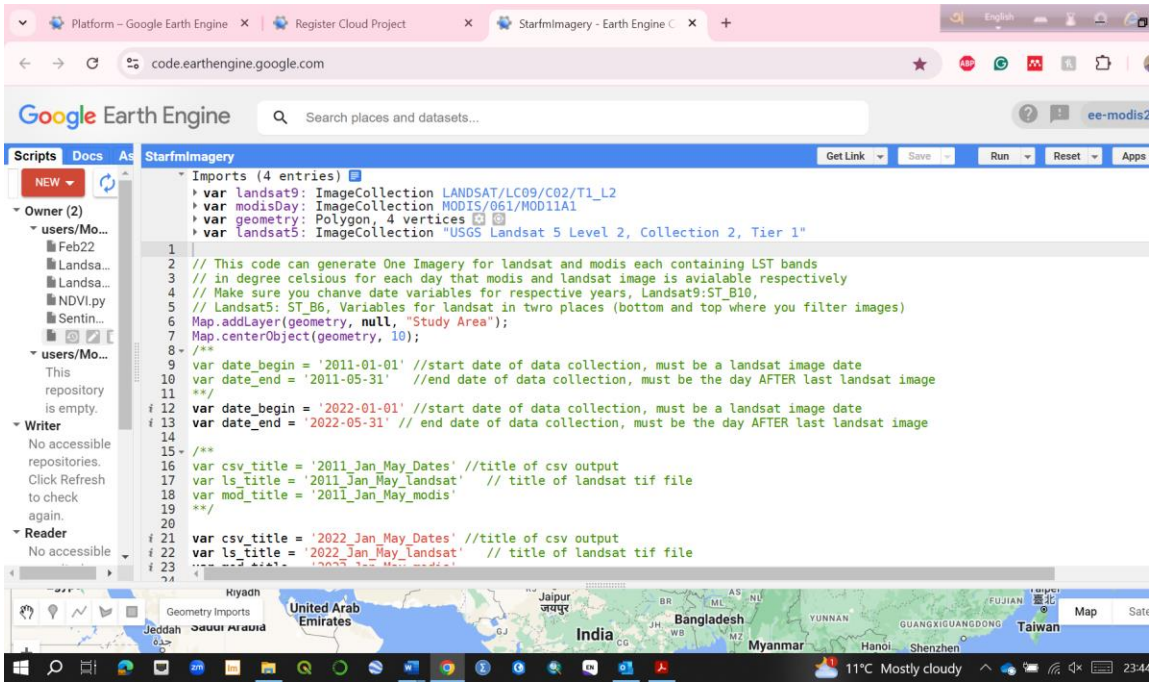

Figure: 34 JavaScript

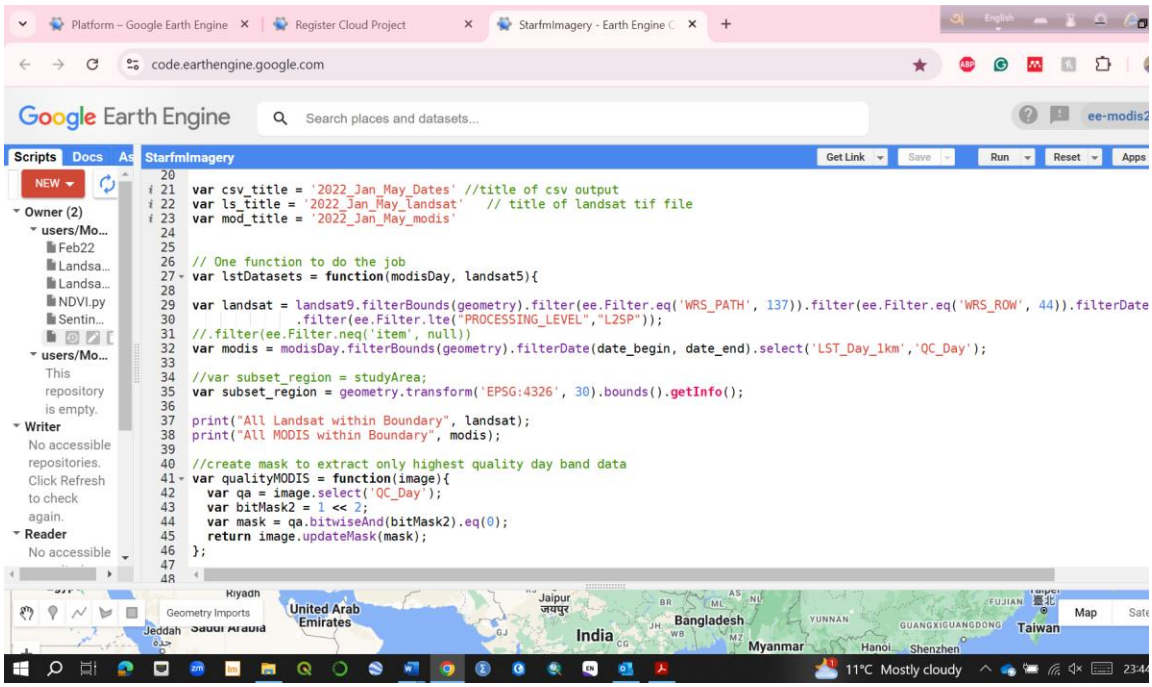

Figure: 35 JavaScript

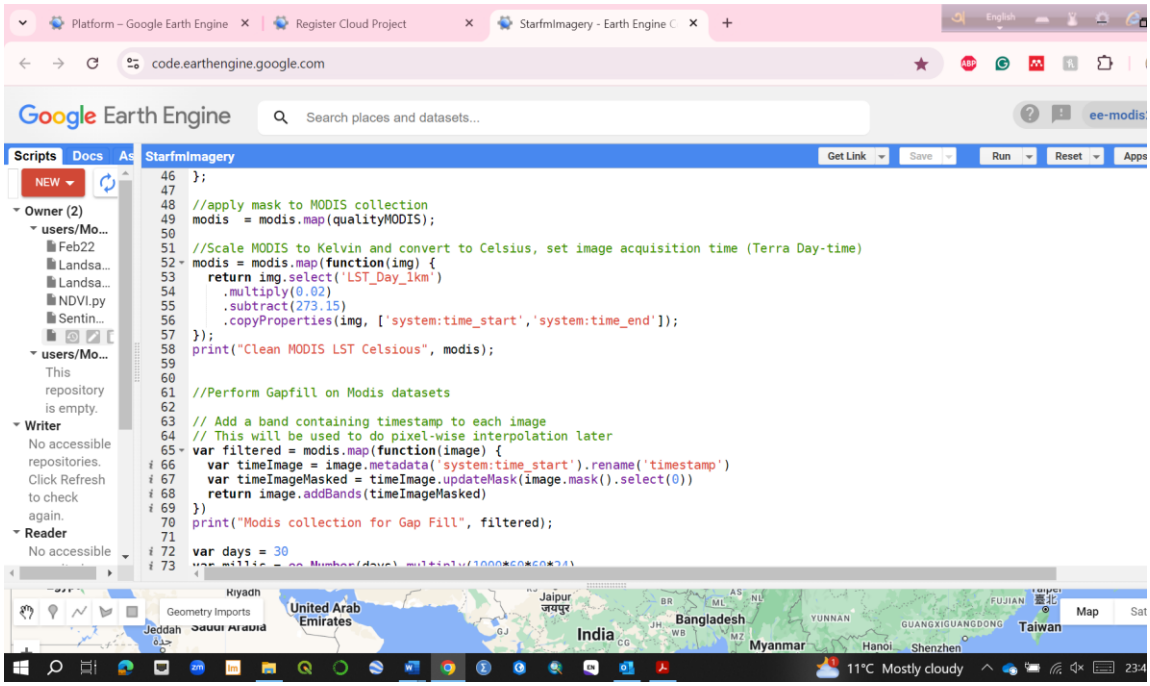

Figure: 36 JavaScript

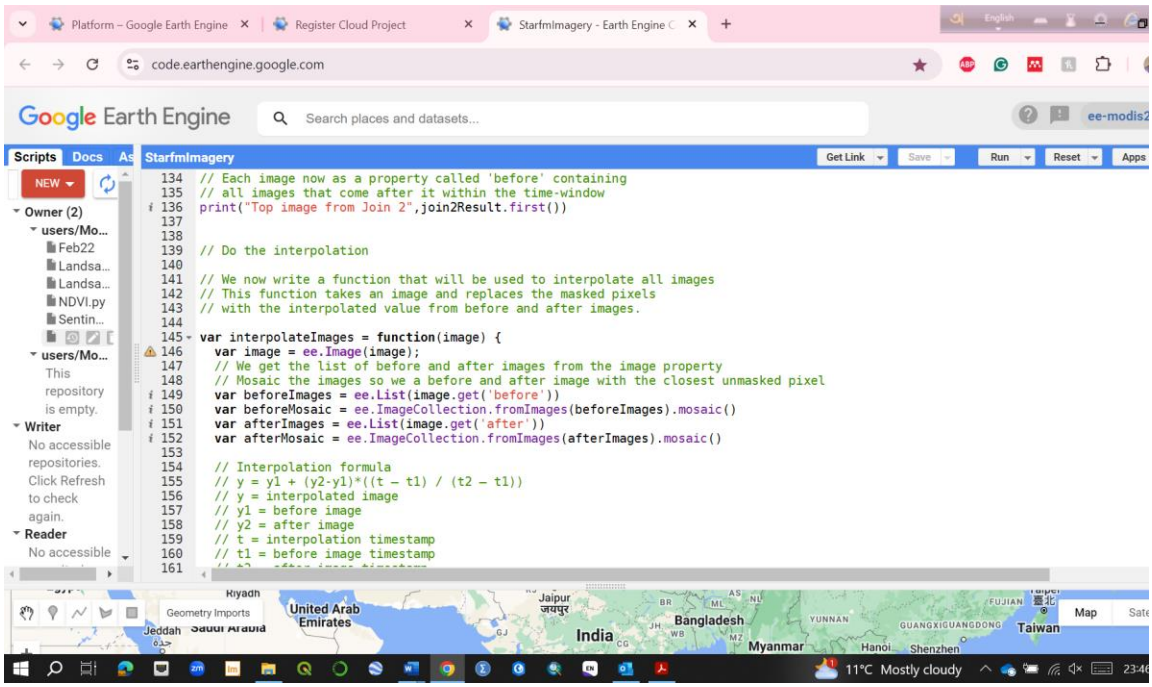

Figure: 37 JavaScript

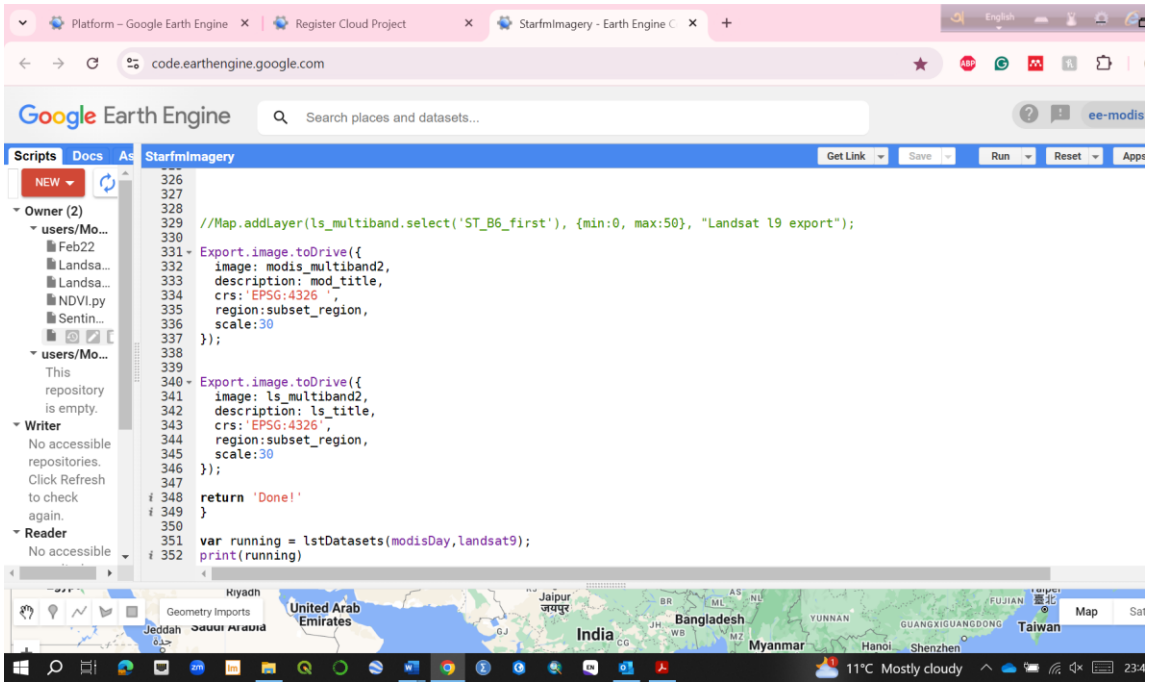

Figure: 38 JavaScript

References

Abebe, G., Getachew, D., & Ewunetu, A. (2022). Analysing land use/land cover changes and its dynamics using remote sensing and GIS in Gubalafito district, Northeastern Ethiopia. SN Applied Sciences, 4(1), 30.

Abineh Tilahun, Bogale Teferie. Accuracy Assessment of Land Use Land Cover Classification using Google Earth. American Journal of Environmental Protection. Vol. 4, No. 4, 2015, pp. 193-198. doi: 10.11648/j.ajep.20150404.14

Abrar R, Sarkar SK, Nishtha KT, Talukdar S, Shahfahad, Rahman, A, Islam, A. R. M. T., & Mosavi, A. (2022). Assessing the Spatial Mapping of Heat Vulnerability under Urban Heat Island (UHI) Effect in the Dhaka Metropolitan Area. Sustainability (Switzerland), 14(9). https://doi.org/10.3390/su14094945.

Abudu, D. & Parvin, N. (2022). A GEE JavaScript program for Landsat and MODIS land surface temperature data pre-processing. Available online at: https://code.earthengine.google.com/a6e641b410d8ccab0816b1aeb0d57bc9

Abudu, D. & Parvin, N. (2022). A Python based script for implementing STARFM fusion algorithm for Landsat and MODIS satellite imagery. Available online at: https://github.com/dandas102/STARFM-fusion-process .

Aflaki, A., Mirnezhad, M., Ghaffarianhoseini, A., Ghaffarianhoseini, A., Omrany, H., Wang, Z. H., & Akbari, H. (2017). Urban heat island mitigation strategies: A state-of-the-art review on Kuala Lumpur, Singapore and Hong Kong. Cities, 62, 131-145.

Ahmed, B., Kamruzzaman, M. D., Zhu, X., Rahman, M. S., & Choi, K. (2013). Simulating land cover changes and their impacts on land surface temperature in Dhaka, Bangladesh. Remote sensing, 5(11), 5969-5998.

Ahmed, I. (2014). Factors in building resilience in urban slums of Dhaka, Bangladesh. *Procedia Economics and Finance*, *18*, 745-753.

Alademomi, A. S., Okolie, C. J., Daramola, O. E., Akinnusi, S. A., Adediran, E., Olanrewaju, H. O., ... & Odumosu, J. (2022). The interrelationship between LST, NDVI, NDBI, and land cover change in a section of Lagos metropolis, Nigeria. Applied Geomatics, 14(2), 299-314.

Ali, S. H., Fallah, M. P., McCarthy, J. M., Keil, R., & Connolly, C. (2022). Mobilizing the social infrastructure of informal settlements in infectious disease response–the case of Ebola virus disease in West Africa. Landscape and Urban Planning, 217, 104256.

Allan, A., Soltani, A., Abdi, M. H., & Zarei, M. (2022). Driving forces behind land use and land cover change: A systematic and bibliometric review. Land, 11(8), 1222.

Almeida, D. Q., Paciência, I., Moreira, C., Rufo, J. C., Moreira, A., Santos, A. C., ... & Ribeiro, A. I. (2022). Green and blue spaces and lung function in the Generation XXI cohort: a life-course approach. European Respiratory Journal, 60(6).

Amati, M. (Ed.). (2016). Urban green belts in the twenty-first century. Routledge.

Amin, S. M. A., & Rahman, A. (2014). Opportunities and challenges of urban and Peri-urban agriculture to face climate change: a critical analysis of policy and urban governance of Dhaka City. The Security of Water, Food, Energy and Liveability of Cities: Challenges and Opportunities for Peri-Urban Futures, 365-382.

Anderson, J. R. (1976). A land use and land cover classification system for use with remote sensor data (Vol. 964). US Government Printing Office.

Arafaine, Z., & Asefa, A. (2019). Dynamics of land use and land cover in the Kafta-Sheraro national park, NW Ethiopia: patterns, causes and management implications. Momona Ethiop J Sci 11: 239–257.

Aronson, M. F., Lepczyk, C. A., Evans, K. L., Goddard, M. A., Lerman, S. B., MacIvor, J. S., ... & Vargo, T. (2017). Biodiversity in the city: key challenges for urban green space management. Frontiers in Ecology and the Environment, 15(4), 189-196.

Assede, E. S., Orou, H., Biaou, S. S., Geldenhuys, C. J., Ahononga, F. C., & Chirwa, P. W. (2023). Understanding drivers of land use and land cover change in Africa: A review. Current Landscape Ecology Reports, 8(2), 62-72.

Bachir, N., Bounoua, L., Aiche, M., Maliki, M., Nigro, J., & El Ghazouani, L. (2021). The simulation of the impact of the spatial distribution of vegetation on the urban microclimate: A case study in Mostaganem. Urban Climate, 39, 100976.

Bangladesh Bureau of statistics (BBS), Population and Housing Census 2011,

Bangladesh Bureau of statistics (BBS), Population and Housing Census 2022,

Bangladesh Bureau of statistics (BBS), Population and Housing Census 2001,

Bangladesh Meteorological Department (BMD), 2022, Daily Temperature data for Dhaka and other station.

Basheer, S., Wang, X., Farooque, A. A., Nawaz, R. A., Liu, K., Adekanmbi, T., & Liu, S. (2022). Comparison of land use land cover classifiers using different satellite imagery and machine learning techniques. Remote Sensing, 14(19), 4978.

Bohnenstengel, S. I., Hamilton, I., Davies, M., & Belcher, S. E. (2014). Impact of anthropogenic heat emissions on London's temperatures. Quarterly Journal of the Royal Meteorological Society, 140(679), 687-698.

Burkart, K. G., Brauer, M., Aravkin, A. Y., Godwin, W. W., Hay, S. I., He, J., ... & Stanaway, J. D. (2021). Estimating the cause-specific relative risks of non-optimal temperature on daily mortality: a two-part modelling approach applied to the Global Burden of Disease Study. The Lancet, 398(10301), 685-697.

Byomkesh, T., Nakagoshi, N., & Dewan, A. M. (2012). Urbanization and green space dynamics in Greater Dhaka, Bangladesh. Landscape and Ecological Engineering, 8, 45-58.

Centre for Environmental and Geographic Information System (CEGIS), Ministry of Local government engineering department (LGED), Bangladesh.

Chowdhury, F. K., & Rahman, S. Z. (2023). Slums and entrepreneurship as an impact of urban poverty and social exclusion in Dhaka, Bangladesh. World Review of Entrepreneurship, Management and Sustainable Development, 19(6), 502-519.

Chua, P., Ng, C. F. S., Tobias, A., Seposo, X., & Hashizume, M. (2021). Associations between ambient temperature and enteric infections by aetiology: a systematic review and meta-analysis. Available at SSRN 3822570.

Chughtai, A. H., Abbasi, H., & Karas, I. R. (2021). A review on change detection method and accuracy assessment for land use land cover. Remote Sensing Applications: Society and Environment, 22, 100482

Cobbinah, P. B., Asibey, M. O., Zuneidu, M. A., & Erdiaw-Kwasie, M. O. (2021). Accommodating green spaces in cities: Perceptions and attitudes in slums. Cities, 111, 103094.

Corner, R. J., Dewan, A. M., & Chakma, S. (2014). Monitoring and prediction of land-use and land-cover (LULC) change. Dhaka megacity: geospatial perspectives on urbanisation, environment and health, 75-97.

Deilami, K., Kamruzzaman, M., & Liu, Y. (2018). Urban heat island effect: A systematic review of spatio-temporal factors, data, methods, and mitigation measures. In International Journal of Applied Earth Observation and Geoinformation (Vol. 67, pp. 30–42). Elsevier B.V. https://doi.org/10.1016/j.jag.2017.12.009

Deng, J. Y., & Wong, N. H. (2020). Impact of urban canyon geometries on outdoor thermal comfort in central business districts. Sustainable Cities and Society, 53, 101966.

Dewan, A. M., & Yamaguchi, Y. (2009). Land use and land cover change in Greater Dhaka, Bangladesh: Using remote sensing to promote sustainable urbanization. Applied geography, 29(3), 390-401.

Dewan, A., Kiselev, G., Botje, D., Mahmud, G. I., Bhuian, M. H., & Hassan, Q. K. (2021). Surface urban heat island intensity in five major cities of Bangladesh: Patterns, drivers and trends. Sustainable Cities and Society, 71, 102926.

Dhaka north city corporation (DNCC), 2023.

Dhaka south city corporation (DSCC), 2023.

Diviacco, P., Iurcev, M., Carbajales, R. J., & Potleca, N. (2022). First Results of the Application of a Citizen Science-Based Mobile Monitoring System to the Study of Household Heating Emissions. Atmosphere, 13(10), 1689.

Dutta, K., Basu, D., & Agrawal, S. (2021). Synergetic interaction between spatial land cover dynamics and expanding urban heat islands. Environmental Monitoring and Assessment, 193, 1-22.

Eastin, M. D., Baber, M., Boucher, A., Di Bari, S., Hubler, R., Stimac-Spalding, B., & Winesett, T. (2018). Temporal variability of the Charlotte (sub) urban heat island. Journal of Applied Meteorology and Climatology, 57(1), 81-102.

Emelyanova, I. V., McVicar, T. R., Van Niel, T. G., Li, L. T., & Van Dijk, A. I. (2013). Assessing the accuracy of blending Landsat–MODIS surface reflectances in two landscapes with contrasting spatial and temporal dynamics: A framework for algorithm selection. Remote Sensing of Environment, 133, 193-209.

Eskandari, S., Reza Jaafari, M., Oliva, P., Ghorbanzadeh, O., & Blaschke, T. (2020). Mapping land cover and tree canopy cover in Zagros forests of Iran: Application of Sentinel-2, Google Earth, and field data. Remote Sensing, 12(12), 1912.

European Environment Agency (EEA), Climate change as a threat to health and well-being in Europe – Focus on heat and infectious diseases, Publications Office of the European Union, 2022, https://data.europa.eu/doi/10.2800/67519

Feng, C., Zhang, H., Xiao, L., & Guo, Y. (2022). Land use change and its driving factors in the rural–urban fringe of Beijing: A Production–Living–Ecological perspective. Land, 11(2), 314.

Feng, X., Astell-Burt, T., Standl, M., Flexeder, C., Heinrich, J., & Markevych, I. (2022). Green space quality and adolescent mental health: do personality traits matter? Environmental Research, 206, 112591.

Flood Action Plan (FAP) 8A. (1991). Master plan study for Greater Dhaka protection project.

Fonseca, L. M., Domingues, J. P., & Dima, A. M. (2020). Mapping the sustainable development goals relationships. Sustainability, 12(8), 3359.

Foody, G. M. (2020). Explaining the unsuitability of the kappa coefficient in the assessment and comparison of the accuracy of thematic maps obtained by image classification. Remote Sensing of Environment, 239, 111630

Forkuor, G., Dimobe, K., Serme, I., & Tondoh, J. E. (2018). Landsat-8 vs. Sentinel-2: examining the added value of sentinel-2's red-edge bands to land-use and land-cover mapping in Burkina Faso. GIScience & remote sensing, 55(3), 331-354.

Frimpong, A., Kwabena Forkuo, E., & Matthew Osei, E. (2023). A comparative estimate of air temperature from modis land surface temperatures in Ghana. Cogent Engineering, 10(1), 2216047.

Gao, B. C. (1996). NDWI—A normalized difference water index for remote sensing of vegetation liquid water from space. Remote sensing of environment, 58(3), 257-266.

Gao, F., Masek, J., Schwaller, M., & Hall, F. (2006). On the blending of the Landsat and MODIS surface reflectance: Predicting daily Landsat surface reflectance. IEEE Transactions on Geoscience and Remote sensing, 44(8), 2207-2218.

Gartland, L. M. (2012). Heat islands: understanding and mitigating heat in urban areas. Routledge.

Gaston, K. J. (Ed.). (2010). Urban ecology. Oxford University Press.

Gorelick, N., Hancher, M., Dixon, M., Ilyushchenko, S., Thau, D., & Moore, R. (2017). Google Earth Engine: Planetary-scale geospatial analysis for everyone. Remote sensing of Environment, 202, 18-27.

Guan, X., Huang, C., & Zhang, R. (2021). Integrating MODIS and Landsat data for land cover classification by multilevel decision rule. Land, 10(2), 208.

Guo, G., Wu, Z., Xiao, R., Chen, Y., Liu, X., & Zhang, X. (2015). Impacts of urban biophysical composition on land surface temperature in urban heat island clusters. Landscape and Urban Planning, 135, 1-10.

Habitat, U. N. (2018). Tracking Progress Towards Inclusive, Safe, Resilient and Sustainable Cities and Human Settlements. SDG 11 Synthesis Report-High Level Political Forum 2018.

Halicioglu, K., Erten, E., & Rossi, C. (2021). Monitoring deformations of Istanbul metro line stations through Sentinel-1 and levelling observations. Environmental Earth Sciences, 80(9), 361.

Han, D., Zhang, T., Qin, Y., Tan, Y., & Liu, J. (2023). A comparative review on the mitigation strategies of urban heat island (UHI): a pathway for sustainable urban development. Climate and Development, 15(5), 379-403.

Hazaymeh, K., & Hassan, Q. K. (2015). Fusion of MODIS and Landsat-8 surface temperature images: A new approach. PLoS One, 10(3), e0117755.

Helmer, E. H., Brown, S., & Cohen, W. B. (2000). Mapping montane tropical forest successional stage and land use with multi-date Landsat imagery. International journal of remote sensing, 21(11), 2163-2183.

Hossain, A. M., Fien, J., & Horne, R. (2018). Megacity Dhaka: ‘water security syndrome’and implications for the scholarship of sustainability. Sustainable Water Resources Management, 4, 63-78.

Hossain, M. S. (2017). Mapping Urban Encroachment in the Rivers around Dhaka City: An Example from the Turag River. Journal of Environment and Earth Science, 7(10), 79-88.

Hou, H., Longyang, Q., Su, H., Zeng, R., Xu, T., & Wang, Z. H. (2023). Prioritizing environmental determinants of urban heat islands: A machine learning study for major cities in China. International Journal of Applied Earth Observation and Geoinformation, 122, 103411.

Hsu, A., Sheriff, G., Chakraborty, T., & Manya, D. (2021). Disproportionate exposure to urban heat island intensity across major US cities. Nature communications, 12(1), 2721.

https://earthobservatory.nasa.gov/images/150274/rising-flood-risks-in-bangladesh

https://sdgs.un.org/goals

https://www.eiu.com/default.aspx

https://www.eiu.com/n/campaigns/global-liveability-index-2023/#:~:text=EIU's%20index%20quantifies%20the%20challenges,and%20education%20in%20developing%20countries.

https://www.macrotrends.net/cities/20119/dhaka/population

https://www.usgs.gov/

Hu, J., Yang, Y., Zhou, Y., Zhang, T., Ma, Z., & Meng, X. (2022). Spatial patterns and temporal variations of footprint and intensity of surface urban heat island in 141 China cities. Sustainable Cities and Society, 77, 103585.

Huang, B., Wang, J., Song, H., Fu, D., & Wong, K. (2013). Generating high spatiotemporal resolution land surface temperature for urban heat island monitoring. IEEE Geoscience and Remote Sensing Letters, 10(5), 1011-1015.

Huang, Y., Lin, T., Zhang, G., Jones, L., Xue, X., Ye, H., & Liu, Y. (2022). Spatiotemporal patterns and inequity of urban green space accessibility and its relationship with urban spatial expansion in China during rapid urbanization period. Science of the Total Environment, 809, 151123.

Hulley, G., & Nickeson, J. (2020). M∗ D21 (MYD21/MOD21) and M∗ D11 (MYD11/MYD21) land surface temperature and emissivity (LST&E) products status

report. NASA, Washington, DC.

Hulley, G., Malakar, N., Hughes, T., Islam, T., & Hook, S. (2016). Moderate resolution imaging spectroradiometer (MODIS) MOD21 land surface temperature and emissivity algorithm theoretical basis document (No. JPL-Publ-12-17, Rev. 2).

Hussain, N., Ahmed, S. S., & Shumi, A. M. (2023). Remote sensing-based geostatistical hot spot analysis of Urban Heat Islands in Dhaka, Bangladesh. Singapore Journal of Tropical Geography, 44(3), 438-458.

Hussain, S., Mubeen, M., Ahmad, A., Akram, W., Hammad, H. M., Ali, M., ... & Nasim, W. (2020). Using GIS tools to detect the land use/land cover changes during forty years in Lodhran District of Pakistan. Environmental Science and Pollution Research, 27, 39676-39692.

Hussain, S., Mubeen, M., Ahmad, A., Majeed, H., Qaisrani, S. A., Hammad, H. M., ... & Nasim, W. (2022). Assessment of land use/land cover changes and its effect on land surface temperature using remote sensing techniques in Southern Punjab, Pakistan. Environmental Science and Pollution Research, 1-17.

Idrees, M. O., Omar, D. M., Babalola, A., Ahmadu, H. A., Yusuf, A., & Lawal, F. O. (2022). Urban land use land cover mapping in tropical savannah using Landsat-8 derived normalized difference vegetation index (NDVI) threshold. South African Journal of Geomatics, 11(1).

Ignatieva, M., Haase, D., Dushkova, D., & Haase, A. (2020). Lawns in cities: from a globalised urban green space phenomenon to sustainable nature-based solutions. Land, 9(3), 73.

Imai, C., Armstrong, B., Chalabi, Z., Mangtani, P., & Hashizume, M. (2015). Time series regression model for infectious disease and weather. Environmental research, 142, 319-327.

Irfeey, A. M. M., Chau, H. W., Sumaiya, M. M. F., Wai, C. Y., Muttil, N., & Jamei, E. (2023). Sustainable mitigation strategies for urban heat island effects in urban areas. Sustainability, 15(14), 10767.

Ishola, K. A., Okogbue, E. C., & Adeyeri, O. E. (2016). Dynamics of surface urban biophysical compositions and its impact on land surface thermal field. Modeling Earth Systems and Environment, 2, 1-20.

Islam, M. M., Hossain, M. A., & Sanjowal, R. K. (2022). Bangladesh at Fifty: changes and challenges in population and development. Journal of Governance, Security & Development, 3(1), 1-38.

Ivajnšič, D., & Žiberna, I. (2019). The effect of weather patterns on winter small city urban heat islands. Meteorological Applications, 26(2), 195-203.

Jain, N., Kourampi, I., Umar, T. P., Almansoor, Z. R., Anand, A., Rehman, M. E. U., ... & Reinis, A. (2023). Global population surpasses eight billion: Are we ready for the next billion? AIMS Public Health, 10(4), 849-866.

Jalal, M. (2022). Assessing the role of land use landcover transition factors in mitigating surface urban heat risk: a study on Dhaka North city. https://urn.fi/URN:NBN:fi:amk-2022112524193.

Jim, C. Y., & Chen, W. Y. (2006). Perception and attitude of residents toward urban green spaces in Guangzhou (China). Environmental management, 38, 338-349.

Jin, H., Chen, X., Wang, Y., Zhong, R., Zhao, T., Liu, Z., & Tu, X. (2021). Spatio-temporal distribution of NDVI and its influencing factors in China. Journal of Hydrology, 603, 127129.

Jones, K. R. (2018). 'The Lungs of the City': Green Space, Public Health and Bodily Metaphor in the Landscape of Urban Park History. Environment and History, 24(1), 39-58.

Kafy, A. A., Al Rakib, A., Akter, K. S., Jahir, D. M. A., Sikdar, M. S., Ashrafi, T. J., ... & Rahman, M. M. (2021). Assessing and predicting land use/land cover, land surface temperature and urban thermal field variance index using Landsat imagery for Dhaka Metropolitan area. Environmental Challenges, 4, 100192.

Kafy, A. A., Dey, N. N., Al Rakib, A., Rahaman, Z. A., Nasher, N. R., & Bhatt, A. (2021). Modeling the relationship between land use/land cover and land surface temperature in Dhaka, Bangladesh using CA-ANN algorithm. Environmental Challenges, 4, 100190.

Kamali Maskooni, E., Hashemi, H., Berndtsson, R., Daneshkar Arasteh, P., & Kazemi, M. (2021). Impact of spatiotemporal land-use and land-cover changes on surface urban heat islands in a semiarid region using Landsat data. International Journal of Digital Earth, 14(2), 250-270.

Kang, L., Yang, Z., & Han, F. (2021). The impact of urban recreation environment on residents' happiness—based on a case study in China. Sustainability, 13(10), 5549.

Kaplan, G., & Avdan, U. (2017). Object-based water body extraction model using Sentinel-2 satellite imagery. European Journal of Remote Sensing, 50(1), 137-143.

Karakuş, C. B. (2019). The impact of land use/land cover (LULC) changes on land surface temperature in Sivas City Center and its surroundings and assessment of Urban Heat Island. Asia-Pacific Journal of Atmospheric Sciences, 55(4), 669-684.

Karim, M. N., Munshi, S. U., Anwar, N., & Alam, M. S. (2012). Climatic factors influencing dengue cases in Dhaka city: A model for dengue prediction. The Indian Journal of Medical Research, 136(1), 32. /pmc/articles/PMC3461715/

Karim, R., Pk, M. B., Dey, P., Akbar, M. A., & Osman, M. S. (2024). A study about the prediction of population growth and demographic transition in Bangladesh. Journal of Umm Al-Qura University for Applied Sciences, 1-13.

Khan, A., Chatterjee, S., Akbari, H., Bhatti, S. S., Dinda, A., Mitra, C., ... & Doan, Q. V. (2019). Step-wise Land-class Elimination Approach for extracting mixed-type built-up areas of Kolkata megacity. Geocarto international, 34(5), 504-527.

Kruize H, van der Vliet N, Staatsen B, Bell R, Chiabai A, Muiños G, Higgins S, Quiroga S, Martinez-Juarez P, Aberg Yngwe M, Tsichlas F, Karnaki P, Lima ML, García de Jalón S, Khan M, Morris G, Stegeman I. Urban Green Space: Creating a Triple Win for Environmental Sustainability, Health, and Health Equity through Behavior Change. Int J Environ Res Public Health. 2019 Nov 11;16(22):4403. doi: 10.3390/ijerph16224403. PMID: 31717956; PMCID: PMC6888177.

Kulkarni, G., Muley, A., Deshmukh, N., & Bhalchandra, P. (2020). Land use land cover change detection through GIS and unsupervised learning technique. In Information and Communication Technology for Sustainable Development: Proceedings of ICT4SD 2018 (pp. 239-247). Springer Singapore.

Laonamsai, J., Julphunthong, P., Saprathet, T., Kimmany, B., Ganchanasuragit, T., Chomcheawchan, P., & Tomun, N. (2023). Utilizing NDWI, MNDWI, SAVI, WRI, and AWEI for Estimating Erosion and Deposition in Ping River in Thailand. Hydrology, 10(3), 70.

Li, Q., Ding, F., Wu, W., & Chen, J. (2016, July). Improvement of ESTARFM and its application to fusion of Landsat-8 and MODIS land surface temperature images. In 2016 4th International Workshop on Earth Observation and Remote Sensing Applications (EORSA) (pp. 33-37). IEEE.

Liang, X., Guan, Q., Clarke, K. C., Liu, S., Wang, B., & Yao, Y. (2021). Understanding the drivers of sustainable land expansion using a patch-generating land use simulation (PLUS) model: A case study in Wuhan, China. Computers, Environment and Urban Systems, 85, 101569.

Lin, M., Hou, L., Qi, Z., & Wan, L. (2022). Impacts of climate change and human activities on vegetation NDVI in China's Mu Us Sandy Land during 2000–2019. Ecological Indicators, 142, 109164.

Liu, C., Li, W., Zhu, G., Zhou, H., Yan, H., & Xue, P. (2020). Land use/land cover changes and their driving factors in the Northeastern Tibetan Plateau based on Geographical Detectors and Google Earth Engine: A case study in Gannan Prefecture. Remote Sensing, 12(19), 3139.

Liu, H., & Weng, Q. (2018). Scaling effect of fused ASTER-MODIS land surface temperature in an urban environment. Sensors, 18(11), 4058.

Liu, J., Varghese, B. M., Hansen, A., Zhang, Y., Driscoll, T., Morgan, G., ... & Bi, P. (2022). Heat exposure and cardiovascular health outcomes: a systematic review and meta-analysis. The Lancet Planetary Health, 6(6), e484-e495.

Liu, Y., Li, Q., Yang, L., Mu, K., Zhang, M., & Liu, J. (2020). Urban heat island effects of various urban morphologies under regional climate conditions. Science of the total environment, 743, 140589.

Long, D., Yan, L., Bai, L., Zhang, C., Li, X., Lei, H., & Shi, C. (2020). Generation of MODIS-like land surface temperatures under all-weather conditions based on a data fusion approach. Remote Sensing of Environment, 246, 111863.

Lovell, D., Miller, D., Capra, J., & Bradley, A. (2022). Never mind the metrics--what about the uncertainty? Visualizing confusion matrix metric distributions. arXiv preprint arXiv:2206.02157.

Lu, D., & Weng, Q. (2007). A survey of image classification methods and techniques for improving classification performance. International journal of Remote sensing, 28(5), 823-870.

MacKaye, B. (1990). The new exploration: A philosophy of regional planning. University of Illinois Press.

Maharajan, M., Aryal, A., Man Shakya, B., Talchabhadel, R., Thapa, B. R., & Kumar, S. (2021). Evaluation of Urban Heat Island (UHI) Using Satellite Images in Densely Populated Cities of South Asia. Earth, 2(1), 86–110. https://doi.org/10.3390/earth2010006

Manisalidis, I., Stavropoulou, E., Stavropoulos, A., & Bezirtzoglou, E. (2020). Environmental and health impacts of air pollution: a review. Frontiers in public health, 8, 505570. Maharjan

Martilli, A., Krayenhoff, E. S., & Nazarian, N. (2020). Is the Urban Heat Island intensity relevant for heat mitigation studies? Urban Climate, 31, 100541.

Masek, J. G., Vermote, E. F., Saleous, N. E., Wolfe, R., Hall, F. G., Huemmrich, K. F., ... & Lim, T. K. (2006). A Landsat surface reflectance dataset for North America, 1990-2000. IEEE Geoscience and Remote Sensing Letters, 3(1), 68-72.

Masrur, A., Dewan, A., Botje, D., Kiselev, G., & Murshed, M. M. (2022). Dynamics of human presence and flood-exposure risk in close proximity to Bangladesh's river network: an evaluation with multitemporal satellite imagery. Geocarto International, 37(27), 14946-14962.

McDonald, R. I., Mansur, A. V., Ascensão, F., Colbert, M. L., Crossman, K., Elmqvist, T., ... & Ziter, C. (2020). Research gaps in knowledge of the impact of urban growth on biodiversity. Nature Sustainability, 3(1), 16-24.

Mileva, N., Mecklenburg, S. & Gascon, F. (2018). New tool for spatiotemporal image fusion in remote sensing - a case study approach using Sentinel-2 and Sentinel-3 data. In Bruzzone, L. & Bovolo, F. (Eds.), SPIE Proceedings Vol. 10789: Image and Signal Processing for Remote Sensing XXIV. Berlin, Germany: International Society for Optics and Photonics. https://doi.org/10.1117/12.2327091

Mohan, M., Sati, A. P., & Bhati, S. (2020). Urban sprawl during five decadal period over National Capital Region of India: Impact on urban heat island and thermal comfort. Urban

climate, 33, 100647.

MohanRajan, S. N., Loganathan, A., & Manoharan, P. (2020). Survey on Land Use/Land Cover (LU/LC) change analysis in remote sensing and GIS environment: Techniques and Challenges. Environmental Science and Pollution Research, 27(24), 29900-29926.

Morabito, M., Crisci, A., Messeri, A., Orlandini, S., Raschi, A., Maracchi, G., & Munafò, M. (2016). The impact of built-up surfaces on land surface temperatures in Italian urban areas. Science of the Total Environment, 551, 317-326.

Moshfika, Mehanaz, Subir Biswas, and M. Shahjahan Mondal. "Assessing groundwater level declination in Dhaka city and identifying adaptation options for sustainable water supply." Sustainability 14, no. 3 (2022): 1518.

Mowla, Q. A. (2011, January). Crisis in the built environment of Dhaka: an overview. In Conference on 'Engineering, Research, Innovation and Education (pp. 11-13). Shahjalal University of Science and Technology Sylhet.

Mushtaha, E., Shareef, S., Alsyouf, I., Mori, T., Kayed, A., Abdelrahim, M., & Albannay, S. (2021). A study of the impact of major Urban Heat Island factors in a hot climate courtyard: The case of the University of Sharjah, UAE. Sustainable Cities and Society, 69, 102844.

Nasrollahi, N., & Rostami, E. (2023). The impacts of urban canyons morphology on daylight availability and energy consumption of buildings in a hot-summer Mediterranean climate. Solar Energy, 266, 112181.

Nawar, N., Sorker, R., Chowdhury, F. J., & Rahman, M. M. (2022). Present status and historical changes of urban green space in Dhaka city, Bangladesh: A remote sensing driven approach. Environmental Challenges, 6, 100425.

Nguyen, H. T. T., Doan, T. M., Tomppo, E., & McRoberts, R. E. (2020). Land Use/land cover mapping using multitemporal Sentinel-2 imagery and four classification methods—A case study from Dak Nong, Vietnam. Remote Sensing, 12(9), 1367.

Nitoslawski, S. A., Galle, N. J., Van Den Bosch, C. K., & Steenberg, J. W. (2019). Smarter ecosystems for smarter cities? A review of trends, technologies, and turning points for smart urban forestry. Sustainable Cities and Society, 51, 101770.

Oke, T. R. (1976). The distinction between canopy and boundary-layer urban heat islands. Atmosphere, 14(4), 268-277.

Oke, T. R. (1982). The energetic basis of the urban heat island. Quarterly journal of the royal meteorological society, 108(455), 1-24.

Oke, T. R., Mills, G., Christen, A., & Voogt, J. A. (2017). *Urban climates*. Cambridge University Press.

P. Dou and Z. Han, "Quantifying Land Use/Land Cover Change and Urban Expansion in Dongguan, China, From 1987 to 2020," in IEEE Journal of Selected Topics in Applied Earth Observations and Remote Sensing, vol. 15, pp. 201-209, 2022, doi: 10.1109/JSTARS.2021.3133703.

Padmanaban, R., Bhowmik, A. K., & Cabral, P. (2019). Satellite image fusion to detect changing surface permeability and emerging urban heat islands in a fast-growing city. PloS one, 14(1), e0208949.

Parvin, N., Abudu, D. (2017). Estimating Urban Heat Island Intensity using Remote Sensing Techniques in Dhaka City. International Journal of Scientific & Engineering Research, 8(4), 289–298. https://doi.org/10.14299/ijser.2017.04.009

Peplau, T., Poeplau, C., Gregorich, E., & Schroeder, J. (2023). Deforestation for agriculture leads to soil warming and enhanced litter decomposition in subarctic soils. Biogeosciences, 20(5), 1063-1074.

Pineo, H. (2022). Towards healthy urbanism: inclusive, equitable and sustainable (THRIVES)–an urban design and planning framework from theory to praxis. Cities & health, 6(5), 974-992.

Proutsos, N. D., Liakatas, A., Alexandris, S. G., Tsiros, I. X., Tigkas, D., & Halivopoulos, G. (2022). Atmospheric factors affecting global solar and photosynthetically active radiation relationship in a mediterranean forest site. Atmosphere, 13(8), 1207.

Qin, X., Wei, Y. D., Yu, Z., & Xiong, N. (2022). Urbanization, Suburbanization, and Population Redistribution in Urban China: A Case Study of Nanjing. Journal of Urban Planning and Development, 148(4), 05022034.

Qu, S., Wang, L., Lin, A., Yu, D., & Yuan, M. (2020). Distinguishing the impacts of climate change and anthropogenic factors on vegetation dynamics in the Yangtze River Basin, China. Ecological Indicators, 108, 105724.

Qureshi, A. M., & Rachid, A. (2022). Heat Vulnerability Index Mapping: A Case Study of a Medium-Sized City (Amiens). Climate, 10(8), 113. https://doi.org/10.3390/cli10080113.

Rahimi-Ajdadi, F., & Khani, M. (2022). Multi-Temporal Detection of Agricultural Land Losses Using Remote Sensing and Gis Techniques, Shanderman, Iran. Acta Technologica Agriculturae, 25(2), 67-72.

Rahman, M. M., Avtar, R., Yunus, A. P., Dou, J., Misra, P., Takeuchi, W., ... & Agustiono Kurniawan, T. (2020). Monitoring effect of spatial growth on land surface temperature in Dhaka. Remote Sensing, 12(7), 1191.

Raj, S. I., & Naem, A. J. (2022). SOCIOECONOMIC IMPACT OF THE FIRST MASS RAPID TRANSIT (MRT) IN DHAKA. Seminario Internacional de Investigación en Urbanismo, (14).

Raja, D. R., Hredoy, M. S. N., Islam, M. K., Islam, K. M. A., & Adnan, M. S. G. (2021). Spatial distribution of heatwave vulnerability in a coastal city of Bangladesh. Environmental Challenges, 4(May), 100122. https://doi.org/10.1016/j.envc.2021.100122

Rashid, N., Alam, J. M., Chowdhury, M. A., & Islam, S. L. U. (2022). Impact of landuse change and urbanization on urban heat island effect in Narayanganj city, Bangladesh: A remote sensing-based estimation. Environmental Challenges, 8, 100571.

Romshoo, S. A., Murtaza, K. O., Shah, W., Ramzan, T., Ameen, U., & Bhat, M. H. (2022). Anthropogenic climate change drives melting of glaciers in the Himalaya. Environmental Science and Pollution Research, 29(35), 52732-52751.

Roy, S., Sowgat, T., Islam, S. T., & Anjum, N. (2021). Sustainability challenges sprawling Dhaka. Environment and Urbanization Asia, 12(1_suppl), S59-S84.

Rwanga, S. S., & Ndambuki, J. M. (2017). Accuracy assessment of land use/land cover classification using remote sensing and GIS. International Journal of Geosciences, 8(04), 611.

Salah, M. (2017). A survey of modern classification techniques in remote sensing for improved image classification. Journal of Geomatics, 11(1), 21.

Santamouris, M. (2014). Cooling the cities–a review of reflective and green roof mitigation technologies to fight heat island and improve comfort in urban environments. Solar energy, 103, 682-703.

Seraj, T. M., & Islam, M. A. (2013). Detailed Area Plan: Proposals to Meet Housing Demand in Dhaka. Dhaka Metropolitan Development Area and Its Planning Problems, Issues and Policies, Bangladesh Institute of Planners.

Sharmin, T., & Steemers, K. (2020). Effects of microclimate and human parameters on outdoor thermal sensation in the high-density tropical context of Dhaka. International journal of biometeorology, 64(2), 187-203.

Shen, H., Huang, L., Zhang, L., Wu, P., & Zeng, C. (2016). Long-term and fine-scale satellite monitoring of the urban heat island effect by the fusion of multi-temporal and multi-sensor remote sensed data: A 26-year case study of the city of Wuhan in China. Remote Sensing of Environment, 172, 109-125.

Shi, S., Yu, J., Wang, F., Wang, P., Zhang, Y., & Jin, K. (2021). Quantitative contributions of climate change and human activities to vegetation changes over multiple time scales on the Loess Plateau. Science of the Total Environment, 755, 142419.

Singh, V. K., Mohan, M., & Bhati, S. (2023). Industrial heat island mitigation in Angul-Talcher region of India: evaluation using modified WRF-Single Urban Canopy Model. Science of The Total Environment, 858, 159949. Stewart, I. D. (2011). Redefining the urban heat island (Doctoral dissertation, University of British Columbia.

Smith, C., Lindley, S., & Levermore, G. (2009). Estimating spatial and temporal patterns of urban anthropogenic heat fluxes for UK cities: the case of Manchester. Theoretical and Applied Climatology, 98, 19-35.

Subedi, P. B., Ojha, P., Adhikari, A., Acharya, S., & Acharya, S. (2022). Mapping of Major Land Use Land Cover Dynamics and Its Driving Factors: A Case Study of Nepalgunj Sub-Metropolitan City, Banke, Nepal. Indonesian Journal of Social and Environmental Issues (IJSEI), 3(1), 67-80.

Sultana, S., Mannan, M. A., Khan, M. A. R., Khandaker, R., & Md Kamrujjaman, -. (2020). Pre-Existing Weather Phenomena for Spreading Dengue Fever Over Dhaka in 2019. Journal of Engineering Science, 11(2), 99–106. https://doi.org/10.3329/jes.v11i2.50901

Sun, X., Ge, F., Fan, Y., Zhu, S., & Chen, Q. (2022). Will population exposure to heat extremes intensify over Southeast Asia in a warmer world? Environmental Research Letters, 17(4), 044006.

Szabo, S., Gácsi, Z., & Balazs, B. (2016). Specific features of NDVI, NDWI and MNDWI as reflected in land cover categories. *Acta Geographica Debrecina. Landscape & Environment Series*, *10*(3/4), 194.

Talukdar, S., Singha, P., Mahato, S., Pal, S., Liou, Y. A., & Rahman, A. (2020). Land-use land-cover classification by machine learning classifiers for satellite observations—A review. *Remote Sensing*, *12*(7), 1135.

Tashnim, J., & Anwar, A. (2016, February). Reasons and remides of heat island phenomena for Dhaka City: A review. In Proceedings of the 3rd international conference on civil engineering for sustainable development (ICCESD 2016) (pp. 228-234).

Tavares, P. A., Beltrão, N. E. S., Guimarães, U. S., & Teodoro, A. C. (2019). Integration of sentinel-1 and sentinel-2 for classification and LULC mapping in the urban area of Belém, eastern Brazilian Amazon. *Sensors*, *19*(5), 1140.

Tepanosyan, G., Muradyan, V., Hovsepyan, A., Pinigin, G., Medvedev, A., & Asmaryan, S. (2021). Studying spatial-temporal changes and relationship of land cover and surface Urban Heat Island derived through remote sensing in Yerevan, Armenia. Building and Environment, 187, 107390.

Tilahun, A., & Teferie, B. (2015). Accuracy assessment of land use land cover classification using Google Earth. American Journal of Environmental Protection, 4(4), 193-198.

Ting, D. S. (2012). Heat Islands–Understanding and Mitigating Heat in Urban Areas.

Tomlinson, C.J., Chapman, L., Thornes, J.E. and Baker, C.J. (2012), Derivation of Birmingham's summer surface urban heat island from MODIS satellite images. Int. J. Climatology, 32: 214-224. https://doi.org/10.1002/joc.2261.

Topaloğlu, R. H., Aksu, G. A., Ghale, Y. A. G., & Sertel, E. (2022). High-resolution land use and land cover change analysis using GEOBIA and landscape metrics: A case of Istanbul, Turkey. Geocarto International, 37(25), 9071-9097.

Turner, B.L., Meyer, W.B., & Skole, D.L. (1994). Global land-use/land-cover change: towards an integrated study.

U.S. Environmental Protection Agency (2017).

Uddin, A. S., Khan, N., Islam, A. R. M. T., Kamruzzaman, M., & Shahid, S. (2022). Changes in urbanization and urban heat island effect in Dhaka city. Theoretical and Applied Climatology, 147(3), 891-907.

Ukrainski, P. (2019). Classification accuracy assessment. Confusion matrix method. 50 degrees. North.

Ullah, S., Ahmad, K., Sajjad, R. U., Abbasi, A. M., Nazeer, A., & Tahir, A. A. (2019). Analysis and simulation of land cover changes and their impacts on land surface temperature in a lower Himalayan region. Journal of environmental management, 245, 348-357.

UN. (2018). 68% of the world population is projected to live in urban areas by 2050, says UN. Department of Economic and Social Affairs. https://www.un.org/development/desa/en/news/population/2018-revision-of-world-urbanization-prospects.html

United Nation Environmental Programme (UNEP, 2022).

United Nations Population Fund (UNFPA, 2023). https://www.unfpa.org/swp2023.

Varentsov, M. I., Grishchenko, M. Y., & Wouters, H. (2019). Simultaneous assessment of the summer urban heat island in Moscow megacity based on in situ observations, thermal satellite images and mesoscale modeling. Geography, Environment, Sustainability, 12(4), 74-95.

Vidal, C., Lyman, C., Brown, G., & Hynson, B. (2022). Reclaiming public spaces: The case for the built environment as a restorative tool in neighborhoods with high levels of community violence. Journal of community psychology, 50(5), 2399-2410.

Vieira, S. M., Kaymak, U., & Sousa, J. M. (2010, July). Cohen's kappa coefficient as a performance measure for feature selection. In International conference on fuzzy systems (pp. 1-8). IEEE.

Vinayak, B., Lee, H. S., & Gedem, S. (2021). Prediction of Land Use and Land Cover

Changes in Mumbai City, India, Using Remote Sensing Data and a Multilayer Perceptron Neural Network-Based Markov Chain Model. Sustainability, 13(2), 471. https://doi.org/10.3390/su13020471

Vujovic, S., Haddad, B., Karaky, H., Sebaibi, N., & Boutouil, M. (2021). Urban heat island: Causes, consequences, and mitigation measures with emphasis on reflective and permeable pavements. CivilEng, 2(2), 459-484.

Walawender, J. P., Szymanowski, M., Hajto, M. J., & Bokwa, A. (2014). Land surface temperature patterns in the urban agglomeration of Krakow (Poland) derived from Landsat-7/ETM+ data. Pure and Applied Geophysics, 171, 913-940.

Walker, J.J., De Beurs, K.M., Wynne, R.H. and Gao, F., 2012. Evaluation of Landsat and MODIS data fusion products for analysis of dryland forest phenology. Remote Sensing of Environment, 117, pp.381-393.

Wan, Z. (1999). MODIS Land-Surface Temperature Algorithm Basis Document (LST ATBD): version 3.3. http://modis. gsfc. nasa. gov/data/atbd.

Wang, Chunyan, Yijing Long, Wenwen Li, Wei Dai, Shaohua Xie, Yuanling Liu, Yinchenxi Zhang et al. "Exploratory study on classification of lung cancer subtypes through a combined K-nearest neighbor classifier in breathomics." Scientific reports 10, no. 1 (2020): 5880.

Wang, J., Lin, Y., Zhai, T., He, T., Qi, Y., Jin, Z., & Cai, Y. (2018). The role of human activity in decreasing ecologically sound land use in C hina. Land degradation & development, 29(3), 446-460.

Wang, Y., Wang, A., Zhai, J., Tao, H., Jiang, T., Su, B., Yang, J., Wang, G., Liu, Q., Gao, C., Kundzewicz, Z. W., Zhan, M., Feng, Z., & Fischer, T. (2019). Tens of thousands additional deaths annually in cities of China between 1.5 °C and 2.0 °C warming. Nature Communications, 10(1), 3376. https://doi.org/10.1038/s41467-019-11283-w

Weng, Q., Fu, P., & Gao, F. (2014). Generating daily land surface temperature at Landsat resolution by fusing Landsat and MODIS data. Remote sensing of environment, 145, 55-67.

Wong, N. H., & Yu, C. (2005). Study of green areas and urban heat island in a tropical city. Habitat international, 29(3), 547-558.

Wu, J., Yunus, M., Ali, M., Escamilla, V., & Emch, M. (2018). Influences of heatwave, rainfall, and tree cover on cholera in Bangladesh. Environment International, 120, 304–311. https://doi.org/10.1016/J.ENVINT.2018.08.012

Xiang, S., Zhou, M., Huang, L., Shan, L., & Wang, K. (2023). Assessing the dynamic land utilization efficiency and relevant driving mechanism in in-situ urbanized rural areas: A case study of 1979 administrative villages in Hangzhou. Environmental Impact Assessment Review, 101, 107111.

Xu, X., Zhou, G., Du, H., Mao, F., Xu, L., Li, X., & Liu, L. (2020). Combined MODIS land surface temperature and greenness data for modeling vegetation phenology, physiology, and gross primary production in terrestrial ecosystems. Science of the Total Environment, 726, 137948.

Yadeta, T., Tessema, Z. K., Kebede, F., Mengesha, G., & Asefa, A. (2022). Land use land cover change in and around Chebera Churchura National Park, Southwestern Ethiopia: implications for management effectiveness. Environmental Systems Research, 11(1), 21.

Yin, H., Islam, M. S., & Ju, M. (2021). Urban river pollution in the densely populated city of Dhaka, Bangladesh: Big picture and rehabilitation experience from other developing countries. Journal of Cleaner Production, 321, 129040. https://doi.org/10.1016/j.jclepro.2021.129040

Yin, L., Dai, E., Zheng, D., Wang, Y., Ma, L., & Tong, M. (2020). What drives the vegetation dynamics in the Hengduan Mountain region, southwest China: Climate change or human activity? Ecological Indicators, 112, 106013.

Yin, S., Shen, Z., Zhou, P., Zou, X., Che, S., & Wang, W. (2011). Quantifying air pollution attenuation within urban parks: An experimental approach in Shanghai, China. Environmental pollution, 159(8-9), 2155-2163.

Zaldo-Aubanell, Q., Serra, I., Sardanyés, J., Alsedà, L., & Maneja, R. (2021). Reviewing the reliability of Land Use and Land Cover data in studies relating human health to the environment. Environmental Research, 194, 110578.

Zhao, C. (2018). Studying surface urban heat island phenomenon using remote sensing in three metropolitan areas of texas, USA.

Zhao, G., Zhang, Y., Tan, J., Li, C., & Ren, Y. (2020). A data fusion modeling framework for retrieval of land surface temperature from Landsat-8 and MODIS Data. Sensors, 20(15), 4337.

Zhou, D., Xiao, J., Bonafoni, S., Berger, C., Deilami, K., Zhou, Y., ... & Sobrino, J. A. (2018). Satellite remote sensing of surface urban heat islands: Progress, challenges, and perspectives. Remote Sensing, 11(1), 48.

Zou, Z., Yan, C., Yu, L., Jiang, X., Ding, J., Qin, L., ... & Qiu, G. (2021). Impacts of land use/land cover types on interactions between urban heat island effects and heat waves. Building and environment, 204, 108138.